# DEFECTIVE BRANCHED-CHAIN AMINO ACIDS (BCAAs) CATABOLISM ALTERS GLUCOSE METABOLISM AND INDUCES PANCREATIC β-CELL DYSFUNCTION IN TYPE 2 DIABETES

**LIN HUIGE**

**PhD**

The Hong Kong Polytechnic University

2021

The Hong Kong Polytechnic University

Department of Health Technology and Informatics

# Defective Branched-chain Amino Acids (BCAAs) Catabolism Alters Glucose Metabolism and Induces Pancreatic β-cell Dysfunction in Type 2 Diabetes

**LIN HUIGE**

A thesis submitted in partial fulfilment of the requirements for the degree of Doctor of Philosophy

September 2020

# CERTIFICATE OF ORIGINALITY

I hereby declare that this thesis is my own work and that, to the best of my knowledge and belief, it reproduces no material previously published or written, nor material that has been accepted for the award of any other degree or diploma, except where due acknowledgement has been made in the text.

_____ (Signed)

LIN HUIGE
_____(Name of student)

# Abstract

Blood glucose homeostasis is tightly controlled by the secretion and actions of insulin, a hormone that is specifically produced and released by pancreatic β-cells. Pancreatic β-cell dysfunction, characterized by defective insulin secretion and reduced β-cell mass, leads to type 2 diabetes (T2D). However, the driving force for β-cell dysfunction remains elusive.

Circulating levels of branched-chain amino acid (BCAA, including leucine, isoleucine and valine) is strikingly increased in human with T2D. This elevation has recently been identified to precede the onset of T2D and associate with β-cell dysfunction. However, the underlying mechanisms have not been explored before. The primary purpose of this study is to examine whether and how BCAA catabolism contributes to β-cell dysfunction. Our *in vivo* and *in vitro* studies showed that glucose metabolism in β-cells is impaired by defective BCAA catabolism, contributing to β-cell dysfunction and T2D.

***Key findings:***

1. Pancreatic β-cells consist of an intact BCAA catabolic pathway. However, this BCAA catabolic capacity is impaired in *db/db* T2D mice, as evidenced by an accumulation of intracellular BCAA related catabolites and reduced activity of BCKDH-A (the key enzyme of BCAA metabolism).
2. *In vitro* studies revealed that branched-chain α-keto acids (BCKA, the first metabolites of BCAA catabolism), but not BCAA or downstream acylcarnitines, induces defective glucose-induced insulin secretion (GSIS) in MIN6 β-cells. C57BL/6 male mice with chronic BCKA feeding displayed defective GSIS and glucose intolerance when compared to those treated with vehicle.

3. Promoting BCAA catabolism using 3,6-dichlorobenzo[b]thiophene-2-carboxylic acid (BT2, pharmacological activator of BCKA oxidation) alleviated glucose intolerance by enhancing GSIS in *db/db* diabetic mice.
4. The expression of PPM1K (a positive regulator of BCKDH-A activity) was decreased in islet from *db/db* diabetic mice compared with those from healthy controls. Genetic deletion of PPM1K or siRNA mediated silencing of PPM1K deficiency led to excessive BCKA and impaired GSIS in pancreatic islets and INS-1E β-cells, respectively.
5. Aberrant BCKA catabolism (induced by chronic treatment with a high concentration of BCKA or silencing of PPM1K) impaired glycolysis, leading to reduced production of ATP for induction of insulin secretion.
6. The inhibitory effects of BCKA on GSIS is glucose specific, because potassium chloride or methyl pyruvate (end-product of glycolysis)-stimulated insulin secretion was normal in MIN6 β-cells treated with BCKA.

Taken together, these data suggest that aberrant BCAA catabolic pathway results in excessive accumulation of BCKA in pancreatic β-cells, which in turn further exaggerates β-cell dysfunction by impairing glucose metabolism and subsequent GSIS, leading to T2D.

Additionally, my second project is to investigate how the adaptor protein APPL2 (a downstream regulator of adiponectin and insulin signaling) controls GSIS. Our data demonstrated that APPL2 interacts with RacGAP1 to antagonize the inhibitory effect of RacGAP1 on Rac1 activation, enhancing glucose-induced F-actin remodeling and GSIS in pancreatic β-cells.

# Acknowledgements

First of all, I would like to express my heart-felt gratitude to my supervisor, Dr. Kenneth Cheng. I learned a lot from his immense knowledge, valuable advices and ideas on my research project and thesis writing. His continuous support, guidance and patience have always kept me going ahead during my PhD study. Without his guidance, I would not have been able to accomplish much of my studies.

A great thank to my team mates, Miss Xi Chen, Mr. Kekao Long, Mr. Kalok Wu, Mr. Kai Wang and Miss Kaying Chan for their kind assistance and technical support in my daily study. Thank to Ms. Baile Wang for her great contribution in our collaborative project. I also want to thank the staffs in the University Research Facility in Life Science of The Hong Kong Polytechnic University for their help in the analyses of metabolomics, confocal microscopy and Seahorse.

Last but not least, a great appreciation to my family members for their love and support which encourage me to continue my research career.

# Publications arising from the thesis

1. Baile Wang*, Huige Lin*, Xiaomu Li, Wenqi Lu, Jae Bum Kim, Aimin Xu, Kenneth K. Y. Cheng; The adaptor protein APPL2 controls glucose-stimulated insulin secretion via F-actin remodeling in pancreatic β-cells; Proceedings of the National Academy of Sciences Nov 2020, 117 (45) 28307-28315; *Co-first author.

# Conference abstracts

1. **Huige Lin**, Kenneth KY Cheng. The role of branched-chain amino acids (BCAAs) metabolism in pancreatic beta cells functions. 14th International Symposium on Healthy Aging "Embrace the Golden Years. Hong Kong. 16-17 March 2019

2. ***Huige Lin**, *Baile Wang, Xiaomu Li, Wenqi Lu, Aimin Xu, Kenneth KY Cheng. APPL2 Deficiency Diminishes Glucose-Smulated Insulin Secreon in Pancreatic Beta Cells. American Diabetes Association's 80th Scientific Sessions Virtual Meeting. Chicago, USA, 12-16 June 2020.

# Table of Contents

# List of Figures

# List of Tables

# List of Abbreviations

| | |
|---|---|
| T2D | type 2 diabetes |
| T1D | type 1 diabetes |
| BMI | body mass index |
| BCAA | branched-chain amino acids |
| BCATm | branched-chain aminotransferase, mitochondrial |
| BCATc | branched-chain aminotransferase, cytosolic |
| BCKDH | branched-chain α keto-acid dehydrogenase complex |
| BCKDH-A | branched-chain α keto-acid dehydrogenase complex E1α |
| KIC | α-ketoisocaproate |
| KMV | α-keto-β-methyl valerate |
| KIV | α-ketoisovalerate |
| BCKA | branched-chain α keto-acid |
| TCA | tricarboxylic acid cycle. |
| PP2CM | protein phosphatase 2C family member |
| PPM1K | phosphatase 1K |
| BDK | branched-chain α-ketoacid dehydrogenase kinase |
| MUSD | maple syrup urine disease |
| mTORC | mammalian target of rapamycin complex |
| 3-HIB | 3-hydroxyisobutyrate |
| BT2 | 3,6-dichlorobenzo[b]thiophene-2-carboxylic acid |
| MPTP | mitochondrial membrane permeability transition pore |
| SNPs | single nucleotide polymorphisms |
| ACL | ATP-citrate lyase |
| GSIS | glucose-stimulated insulin secretion |
| CREB | cAMP response element-binding protein |
| KLF15 | Krüppel-like factors 15 |
| LARS1 | leucyl-tRNA synthetase 1 |
| ULK1 | Unc-51 like autophagy activating kinase 1 |

| | |
|---|---|
| PDH | pyruvate dehydrogenase |
| O-GlcNAc | O-linked-N-acetylglucosamine |
| *PYGL* | *glycogen phosphorylase* |
| HSCs | hematopoietic stem cells |
| LC-MS/MS | liquid chromatography tandem-mass spectrometry |
| HPLC | high performance liquid chromatography |
| m/z | mass-to-charge ratio |
| pBCKDH-A | phosphorylated BCKDH |
| ATP | Adenosine triphosphate |
| GTT | glucose tolerance test |
| ITT | Insulin tolerance test |
| KATP | ATP-sensitive K+ |
| ECAR | extracellular acidification rate |
| OCR | oxygen consumption rate |
| CE-MS | Capillary Electrophoresis–Mass Spectrometry |
| DHAP | dihydroxyacetone phosphate |
| α-KG | α-Ketoglutarate |
| BAR | Bin/Amphiphysin/Rvs |
| PH | pleckstrin homology |
| PTB | phosphotyrosine binding |
| APPL1 | Adaptor protein 1 |
| APPL2 | Adaptor protein 2 |
| SNARE | soluble N-ethylmaleimide-sensitive factor attachment protein receptor |
| RIP-APPL2 KO | β cell-specific APPL2 knockout |
| TBC1D1 | TBC1 Domain Family Member 1 |
| Rac1 | Ras-related C3 botulinum toxin substrate 1 |
| GTPase | a guanosine triphosphatase |
| Cdc42 | cell division cycle 42 |
| Q61L | constitutively active mutant of human Rac1 |

| | |
|---|---|
| RacGAP1 | Rac GTPase activating protein 1 |
| IP | immunoprecipitation |
| GEF | regulator guanine exchange factors |
| Rho-GDIs | Rho GDP-dissociation inhibitors |
| KGDH | α-ketoglutarate dehydrogenase |
| PFKM2 | phosphofructokinase |
| PDHA2 | pyruvate dehydrogenase E1 alpha subunit |
| AAV | adeno-associated virus |

# Chapter 1 Introduction

## 1.1 Pancreatic β cell dysfunction in type 2 diabetes (T2D)

### 1.1.1 The prevalence and risk of T2D

In recent decades, the prevalence of diabetes is rapidly expanding across the world, most markedly in middle-income countries, which imposes a heavy burden on the health-care system and individual economy (1). Diabetes is a chronic metabolic disorder with abnormal high blood glucose/sugar level, and over time leads to a large number of serious complications, such as kidney failure, heart attack, stroke, nerve damage and vision loss and so forth (2, 3), which increases the overall risk of premature death. According to the newest global diabetes report by the World Health Organization, in 2014, 8.5% of adults were living with diabetes. In 2016, diabetes directly accounted for 1.6 million deaths, becoming the seventh leading cause of mortality (1). In 2040, it is estimated a 10.4 % of raise in the prevalence of diabetes (4).

There are two main types of diabetes - type 1 and type 2, both of which cannot use and store glucose properly. Type 1 diabetes (T1D) happens when insufficient or no insulin (a hormone that regulates blood glucose) is produced by pancreas. This condition is also knowns as juvenile or childhood-onset diabetes since it usually happens in children and adolescents. In T1D, insulin-producing β-cells are destroyed by immune cells such as inflammatory T cells and macrophages. The exact causes of T1D remain unknown, but it is generally accepted that an interplay of genetic and environmental factors plays a critical role. No method has been found to prevent T1D and the patients require lifelong administration of insulin to keep normal blood glucose level for survival (1, 5).

Compared with T1D, the majority of type 2 diabetes (T2D) occurs in adults, although the incidence in young age tends to be increased recently (6). Based on the report made

by the Chinese Diabetes Society, it is estimated that more than 90 % of the population with diabetes are diagnosed with type 2 while less than 5 % are type 1 diabetes and other types (such as gestational diabetes) only account for 0.7% of the diabetic cases in China (7). T2D develops when the body becomes blunted to insulin signal (so-called insulin resistance) and/or the pancreatic β-cells cannot produce enough insulin to meet the need for glucose controlling (1). Similar to T1D, T2D is also a lifelong disease with hyperglycemia as a result of the interaction between genetic and environmental factors. It has been demonstrated the risk of T2D is positively and strongly related to age, body mass index (BMI), obesity and unhealthy diet. T2D can be effectively prevented and alleviated by multiple approaches, including loss of overweight, physical activity and a balanced diet, which is the most significant difference in the prevention between type 1 and type 2 diabetes (8).

### 1.1.2 Insulin regulates glucose homeostasis

The pancreatic islets are dense clusters of approximately 1000 cells which constitute 1–2% of the pancreas mass. They are endocrine unit of the pancreas that consist of four different types of hormone-producing cells that work collectively to maintain normoglycemia. Pancreatic β-cells, which are exclusively responsible for generating and releasing insulin, are the most prominent cell type contributing 60–70% to the human islet mass and 80-90% to the mouse islet. Pancreatic α-cells produce the hormone glucagon and only account for around 20% of each islet mass (9, 10). Systemic glucose homeostasis is tightly controlled by the secretion and actions of insulin and glucagon. In a fasted state with low blood glucose level, glucagon is secreted from α-cells to stimulate hepatic glucose production to raise blood glucose level. On the contrary, in a feeding state with elevated blood glucose, insulin is rapidly released from pancreatic β-cells into the circulation, and then targets to insulin receptors located on the cell surfaces of peripheral tissues, triggering multiple intracellular signal transductions to promote glucose uptake and inhibit glucose production, therefore blood glucose is decreased to normal level (Figure 1.1). In summary, intact insulin signaling in peripheral tissues and normal pancreatic β-cell function are essential to prevent hyperglycemia and diabetes.

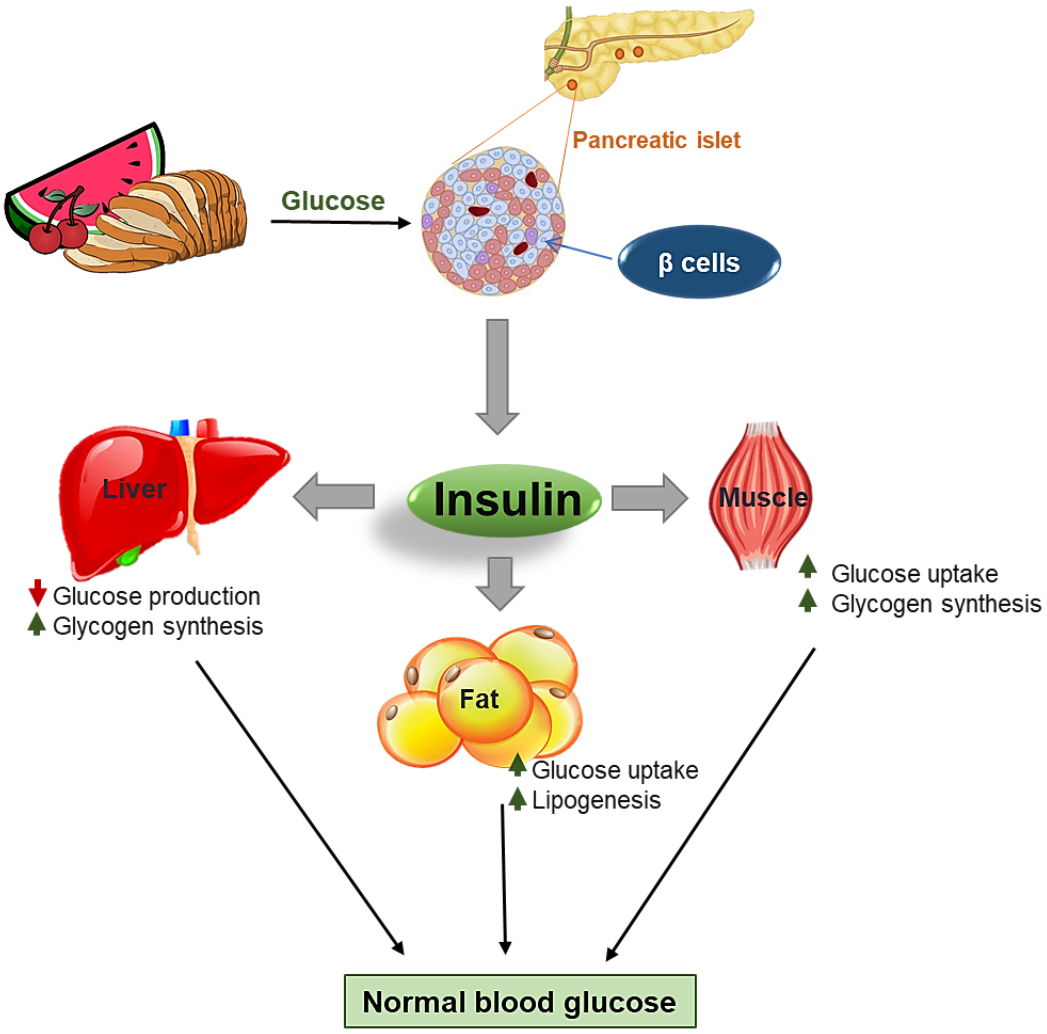


**Figure 1.1. Role of insulin in systemic glucose homeostasis.**

In response to carbohydrate uptake and elevated blood glucose, insulin is secreted from pancreatic β-cells into the bloodstream and then bind with insulin receptors on the cell surfaces, triggering intracellular signal pathway transductions to enhance glucose uptake and inhibit glucose production in the peripheral tissues, eventually lowering blood glucose to normal level.

### 1.1.3 Pathogenesis of pancreatic β-cell dysfunction

Pancreatic β-cell dysfunction is the key determinant for the progress of prolonged hyperglycemia and T2D. In pre-diabetes, typically in obese individuals, blood glucose can be maintained within the physiological range even when insulin resistance has been established. This is because pancreatic β-cells can produce and secrete more insulin to compensate for insulin resistance. However, severe T2D occurs when pancreatic β-cell function compromises due to long-term demand of insulin production and secretion (11). The major characteristics of pancreatic β-cell dysfunction is featured by reduction of β-cell mass and defective insulin secretion, which are irreversible and so far there is no effective clinical treatment.

Several pathogenic mechanisms explain the progressive pancreatic β-cell dysfunction in T2D. Under excess nutrient states such as chronic elevation in blood glucose and lipid in obesity, β-cells initially undergo compensatory insulin hypersecretion and increase of β-cell mass by adaptive cell proliferation (12, 13). However, at the later stage, synthesis and secretion of massive insulin exert a sustained demand on the Endoplasmic Reticulum (ER). Misfolded or unfolded proteins are increasingly accumulated in the ER lumen, leading to activation of ER stress and apoptosis (14, 15). In addition, β-cell mass reduces due to dedifferentiation and cell death by apoptosis and autophagy (16-18). Furthermore, pro-inflammatory cytokine and elevated fatty acid and glucose can induce oxidative stress and inflammation, which may alter the expression of genes associated with insulin secretion and cell survival (19, 20). Despite the above findings, pathogenesis underlying pancreatic β cell dysfunction still remains largely elusive.

## 1.2 Branched-chain amino acids (BCAA) metabolism

### 1.2.1 Basic information of BCAA

Branched-chain amino acids (BCAA, including leucine, isoleucine and valine) share a common structure of a central carbon atom bound to branched-chain consisting of three or more carbon atoms (21). They are the most abundant essential amino acids accounting for 35-40% of the nine essential amino acids in muscle proteins and more than 20% of the total amino acids in body proteins (22). BCAA does not only serve as nutrient substrates but also as critical regulators in intestinal functions, immunity and metabolic health. Supplementation with BCAA improved intestinal development, nutrient transportion and resistance to diseases in humans and animals (23, 24). BCAA also supports immune function as evidenced by the impairment in innate immune reaction and shortage of lymphocytes and white blood cells when BCAA was deficient (25).

Besides, studies showed that BCAA has a positive effect on the regulation of systematic glucose and lipid metabolism. Dietary supplementation of BCAA improved glucose homeostasis in humans (26, 27). Oral administration of isoleucine enhanced glucose uptake in skeletal muscle and significantly reduced plasma glucose via activation of AMPK alpha2 activity in rats (28). BCAA deficient diet suppressed lipogenesis in the liver and stimulated fat loss. Such effects were associated with increased energy expenditure in the brown adipose tissue and increased lipolysis in the white adipose tissue (29). In spite of the aforementioned beneficial impacts of BCAA on metabolic health, an adverse role of BCAA has been suggested by mounting evidences, which will be discussed in the following section.

### 1.2.2 Elevated circulating BCAA as a predictor for risk of future T2D

Emerging evidences indicate a strong association between circulating BCAA and the severity of insulin resistance, obesity or T2D in human (30-32). In 1969, it was the first time to identify the elevation of circulating BCAA in obese human with insulin resistance (33). During the past decades, multiple prospective cohort studies were conducted separately and independently by different research groups to follow up populations in different countries and regions, including America, Germany, China, Europe and Asia for 5-19 years. These long-term follow-up examinations revealed that among those developing diabetes, circulating concentrations of BCAA were elevated prior to the onset of diabetes (34-38). Similarly, in progressive T2D mouse models under genetic background of β cell-specific prohibitin-2 knockout or leptin receptor–mutant (*db/db*), increased plasma level of BCAA was found to precede the onset of severe diabetes(39). Therefore, increased circulating level of BCAA is recognized as a predictor and robust biomarker for future risk of T2D (40, 41).

The adverse role of BCAA in glucose homeostasis was reinforced by numerous dietary studies of BCAA supplementation or BCAA deprivation in animals and human. Dudley W.L *et al*. found that BCAA-restricted diets not only improved glucose tolerance and lowered fasting blood glucose concentration in rat (42), but also prevented fat mass gain and restored insulin sensitivity in obese mice (43). In the high fat diet-induced obese rat, Newgard *et al*. demonstrated that low BCAA diet alleviated insulin resistance in skeletal muscle (44). In *db/db* diabetic mice, dietary BCAA restriction also improved glucose metabolism and this effect was related to GCN2/mTOR/S6K1 and AMPK pathways (45, 46). By contrast, the BCAA-rich diet exerted an adverse effect on glucose homeostasis by impairling insulin sensitivity in obese mice (32). More

investigations are required to elucidate whether and how elevated circulating BCAA acts as a causative factor for future diabetes.

### 1.2.3 BCAA metabolic pathway

Intracellular BCAA concentration is regulated by dietary BCAA intake, protein degradation and utilization for protein synthesis and consumption for mitochondrial oxidation. The key steps of BCAA catabolic pathway are shown in Figure 1.2 and Figure 1.3. Briefly, the first step is the reversible transamination of BCAA mediated by the branched-chain aminotransferase (BCATm) to respective branched-chain α keto-acid (BCKA; leucine to α-ketoisocaproate [α-KIC], isoleucine to α-keto-β-methyl valerate [α-KMV] and valine to α-ketoisovalerate [α-KIV]), in extrahepatic tissues. The second step (also the rate-limiting step) is the oxidative decarboxylation of BCKA, which is mediated by the multienzyme branched-chain α keto-acid dehydrogenase (BCKDH) complex (47). The products of BCKDH complex are further metabolized by multiple mitochondrial-matrix enzymes to produce numerous Co-A derivates, such as isovaleryl-CoA, propionyl-CoA and acetyl-CoA (47). These CoA-derivates further bind with carnitines to form acyl-carnitines (short and medium-chain fatty acids) or undergo further oxidation via the TCA cycle.

There are two types of mammalian BCAT, cytosolic isoform (BCATc) encoded by gene BCAT1 and mitochondrial isoform (BCATm) encoded by gene BCAT2. BCATc exclusively presents in nerve system while BCATm ubiquitously expresses in almost all tissues (48). Oxidative decarboxylation of BCKA by BCKDH complex is the key step of BCAA catabolism. The BCKDH complex consists of three subunits: a heterodimeric decarboxylase (E1α and E1β), a dihydrolipoyl transacylase (E2), and a dihydrolipoyl dehydrogenase (E3). Activity of BCKDH complex is inhibited by covalent phosphorylation of E1α subunits (also known as BCKDH-A), which is positively regulated by the protein phosphatase 1K (PPM1K or PP2CM) and is

negatively regulated by the branched-chain α-ketoacid dehydrogenase kinase (BDK or BCKDK) via dephosphorylation and phosphorylation of BCKDH-A at serine 293, respectively (49, 50).

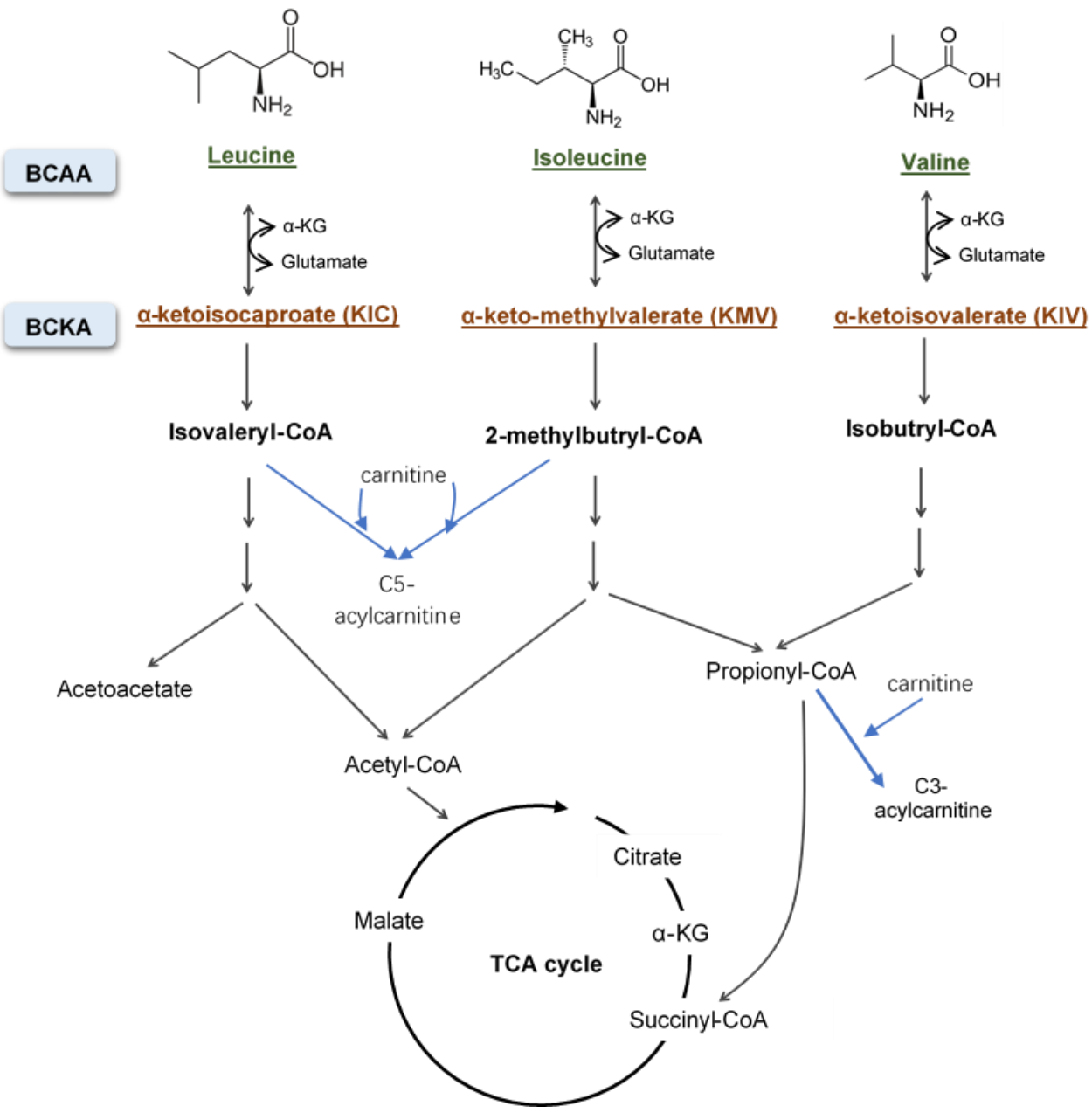


**Figure 1.2. Pathway of BCAA metabolism.**

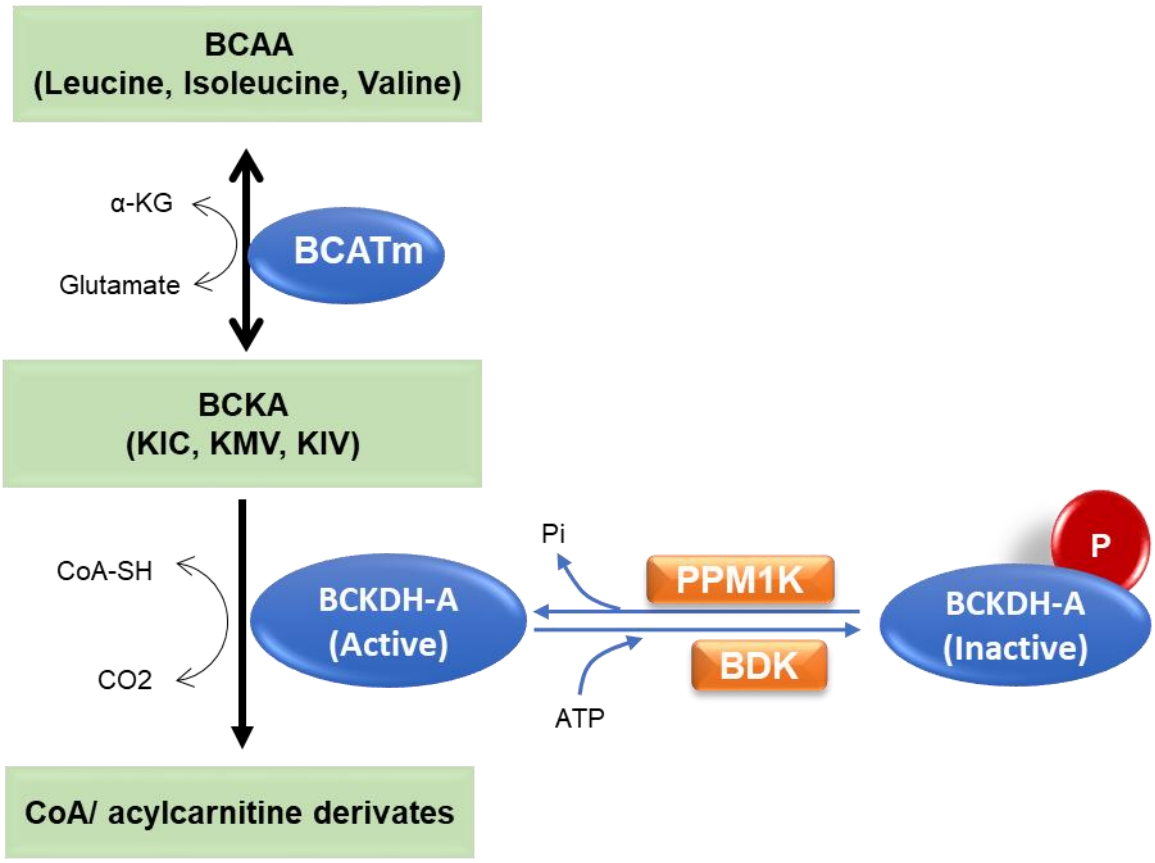


**Figure 1.3. Key enzymes and proteins for BCAA metabolism.**

### 1.2.4 Multiple tissues involve in BCAA homeostasis

Systematic BCAA homeostasis is maintained by the interplay between multiple tissues as illustrated in Figure 1.4. Skeletal muscle, adipose tissue and liver are the three main organs responsible for BCAA metabolism (51). Although BCATm is abundantly expressed in the skeletal muscle and moderately in fat, it is almost absent in the liver. High expression and activity of BCKDH complex are found in the liver whereas skeletal muscle has extremely low expression of BCKDH (51-53). Due to the different BCAA catabolic capacity among tissues, a large amount of dietary BCAA is first transported into muscle cells for transamination by BCATm (54, 55). The product BCKA is then released into the circulation, followed by transportation to adipose tissue and liver for oxidative decarboxylation and catabolism by the BCKDH complex.

Loss of BCAA metabolism in one tissue can be largely compensated by other tissues with intact BCAA metabolic capacity. For instance, transplantation of normal adipose tissue into mice with genetic defects in BCAA metabolism, or transplantation of normal liver into human with maple syrup urine disease (MSUD, a metabolic disorder characterized by BCKDH deficiency and abnormally high blood BCKA) resulted in a reduction of plasma BCAA level (56, 57). This was mostly because the reserved BCAA catabolic capacity in the transplanted tissues was activated in response to the elevated circulating BCAA and BCKA in the recipients. Therefore, physiologically, the body should be well tolerated with excessive dietary BCAA intake due to the compensatory mechanism in other peripheral tissues with intact BCAA catabolic ability.

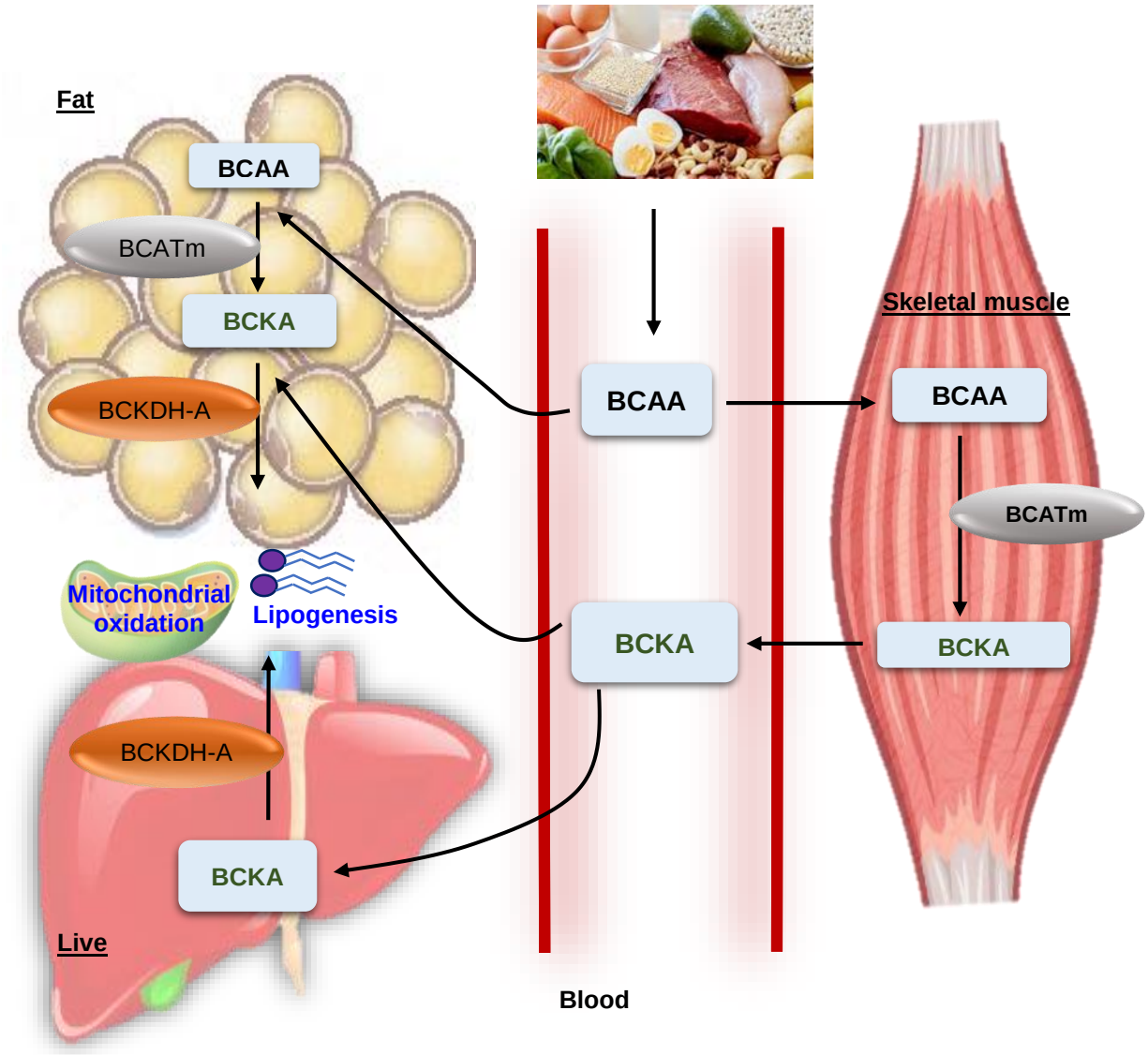


**Figure 1.4. Interorgan BCAA metabolism.**

After food intake, dietary BCAA is transported into the skeletal muscle for transamination by BCATm. The product BCKA is then released into the circulation, followed by transportation into adipose tissue and liver for oxidative decarboxylation by the BCKDH complex. The end-products of BCAA catabolism eventually enter mitochondrial oxidation or lipogenesis.

### 1.2.5 Defective BCAA metabolism in obesity and T2D

Obesity is a key factor for development of insulin resistance and T2D (58). One of the most consistent and robust changes in obesity is a marked reduction in genes related with BCAA metabolism in adipose tissue (41, 59-62). In two obese rodent models (Zucker rats and *ob/ob* mice), Pengxiang She *et al*. showed that the expression and activity of BCATm and BCKDH-A were reduced in adipose tissues and liver but were not changed in skeletal muscles (61). In human and *ob/ob* obese mice, Haipeng Sun *et al.* identified a negative association between BCAA catabolic gene expression and insulin resistance. Besides, obesity related changes of BCAA catabolism differed among tissues. In adipose tissue and liver, mRNA expressions of almost all BCAA catabolic gene were decreased, accompanied by an accumulation of BCKA oxidative product. In skeletal muscle, although no alteration was found in expression of BCAA catabolic gene expression, BCKA was accumulated. Another major difference was that BCAA was increased in fat but decreased in liver under obese state (63).

Michael D.Neinast *et al.* performed a quantitative isotope tracing analysis of whole-body BCAA metabolic fate in *db/db* diabetic mice (51). They found that BCAA oxidation dramatically shifted from white adipose tissue and liver toward skeletal muscle under diabetes (51), although skeletal muscle has a low capacity of BCKA oxidation(51-53). In streptozotocin-induced T2D mice, diminished activity of BCKDH-A was observed in fat, liver and skeletal muscle, which was most likely due to an aberrant expression of PPM1K and BDK (the positive and negative regulator of BCKDH-A, respectively) (64). Genomic studies identified that various mutations in *BCKDH* and *PPM1K genes* were closely associated with the risk of obesity and type 2 diabetes (65-67). These data suggest that systematic BCAA metabolism is altered in

obesity and diabetes, and the changes are different among tissues, indicating that BCAA metabolism might exert distinct functions in different tissues.

### 1.2.6 Cytotoxic effect of BCAA catabolic intermediates in obesity and T2D

Recent studies attempted to define a causal link between defective BCAA metabolism and T2D. 1) The first mechanism suggests that BCAA induces a sustained activation of the nutrient-sensing complex, rapamycin complex 1 (mTORC1), leading to uncoupling of insulin signalling in skeletal muscle of high fat diet-induced obese rodents (32, 44). 2) Similarly, treatment of muscle cells with high BCKA not only caused activation of mTORC1, but also reduced glucose uptake and enhanced lipid accumulation (68). 3) The second potential mechanism indicates that it is BCAA catabolic intermediates but not BCAA itself play a role. For instance, 3-hydroxyisobutyrate (3-HIB), a catabolic intermediate of the valine catabolism, can be released from muscle cells and increase fatty acid uptake in endothelial, leading to lipotoxicity in skeletal muscle and subsequent insulin resistance (69-72). Circulating 3-HIB is elevated in human with hyperglycemia and T2D, positively correlating with insulin resistance. Moreover, 3-HIB modulated metabolism during differentiation of white and brown adipocytes (73). 4) C3 and C5 acylcarnitine, the byproducts of BCAA catabolism, are found to be accumulated in the blood and muscle of human with insulin resistance, obesity and T2D. These short-chain acyl-carnitines are considered as incompletely oxidized lipid species with glucolipotoxicity and can contribute to insulin resistance (74-77).

In addition, glucose intolerance and insulin resistance could be alleviated in Zucker fatty rat, *ob/ob* and diet-induced obese mice by promoting BCAA catabolism using a pharmacological activator 3,6-dichlorobenzo[b]thiophene-2-carboxylic acid (BT2) (63, 78). Previous study identified that BT2 activates the activity of BCKDH-A by binding to BDK, leading to dissociation of BDK from the BCKDH complex (79).

Surprisingly, deletion of the BCATm (the first enzyme responsible for reversible BCAA transamination) increased plasma BCAA and prevented BCKA accumulation the peripheral tissues, accompanied with improved glucose homeostasis, insulin sensitivity and lipid profiles in mice fed with standard chow (80). In addition, a recent study showed that defective BCAA metabolism caused by gene deletion of *PPM1K* improved glucose homeostasis and insulin sensitivity in lean and healthy mice, but its effect on glucose homeostasis under obese condition was not explored (81). Of note, an early study by Newgard *et al*. showed that BCAA only triggered insulin resistance and hyperglycemia rat under high-fat diet feeding but not under standard chow feeding (32). Taken together, current findings support a notion that elevated BCAA catabolic intermediates are detrimental to metabolic health, in particular in control of glucose homeostasis, under obese and diabetic conditions.

### 1.2.7 PPM1K as a T2D susceptibility gene in human islets

Protein phosphatase 1K (PPM1K), also known as protein phosphatase 2C family member (PP2CM), was first discovered by Yibin Wang *et al*. in 2007 (82). PPM1K is highly conserved among vertebrates with a serine/threonine phosphatase domain and exclusively targets to mitochondria matrix. It was found to abundantly express in brain and heart. It has been reported that PPM1K plays a critical role in cell death and cell survival via regulation of mitochondrial membrane permeability transition pore (MPTP) opening (82, 83). The protective effect of PPM1K on cell viability was believed to relate with its regulation in oxidative stress, lipid metabolism, cell death and activation of stress kinases JNK and p38 (49, 82-84).

In 2009, PPM1K was identified as the BCKDH-A phosphatase. PPM1K activates BCKDH-A by inducing its dephosphorylation at serine 293 in the presence of substrate BCKA (49). Mutations in gene of *PPM1K* can lead to elevated plasma levels of BCKA and hence MSUD(84). Global gene ablation of *PPM1K* resulted in an accumulation of BCAA catabolic intermediates in the circulation, as well as an accumulation of BCKA in the liver, skeletal muscle and white adipose tissue (81). A large-scale human genetic and metabolomic study revealed that single nucleotide polymorphisms (SNPs) in the *PPM1K* gene were strong signals linked with the higher incidence of T2D (85). Overexpression of PPM1K could reduce hepatic steatosis and alleviate glucose intolerance in Zucker fatty rats by decreasing phosphorylation of adenosine triphosphate (ATP)-citrate lyase (ACL) and *de novo* lipogenesis in the liver (78). Therefore, PPM1K has been recognized as a susceptibility gene that affects risk of T2D (62-64), but our understanding of undelaying mechanism is very limited.

### 1.2.8 Association between BCAA metabolism and pancreatic β-cell function

Although the relationship between BCAA and insulin resistance has been well established, it is uncertain whether and how BCAA metabolism involves in the regulation of pancreatic β-cell function in health and disease conditions. A 12-year follow-up human study further revealed that elevated circulating BCAA was associated with future β-cell dysfunction (measured by functional score HOMA-β) in humans (34). Similarly, another cross-sectional and 7.4-year prospective study also demonstrated the association of BCAA with decreased insulin secretion and elevated blood glucose in over five thousand Finnish Men (86). Besides, in β-cell-specific prohibitin-2 knockout mice and *db/db* mice which develop progressive β-cell failure, plasma BCAA was increased with a reduction of β-cell mass at the early stage of prediabetes before the onset of severe diabetes (39). These findings indicate that BCAA metabolism exert a crucial effect on regulating β-cell function during the onset and progress of T2D.

Studies exploring the effect of BCAAs on β-cell function are relatively limited. Some of them even seem conflicting. Both *in vitro* and *ex vivo* studies showed that short-term treatment with leucine or its direct metabolite KIC induced acute insulin secretion in rodent pancreatic islets (87-89). By contrast, chronic exposure to leucine induced pancreatic β-cell dysfunction by impairing glucose-stimulated insulin secretion (GSIS) in both mouse islets and insulinoma INS-1E cells (90). In human, global gene expression profiles revealed that pancreatic islets collected from over 60 hyperglycemic donors have significantly decreased *PPM1K* mRNA expression when compared with those from normoglycemic donors (66). In mice, disruption of leucine metabolism by genetic deletion of *SIRT4* triggered hyperinsulinemia and subsequent glucose intolerance and abolished GSIS in aged mice (91). Investigations regarding the relation

between BCAA metabolism and pancreatic β cell function are listed in Table 1.1.

A previous study reported that normal rat islet was lack of BCATm but exhibited high expression of BCKDH-A, indicating a potential capacity of β-cells to metabolize BCKA rather than BCAA (92). Further investigation focusing on BCAA and its catabolism is warranted, as little is known on their impact on insulin secretion, apoptosis and β-cell survival in obesity and diabetes.

Table 1.1. Summary of the Effects of BCAA Metabolism on Pancreatic β-Cells Function

| Experimental Model and Subjects | Treatment | Effects on β-cell | Reference |
|---|---|---|---|
| Dog | Injection with 1 mM leucine for 30min | ↑ Insulin secretion | K Sreekumaran Nair *et al.* 2005 |
| Isolated rat pancreas | Perfusion with 5 mM KIC for 40min | ↑ Biphasic insulin secretion that similar with GSIS | JOHN C. HUTTON *et al.* 1980 |
| Islets from obese mice | Perfusion with 10 mM leucine or KIC for 40min | ↑ Insulin secretion | U Panten, J Christians *et al.* 1974 |
| RINm5F cells | Incubation with 0.4- 10 mM leucine for 30min | ↑ signal for βcell growth | Guang Xu *et al.*2001 |
| Isolated rat islets | Incubation with 10mM leucine and glutamine for 30min | ↑ Insulin secretion | Yi-Jia Liu et al. 2003 |
| Isolated rat islets | 10mM leucine for 2 days | ↑ GSIS and ATP production | Jichun Yang *et al.*2006 |
| Isolated rat islets | 10mM leucine for 1 day and 1 week | 1-week treatment enhanced GSIS and ATP production | Jichun Yang *et al.*2004 |
| Isolated rat islets | Culture with 0, 5 or 20 mM glucose for 1 day, followed by stimulation with 10 mM leucine or 10 mM KIC for 20 min | High glucose abolished leucine but not KIC induced insulin secretion | Zhiyong Gao *et al.* 2003 |
| Isolated rat islets | Perfusion with 2 mM glutamine and different concentration of glucose prior to stimulation with 10 mM leucine or KIC for 40 min | Glutamine and low glucose augmented leucine induced insulin secretion while high glucose suppressed it. | Changhong Li et al. 2003 |
| Isolated mice islets | Mice fed with control or low BCAA diets for 11 weeks | ↓GSIS; ↓GTT; ↑Ca2+ oscillation | LuigiFontana *et al.*2016 |
| Pancreatic buds from rat embryos | Incubation with 2% leucine for 7 days | ↓β cell differentiation | Latif Rachdi *et al.* 2012 |
| mouse islet and INS-1E cells | Incubation with 1or 10 mM leucine for 72 hours | ↓GSIS; ↑cholesterol | Zhenping Liu *et al.* 2012 |
| INS-1 cells | Knockdown of PPM1K by siRNA | ↓GSIS | Jalal Taneera *et al.*2012 |

Symbols: ↑ Increase; ↓ Decrease

## 1.3 Glucose-stimulated insulin secretion (GSIS)

### 1.3.1 First- and second phase of glucose-stimulated insulin secretion (GSIS)

Insulin secretion in pancreatic β-cells is collectively governed by nutrient signals, hormones and the nervous system. Among insulin secretagogues, glucose is the major one. Glucose-stimulated insulin secretion (GSIS) is a complicated and highly dynamic process involving aerobic glucose metabolism, calcium influx, membrane depolarization and F-actin remodeling (93). After food intake, pancreatic β-cells sense the elevation of plasma glucose level and glucose is transported into β cells via glucose transporter 2 in human and glucose transporter 1 in the rodent. Upon entering the cells, glucose undergoes breakdown by glycolysis to produce pyruvate, which is further catabolized via the mitochondrial TCA cycle and drives oxidative phosphorylation pathway to produce a large amount of ATP. The increase of ATP/ADP ratio induces closure of the ATP-sensitive K+ (KATP) channel, leading to membrane depolarization and Ca2+ influx, which in turn triggers first-phase insulin secretion (93). This rapid insulin secretory reaction lasts only for a few minutes, followed by a slow and sustained second phase GSIS. In brief, coupling factors such as Ca2+, NADPH, NADH and GTP trigger and amplify second phase GSIS by inducing F-actin remodeling (94). The depolymerization of cortical actin network allows movement and translocation of insulin granules from cytosol storage pools to the plasma membrane for exocytosis (95, 96). Both first- and second-phase GSIS of β cells are disrupted in T2D (93), yet the underlying mechanisms still remain elusive.

### 1.3.2 Interplay between glucose and BCAA metabolism

BCAA catabolism fuels multiple intracellular metabolic processes including glucose metabolism, synthesis of fatty acid and amino acids (97, 98). Several studies suggested a regulatory circuit between glucose and BCAA metabolism. Dan Shao *et al*. showed that high concentration of glucose repressed BCAA catabolism in cardiomyocytes by inhibition of cAMP response element-binding protein (CREB)-stimulated Krüppel-like factors 15 (KLF15) transcription, leading to downregulated mRNA expression of enzymes responsible for BCAA degradation (99). Ina Yoon *et al.* revealed a novel mechanism that glucose regulated protein synthesis via controlling leucine usage. Upon glucose starvation, leucyl-tRNA synthetase 1 (LARS1) was phosphorylated by Unc-51 like autophagy activating kinase 1 (ULK1). Thus its binding residues with leucine were blocked, which shifted leucine utilization from anabolic process to catabolism for supporting cell survival (100).

On the other hand, glucose metabolism is under control of BCAA catabolism. Chronic accumulation of BCAA caused by *PPM1K* gene deletion suppressed glucose uptake and inactivated pyruvate dehydrogenase (PDH) in heart. BCAA treatment also directly inhibited PDH activity in heart lysates. The modulation of PDH activity by BCAA and PPM1K has involved with the protein O-linked-N-acetylglucosamine (O-GlcNAc) modification (101), which has been demonstrated to control the enzyme activities of glycolysis (102-104). In the beef heart, the activity of 2-ketoglutarate dehydrogenase (TCA cycle enzyme) was suppressed by treatment with individual BCKA (KIC, KMV and KIV) (105).

In the liver of *PPM1K* deficient mice, glycogenesis was altered because mRNA expression of *glycogen phosphorylase (PYGL)* and glycogen catabolites were both

elevated, which could replenish glucose and facilitate glycolysis. The upstream of glycolytic metabolites (glucose, glucose 6-phosphate and fructose 6-phosphate) were increased whereas downstream intermediates (fructose-1,6-biphosphate, 3-phosphoglycerate) and TCA metabolites were lower in the *PPM1K* deficient liver. The authors speculated that the alterations were likely because the upstream glycolytic metabolites entered conjoint metabolic pathways such as the pentose phosphate pathway and the polyol pathway (81). They also showed a directly inhibitory impact of BCKA on mRNA expression of *PYGL* in HepG2 hepatocytes as well as on the respiratory Complex II in the isolated liver mitochondria. These data demonstrated that BCAA catabolic defect exerted multiple effects on hepatic glucose metabolism in lean mice (81). In high-fat diet-induced obese mice, feeding with BCAA significantly enhanced fasting blood glucose and diminished pyruvate tolerance. Besides, expression of *Foxo1, PCK1* and *G6PC* (proteins for gluconeogenesis) was increased in the liver, suggesting that BCAA feeding enhanced hepatic gluconeogenesis. Further investigation using primary hepatocytes indicated that BCAA and BCKA enhanced hepatic glucose production by inhibition of mTOR-Akt2 signaling (106).

In hematopoietic stem cells (HSCs), *PPM1K* deletion impaired glycolytic flux and ATP production via the CDC20-mediated ubiquitination of MEIS1 and p21(107). Despite the above findings of the effect of BCAA metabolic pathway in peripheral tissues, it is unknown whether there is an interplay between BCAA and glucose metabolism in pancreatic β-cells.

## 1.4 General aims of the study

Numerous studies have shown that elevated circulating BCAA and its catabolic intermediates as robust predictors for the future risk of T2D in humans (30-33). Insulin resistance in peripheral tissues and pancreatic β-cell failure are core factors for the development and progression of T2D. Several underlying pathogenetic pathways have been proposed to define the association between BCAA metabolism and insulin resistance in the liver, skeletal muscle and adipose tissue (32, 69-72, 74-78, 82, 105, 108, 109). In brief, the intracellular accumulation of BCAA catabolic intermediates exert an adverse effect on signaling pathways associated with insulin resistance. Alternatively, proteins involved in BCAA metabolism such as PPM1K and BDK play a role in the regulation of hepatic lipogenesis. Noted that the alterations of BCAA metabolic flux (41, 51-55, 59-63) and the effect of defective BCAA metabolism differ among the liver, skeletal muscle and adipose tissue (73, 81), suggesting BCAA metabolism might play different roles among tissues in healthy and diabetic conditions.

On the other hand, progressive pancreatic β-cell failure is a hallmark of T2D and overt hyperglycemia only happens when pancreatic β-cells become dysfunctional. Several long-term follow-up examinations in humans have pointed out that the elevation of circulating BCAA intermediates occurred before the onset of severe T2D. This elevation was associated with pancreatic β-cell dysfunction as measured by the β-cell functional score HOMA-β (34, 39, 86). However, it still remains almost unknown whether and how BCAA catabolism regulates pancreatic β-cells function, especially in T2D.

To address the above question, this study aims to investigate: (1) Does pancreatic β-cells have the capacity for BCAA metabolism? Is this ability altered in T2D? (2) What

is the effect of BCAA catabolism on pancreatic β-cell function? (3) What is the underlying mechanism for BCAA catabolism in the regulation of pancreatic β-cell function?

Apart from the role of BCAA metabolism in pancreatic beta function, my second project is to investigate how the adaptor protein APPL2 (a downstream regulator of adiponectin and insulin signaling) controls GSIS via F-actin remodeling in Chapter 6.

# Chapter 2  Materials and Methods

## 2.1. Materials

### 2.1.1 Chemicals and materials for Mass Spectrometry

| Chemicals or materials | Company | Catalog NO. |
|---|---|---|
| Methanol (HPLC grade) | DUKSAN | 62 |
| Acetonitrile (ACN, LCMS grade) | DUKSAN | 549 |
| Formic acid | Sigma-Aldrich | 695076 |
| Ammonium formate | Sigma-Aldrich | 09735 |
| o-phenylenediamine (OPD) | Sigma-Aldrich | P9029 |
| Hydrochloric acid (HCl, 37%) | Analar Normapur | 20252.420 |
| Ethyl acetate | Sigma-Aldrich | 270989 |
| Sodium sulfate (Na2SO4) | Sigma-Aldrich | 239313 |
| Ammonium acetate | Sigma-Aldrich | A1542 |
| L-Leucine | Sigma-Aldrich | L8000 |
| L-Isoleucine | Sigma-Aldrich | V0500 |
| L-Valine | Sigma-Aldrich | I2752 |
| Sodium α-keto isocaproate (KIC) | Cayman Chemical | 21052 |
| Sodium α-keto β-methylvalerate (KMV) | Sigma-Aldrich | K7125 |
| Sodium α-keto isovalerate (KIV) | Sigma-Aldrich | 198994 |
| C2-acylcarnitine | Sigma-Aldrich | A6706 |
| C3-acylcarnitine | Sigma-Aldrich | 42602 |
| C5-acylcarnitine | Sigma-Aldrich | 51371 |
| $^{13}C_6$ L-leucine | Thermo Fisher Scientific | 88436 |
| $^{13}C_6$-D-Glucose | Sigma-Aldrich | 389374 |
| L-Valine ($D_8$, 98%) | Cambridge Isotope Laboratories | DLM-311-PK |
| KIV ($D_7$, 98%) | Cambridge Isotope Laboratories | DLM-4646-PK |
| D-Mannitol | Sigma-Aldrich | M4125 |
| Chloroform | Sigma-Aldrich | 650498 |
| Methionine sulfone（HPLC grade） | Sigma-Aldrich | M0876 |

| | | |
|---|---|---|
| D-Campher-10-sulfonic acid sodium salt (HPLC grade) | Sigma-Aldrich | C2107 |
| Ultra-free MC centrifugal filter devices | Millipore | UFC3LCC00 |
| Glass insert,150 µL | Waters | WAT094171 |
| HPLC glass brown vial | Waters | 186007200C |
| ACQUITY BEH C18 1.7µM VANGUARD Pre-Col | Waters | 186003975 |
| ACQUITY UPLC BEH C18 1.7µm 2.1x50mm Col | Waters | 186002350 |
| ACQUITY BEH Amide 1.7µm VANGUARD Col | Waters | 186004799 |
| ACQUITY UPLC BEH Amide 1.7µm 2.1x100mm | Waters | 186004801 |

### 2.1.2 Reagents and materials for cell culture and cell studies

All reagents and materials used for cell culture and cell studies are sterilized.

| **Reagents or materials** | **Company** | **Catalog NO.** |
|---|---|---|
| INS-1E β cell line | AddexBio Technologies | C0018009 |
| MIN6 β cell line | AddexBio Technologies | C0018008 |
| Fetal bovine serum (FBS) | Thermo Fisher Scientific | 10270 |
| Penicillin- streptomycin (PS) | Thermo Fisher Scientific | 15140122 |
| Dulbecco's Modified Eagle Medium (DMEM) | Gibco™ | 12800082 |
| RPMI 1640 medium | Gibco™ | 31800105 |
| Beta-mercaptoethanol | Bio-Rad Laboratories, Inc. | 1610710 |
| Trypsin | Gibco™ | 25200056 |
| 3,6-dichlorobenzo[b]thiophene-2-carboxylic acid (BT2) | Santa Cruz Biotechnology | sc-276559 |

| | | |
|---|---|---|
| Opti-MEM I reduced serum medium (Opti-MEM) | Gibco™ | 31985070 |
| Lipofectamine™ RNAi MAX transfection | Invitrogen™ | 13778150 |
| siRNA oligo | Genepharma Co. Ltd | A01004 |
| MILLEX-GP 33MM PES .22UM STERILE | MERCK MILLIPORE | SLGP033RS |
| Leucine-free RPMI 1640 medium | Thermo Fisher Scientific | 88426 |
| Dialyzed BSA | Thermo Fisher Scientific | A3382001 |
| Oligomycin | Cayman Chemical | 11341 |
| 2-deoxy-D-Glucose (2-DG) | Cayman Chemical | 14325 |
| XF DMEM base medium, pH 7.4 | Agilent Technologies, Inc | 103575-100 |
| XF RPMI medium, pH 7.4 | Agilent Technologies, Inc | 103576-100 |
| Seahorse XF calibrant solution | Agilent Technologies, Inc | 100840-000 |
| XFe24 sensor cartridge | Agilent Technologies, Inc | 102340-100 |
| XF24 V7 PS tissue culture microplate | Agilent Technologies, Inc | 100777-004 |
| Black 96-well TC plate with clear bottom | Corning | 3603 |

### 2.1.3 Reagents and materials for pancreatic islet isolation and insulin secretion assay

| **Reagents or materials** | **Company** | **Catalog NO.** |
|---|---|---|
| Collagenase P | Roche | 11213865001 |
| Hanks' Balanced salt solution (HBSS) | Gibco™ | 14025076 |
| Bovine serum albumin (BSA) | Sigma-Aldrich | A7906 |
| Fine test sieves, pore size 500 μm | Sigma-Aldrich | Z289922 |
| 70-μm cell strainer | Falco | 352350 |
| 26G Sterile vein set for single use | Zhejiang Kindly Medical Devices Co., Ltd | 0.45 X 15 I RWLB |
| 3cc Syringe | Terumo | SS-03L |
| Petri dish, 100x15mm | SPL Life Sciences | SPL #: 10100 |

| | | |
|---|---|---|
| Bovine serum albumin, fatty acid free, low endotoxin (BSA) | Sigma-Aldrich | A8806 |
| Glucose | Fluka | 49138 |
| Potassium chloride | Sigma-Aldrich | P9333 |
| Methyl pyruvate | Sigma-Aldrich | 371173 |
| L-Arginine | Sigma-Aldrich | A5006 |
| Cytochalasin B | Sigma-Aldrich | C6762 |
| Ketamine, 10% | Alfasan International B.V. | 0904088-05 |
| Xylazine, 2% | Alfasan International B.V. | 1205117-05 |

### 2.1.4 Reagents and materials for western blot, histology, immunohistochemical and immunofluorescent staining

| Reagent or material | Company | Catalog NO. |
|---|---|---|
| PageRuler™ prestained protein ladder | Thermo Fisher Scientific | 26617 |
| FluoroTrans PVDF transfer membrane | Pall Life Sciences | BSP0161 |
| Medical X-Ray film | Fuji Film | RX1318 |
| ECL western blot detection kit | Bio-Rad | 1705060 |
| Acryl/Bis 30% solution | Sangon Biotech Co., Ltd. | B546018-0500 |
| Ammonium persulfate | Sigma-Aldrich | A3678 |
| TEMED | Thermo Fisher Scientific | 17919 |
| ProLong™ gold antifade mountant with 40, 6-diamidino-2-phenylindole (DAPI) | Thermo Fisher Scientific | P36941 |
| ProLong™ glass antifade mountant with NucBlue™ Stain | Thermo Fisher Scientific | P36985 |
| DPX Mountant for histology | Sigma-Aldrich | 06522 |
| 10% neutral buffered formalin | Thermo Fisher Scientific | 6764240 |
| Xylene | Sigma-Aldrich | 185566 |
| Absolute ethanol | Sigma-Aldrich | 459844 |

| | | |
|---|---|---|
| Hematoxyline | Sigma-Aldrich | HHS32 |
| Eosin | Sigma-Aldrich | 318906 |
| Histological paraffin | Thermo Fisher Scientific | 8331 |
| Sodium citrate dihydrate | Sigma-Aldrich | W302600 |
| 3,3’ diaminobenzidine (DAB) tablets | Sigma-Aldrich | SLBM4338V |
| Anhydrous citric acid | Sigma-Aldrich | C0759 |
| Tween-20 | Sigma-Aldrich | WXBC9582V |
| Superfrost™ ultra plus adhesion slides | Thermo Fisher Scientific | J3800AMNT |
| Super PAP Pen | Thermo Fisher Scientific | 008899 |

### 2.1.5 Antibodies for western blot, immunohistochemical and immunofluorescent staining and immunoprecipitation

| **Antibody** | **Company** | **Catalog NO.** |
|---|---|---|
| Rabbit anti-pBCKDH-A | Abcam | ab200577 |
| Rabbit anti-BCKDH-A | Abcam | ab90691 |
| Rabbit anti-BCATm | Abcam | ab95976 |
| Rabbit anti-PPM1K | Proteintech | 14573-AP |
| Mouse anti-insulin | HyTest Ltd | 2IP10cc D6C4cc |
| Rabbit anti-glucagon | Sigma-Aldrich | SAB4501137 |
| Rabbit anti- APPL2 | | |
| Mouse anti-RacGAP1 | Santa Cruz Biotechnology | sc-166477 |
| Mouse anti-HA | sc-7392 | sc-166477 |
| Rabbit anti-HA | Cell Signaling Technology | 5017 |
| Rabbit anti-FLAG | Sigma-Aldrich | F7425 |
| Mouse anti-Myc | Santa Cruz Biotechnology | sc-40 |
| ANTI-FLAG® M2 Affinity Gel | Sigma-Aldrich | A2220 |
| Rabbit anti-GAPDH | Cell Signaling Technology | 5174 |

| | | |
|---|---|---|
| Rabbit anti-HSP90 | Cell Signaling Technology | 4877 |
| Mouse anti-β-actin | Santa Cruz Biotechnology | sc-8432 |
| HRP-conjugated anti-mouse antibody | Cell Signaling Technology | 7076S |
| HRP-conjugated anti-rabbit antibody | Cell Signaling Technology | 7074S |
| Alexa Fluor™ 488 Goat Anti-Mouse | Thermo Fisher Scientific | A31620 |
| Alexa Fluor™ 594 Goat Anti-Rabbit | Thermo Fisher Scientific | A31632 |

### 2.1.6 Recipe of buffers and solutions

| Buffer or solution | Recipe |
|---|---|
| Krebs buffer | 129 mM NaCl, 4.8 mM KCl, 5 mM NaHCO3, 1.2 mM KH2PO4, 2.5 mM CaCl2, 1.2 mM MgSO4, 0.1 % BSA, 2 mM glucose, pH 7.4 |
| Solution G | 0.1 % in BSA in 1 X HBSS buffer |
| Cell lysis buffer | 150 mM NaCl, 50 mM Tris-Cl (pH7.4), 2 mM EDTA, 1 % NP40 |
| 5 X SDS loading buffer | 0.3 M Tris-HCl, 12 %SDS, 50 % glycerol, 15 % beta-mercaptoethanol, 0.055 % bromophenol blue, pH 6.8 |
| 1 X SDS running buffer | 0.144 M glycine, 20 mM Tris, 0.1% SDS |
| 1 X Transfer buffer | 0.144 M glycine, 20 mM Tris, 20 % methanol |
| 1 X Tris buffer saline with Tween 20 (1 X TBS T) | 50 mM Tris-HCl, 150 mM NaCl, 0.1 %Tween 20, pH 7.4 |
| Blocking buffer | 5 % non-fat dried milk in 1 X TBST |
| Antibody dilution buffer | 5 % BSA in 1 X TBST |
| Phosphate buffered saline (PBS) | 137 mM NaCl, 2.7 mM KCl, 10 mM Na2HPO4, 1.8 mM KH2PO4, pH 7.4 |
| Citrate buffer | 10mM sodium citrate, 0.05 % Tween 20, pH 6.0 |
| 1 X PBST | 0.1 % Tween-20 in 1 X PBS, pH 7.4 |
| BSA blocking buffer | 3% BSA and 10% FBS in PBST |

### 2.1.7 Sequences of oligonucleotides used in this study

| **Genotyping Primers** | |
|---|---|
| **Gene name** | **Sequence** |
| *PPM1K* | Fw: 5’ CCC ATC CTT AGG AGA GGT CG 3’<br>Rv1: 5’ CAG CAG AAT TGG CTC ATC AA 3’<br>Rv2: 5’ ATG GTG GAT CCT GAG ACT GG 3’ |
| *APPL2* | Fw: 5’ CAC ACA GGA GCG TCT GTG GTG GTC 3’<br>Rv: 5’ CCT CCC TCT GTT GAA CCA GGA ACG 3’ |
| *General Cre* | Fw: 5’ GCA TTA CCG GTC GAT GCA ACG AGT G 3’<br>Rv: 5’ GAA CGC TAG AGC CTG TTT TGC ACG TTC 3’ |
| **RNAi duplex oligos** | |
| **Gene** | **Sequence** |
| *Scrambled control* | 5’ UAG CGA CUA AAC ACA UCA AUU 3’<br>5’ AAU UGA UGU GUU UAG UCG CUA 3’ |
| *PPM1K* | 5’ CCG CAU UGA UGA GCC AAU UTT 3’<br>5’AAU UGG CUC AUC AAU GCG GTT 3’ |
| *APPL2* | 5’ CCC UCA CAG ACU ACA CCA A 3’<br>5’ UUG GUG UAG UCU GUG AGG G 3’ |
| *RacGAP1* | 5’ GCU CCG UAC CUC AAG UAA ATT 3’<br>5’ UUU ACU UGA GGU ACG GAG CTT 3’ |
| **qPCR** | |
| *PPM1K* | 5’ TGT CTG CTG ATG CAA GCC TCC TG 3’<br>5’ TGG GGC TGT CCC AGG CTA TTC C 3’ |
| *GAPDH* | 5’ GGA TTT GGC CGT ATC GG 3’<br>5’ GTT GAG GTC AAT GAA GGG 3’ |

### 2.1.8 Plasmids used in this study

| Plasmid | Company | Catalog NO. |
|---|---|---|
| pRK5myc Rac1 Q61L | Addgene | 15903 |

### 2.1.9 Biochemical kits

| Biochemical kits | Company | Catalog NO. |
|---|---|---|
| Mouse insulin ELISA | Mercodia | 10-1247-01 |
| Ultrasensitive human insulin ELISA | Mercodia | 10-1132-01 |
| Wide range mouse insulin ELISA | Antibody and Immunoassay Services (AIS-HKU) | 32380 |
| Glucose uptake-Glo™ assay | Promega | J1341 |
| ATPlite luminescence assay | PerkinElmer Inc | 6016943 |
| Pierce™ BCA protein assay kit | Thermo Fisher Scientific | 23225 |
| Pierce™ 660nm protein assay kit | Thermo Fisher Scientific | 22662 |
| E.Z.N.A.® tissue DNA kit | Omega | D3396-02 |
| EndoFree mini plasmid kit | Omega | DP118-02 |
| Glucose assay kit | Nanjing Jiancheng Bioengineering institute | F006-1-1 |
| TMRE mitochondrial membrane potential assay kit | Cayman Chemical | 701310 |
| Reverse transcription kit | Promega | 15596026 |

### 2.1.10 Other Reagents or materials

| Reagent or material | Company | Catalog NO. |
|---|---|---|
| Latrunculin A | Cayman Chemical | 10010630 |
| SPY555-actin | Cytoskeleton | CY-SC202 |
| Alexa Fluor 488 phalloidin | Cell Signaling Technology | 8878 |
| Protein A-agarose | Santa Cruz Biotechnology | sc-2001 |

| | | |
|---|---|---|
| Protein G PLUS-agarose | Santa Cruz Biotechnology | sc-2002 |
| Insulin, human recombinant | Sigma-Aldrich | 91077C |
| Lab-Tek II 8-well chambered coverglass | Nunc | 155409 |
| Mouse standard diet | Labdiet | 5053 |
| TRIZOL | Invitrogen™ | 5596026 |
| SYBR Green | Roche | 21966100 |

### 2.1.11 Equipment

| Equipment | Company |
|---|---|
| Agilent 6460 Liquid Chromatography – Electrospray Ionisation Triple Quadrupole Mass Spectrometer | Agilent Technologies |
| Refrigerated CentriVap Centrifugal Concentrator and CentriVap Cold Traps | Labconco |
| Varioskan LUX Multimode Microplate Reader | Thermo Fisher Scientific |
| 96 Microplate Reader | Bio-Rad Laboratories |
| NanoDrop 2000 Spectrophotometer | Thermo Fisher Scientific |
| Countess II FL Automatic Cell Counter | Invitrogen™ |
| Accu-Check Performa Glucose Meter | Roche (USA) |
| Agilent Seahorse XFe24 Extracellular Flux Analyser | Agilent Technologies |
| TCS SP8 MP Multiphoton/Confocal Microscope | Leica Microsystems |
| TCS SPE Confocal Microscope | Leica Microsystems |
| Nikon Eclipse Ni-U Fluorescent Microscope | Nikon Instruments Inc. |
| Nikon Y-THPL Microscope | Nikon Instruments Inc. |
| ViiA7 Realtime PCR | Applied Biosystems |
| RM2235 Manual Microtome | Leica Microsystems |
| Excelsior AS Tissue Processor | Thermo Fisher Scientific |
| Paraffin Embedding Station | Thermolyne™ |

| | |
|---|---|
| Capillary electrophoresis (G7100A) - time of flight (TOF) mass spectrometry (G6224A) | Agilent Technologies |
| Real-Time PCR System | Applied Biosystems |

## 2.2. General protocols

### 2.2.1 Measurement of BCAA, BCKA and acylcarnitine by LC/MS/MS

#### 2.2.1.1 Preparation of calibration curve

The standard chemicals leucine, isoleucine, valine, KIC, KMV, KIV, C3- and C5-acylcarnitine and internal standards $D_8$-valine and $D_7$-KIV were dissolved in distilled water at a concentration of 100 mM as stock solutions. Calibration curves of these standards were prepared by a serial dilution from stock solutions for each measurement. Internal standards were diluted in 100 % methanol for analysis for serum samples or in methanol: water (4: 1, v: v) for analysis for cell samples. All the stock solutions were stored at – 80 °C.

#### 2.2.1.2 Serum and plasma samples processing

Plasma collected from human with normoglycemia or hyperglycemia was a kind gift from Dr. Parco Siu (110). 10 μL of human plasma or mouse serum was mixed with 100 μL cold absolute methanol containing 3 μM internal standard $D_8$-valine and $D_7$-KIV. The mixtures were vortexed for 1 minute and centrifuged at 10,000 rpm for 15 minutes under 4 °C. For the measurement of BCAA and C3- and C5-acylcarnitine, 20 μL of the extracted supernatant was transferred into a HPLC glass vial with an insert. 40 μL of the remaining supernatant was transferred into a new 1.5 ml Eppendorf tube and subjected to derivatization procedure for BCKA measurement.

#### 2.2.1.3 Cell sample processing

MIN6 cells were plated into 10-cm cell culture dishes and INS-1E cells were plated into 6-well culture plates for chemical treatment as stated in each figure legend. Cells reached around 80 % confluency in the day of sample processing. The treated cells were

placed on ice to slow down the intracellular metabolism. Culture medium was removed and cells were washed twice with cold PBS to remove excess medium. The cells were then placed on liquid nitrogen for snap freezing, followed by addition of the coldest possible methanol (MeOH: H2O, 4 parts:1 part, 500 μL) containing 1 μM internal standard D8-valine and D7-KIV. The cells were then scraped off and collected into 1.5 ml Eppendorf tubes, sonicated and centrifuged at 10,000 rpm for 15 minutes under 4 °C. 20 μL of cell extraction supernatant was transferred for the detection of BCAA and C3- and C5-acylcarnitines. The remaining supernatant was transferred into a new 1.5 ml tube and dried by evaporation in the Refrigerated CentriVap Centrifugal Concentrator. The residue was then reconstituted with 40 μL of methanol and used for BCKA derivatization.

#### 2.2.1.4 BCKA derivatization and extraction

The above serum and cell samples after methanol extraction were derivatized by incubation with 500 μL of 12.5 mM OPD in 2 M HCL at 80 °C for 20 minutes and then cooled on ice for 10 minutes (111). The derivatized samples were transferred to new 1.5 mL tubes containing 80 mg of Na2SO4, followed by vortex until Na2SO4 powder was completely dissolved. 500 μL of ethyl acetate was added into each tube and mixed by vortex for 1 minute (112). The tubes were then centrifuged at 500 g for 5 minutes at room temperature and the upper layer of ethyl acetate was transferred into new 1.5 mL tubes containing 80 mg of Na2SO4. The lower layer was extracted again by addition of another 500 μL of ethyl acetate. The new upper layer was transferred and combined with the first extraction, and dried by evaporation using the Refrigerated CentriVap Centrifugal Concentrator. The residue was reconstituted with 40 μL of 200 mM ammonium acetate, vortexed and centrifuged at 10,000 rpm for 10 minutes. 20 μL of

the supernatant was transferred into an HPLC glass vial with an insert for BCKA measurement by LC/MS/MS.

#### 2.2.1.5 $^{13}C_6$-labeled leucine tracing experiments

INS-1E cells were plated into 10 cm culture plate and cultured overnight. The cells were cultured with leucine-free RPMI 1640 medium supplemented with 10 % dialyzed FBS for 30 minutes. Medium was removed and cells were incubated with new medium containing 0, 300 mM or 2000 μM of $^{13}C_6$-labelled leucine for 9 or 24 hours as indicated in each figure legend. After treatment, the cells were processed as stated in 2.2.1.3. and 2.2.1.4. for measurement of BCAA, BCKA and acylcarnitine.

#### 2.2.1.6 Metabolomics analyses

The LC/MS/MS target metabolomic analysis was conducted using Agilent 6460 Liquid chromatography system and Electrospray Ionization Triple Quadrupole Mass Spectrometer (Department of University life Science, The Hong Kong PolyU). The temperature of the auto-sampler was set at 4 °C. For measurement of BCAA and acylcarnitine, 2 μL of each sample was injected into an ACQUITY UPLC BEH HILIC Column (1.7 μm, 2.1× 100 mm) for separation and the flow rate of aqueous–organic mobile phase was 0.3 ml/min. Mobile phase A consisted of acetonitrile: water (90:10, v:v), 5 mM ammonium formate and 0.1 % formic acid. Mobile phase B consisted of acetonitrile: water (10:90, v:v), 5 mM ammonium formate and 0.1 % formic acid. The gradient of mobile phase for HILIC separation was listed in Table 2.1. Measurement of BCKA was performed using an ACQUITY UPLC BEH C18 Column (130Å, 1.7 μm, 2.1 mm X 50 mm). Mobile phase A consisted of water and 0.1 % formic acid while mobile phase B consisted of acetonitrile and 0.1 % formic acid. Flow rate was set at 0.3

mL/min and gradient program was listed in Table 2.1. MS/MS data was acquired by multiple reaction monitoring (MRM) in a positive ion mode. The mass spectrometer was operated with the voltage set to 3.5 kV and source temperature held at 300°C. The fragmentor voltage (70-100 V) and collision energy (5- 20 psi) were optimized for each metabolite. The ion transitions and instrumental parameters are listed in Figure 3.1.C and Table 2.2. Enrichment measurement was corrected by internal standard and protein or DNA concentration.

Table 2.1. Gradient of mobile phase in HPLC

| HILIC column | | | C18 column | | |
|---|---|---|---|---|---|
| Time (min) | A (%) | B (%) | Time (min) | A (%) | B (%) |
| 0.00 | 2 | 98 | 0.00 | 98 | 2 |
| 3.00 | 2 | 98 | 2.00 | 98 | 2 |
| 10.00 | 30 | 70 | 5.00 | 60 | 40 |
| 12.00 | 50 | 50 | 6.00 | 40 | 60 |
| 14.00 | 50 | 50 | 9.00 | 40 | 60 |
| 16.00 | 2 | 98 | 11.00 | 98 | 2 |
| 18.00 | 2 | 98 | 13.00 | 98 | 2 |

Table 2.2. Ion transitions and instrumental parameters for isotope tracing analysis

| Analyte | ESI mode | Ion transition (m/z) | Retention time (min) | Fragmentor energy (V) | Collision energy (psi) |
|---|---|---|---|---|---|
| $^{13}C_6$-Leucine | Positive | 138-91 | 9.36 | 55 | 5 |
| $^{13}C_6$-KIC | Positive | 209-209 | 6.11 | 90 | 0 |
| $^{13}C_5$-C5-acylcarnitine | Positive | 251-85 | 10.76 | 100 | 25 |

### 2.2.2 Measurement of glycolytic and TCA cycle metabolites by CE/MS/MS

MIN6 cells were seeded onto 10-cm cell culture dishes and cultured with or without 30 μM BCKA for 48 hours reaching around 60 % confluency. The cells were washed twice with Krebs buffer and then treated with Krebs buffer containing 2 mM or 20 mM $^{13}C_6$-labeled glucose for 30 minutes, followed by rinse with 5 % mannitol (prepared by deionized water) for twice. After completely removing the mannitol solution, the cells were snap-frozen in liquid nitrogen. 1 mL of cold methanol containing 50 μM internal standards (methionine sulfone and D-Campher-10-sulfonic acid sodium salt) was added to the cells. The cells were then scraped off and collected into 1.5 mL tubes and vortexed for 20 seconds. 1 mL of chloroform and 400 μL of deionized water were added into each tube, and vortexed for 20 seconds after each addition. The mixtures were centrifuged at 14,000 g for 15 minutes at 4 ℃. 420 μL of upper layer was transferred and filtered using an Ultra-free MC Centrifugal filter device by centrifugation at 12,000 g for 3 hours at 4 ℃. The filtrates were dried by evaporation using the Refrigerated CentriVap Centrifugal Concentrator. Measurement and analysis of glycolytic and TCA cycle metabolites were performed by Capillary Electrophoresis–Mass Spectrometry (CE-MS) with help from Dr. Hailong Piao from Dalian Institute of Chemical Physics, Chinese Academy of Sciences (83).

### 2.2.3 Animal study

All mouse experiments were performed according to procedures approved by Department of Health HKSAR Government (Ordinance Cap. 340), and the Animal Subjects Ethics Sub-Committee (ASESC) of the Hong Kong Polytechnic University. Male C57BL/J mice were purchased from the Hong Kong Polytechnic University. *db/db* diabetic mice and lean controls were purchased from the Chinese University of

Hong Kong. *PPM1K* knockout mice were a kind share from Dr. Yinbing Wang from the University of California at Los Angeles (83). All mice were housed in the Centralised Animal Facilities of the Hong Kong Polytechnic University and maintained at 23 ℃ ± 1 ℃ on 12:12 light-dark cycle, with ad libitum access to drinking water and standard chow diet.

#### 2.2.3.1 Drug treatment with BT2 and BCKA feeding

BT2 was dissolved in DMSO at a concentration of 150 mM and diluted into 5 % DMSO in 0.1 M sodium bicarbonate, pH 9.0 for injection. 20 to 24-week-old male and female *db/db* mice were assigned into two groups with same fasting blood glucose. The *db/db* mice and their lean littermates were intraperitoneally injected with vehicle control or BT2 at a dose of 20 mg/kg for 4 weeks and 5-6 days each week. Skin disinfectant iodophor was used before and after each injection.

For BCKA feeding, chemicals of KIC, KMV and KIV were dissolved in the drinking water at a concentration of 5 mg/ml and filtered through a 0.22 μm filter. 16-week-old male C57BL/J mice were randomly assigned into two groups having free access to drinking water supplemented with or without BCKA for 4 weeks.

#### 2.2.3.2 Glucose tolerance test (GTT) and insulin tolerance test (ITT).

For GTT, *db/db* diabetic mice were fasted for 16 hours. Glucose were dissolved in sterile PBS for delivery. The fasted *db/db* mice were intraperitoneally injected with glucose (1 g /kg body weight) and blood was collected via tail vein every 20 minutes. Serum was separated within 30 minutes and serum glucose concentration was determined using a glucose assay kit according to the manufacturer's instruction. The mice in BCKA feeding study were fasted for 6 hours and intraperitoneally injected with

glucose (2 g /kg body weight). Blood glucose was measured every 20 minutes with a glucose meter.

For ITT, the mice were fasted for 6 hours and intraperitoneally injected with insulin (1.25 U /kg for *db/db* mice and 0.5 U/kg for BCKA fed mice). Blood glucose was measured every 15 minutes via tail veil using a glucose meter.

#### 2.2.3.3 Glucose and arginine-stimulated insulin secretion

For glucose-stimulated insulin secretion (GSIS), blood samples were collected from tail vein at the 0, 10 and 30 min of GTT. For arginine-stimulated insulin secretion, mice were fasted overnight and intraperitoneally injected with arginine at a dosage of 1g arginine/kg body weight. Blood samples were collected at 0, 4 and 10 min after injection. The serum was separated for measurement of insulin using a mouse insulin ELISA.

### 2.2.4 Isolation of pancreatic islets

The mice were fasted for 4 hours and anesthetized with ketamine/xylazine. The mice's abdomen was opened and bile duct was clamped off at the duodenum. Pancreas were perfused with 3 mL of collagenase P (1.4 mg/ml in HBSS) via bile duct and then separated for digestion at 37 °C for 20 minutes. After vigorously hand shaking for 30 seconds, the pancreas was incubated at 37 °C for another 5 minutes and then added with 15 ml solution G. The digested pancreas was filtered with a 500 μm fine test sieves and filtrate was collected into a 50 ml conical tube, centrifuged at 1,000 rpm for 5 minutes at room temperature. The supernatant was discarded and pellet was resuspended with

15 ml solution G, which was then filtered with a 70 μm cell strainer, resulting in two fractions: flow-through fraction containing exocrine cells (non-islet fraction) and captured fraction (islets). The captured islets were washed down by solution G and cultured in RPMI 1640 medium with 10 % FBS and 50 μM beta-mercaptoethanol at 37 °C overnight. The islets were manually picked under a microscope for insulin secretion assay or LC/MS/MS targeted metabolomic study.

### 2.2.5 Cell culture and glucose-stimulated insulin secretion (GSIS)

Insulinoma INS-1E cells were maintained in RPMI 1640 and MIN 6 β-cells were maintained in DMEM, and both media were supplemented with 10% FBS, 1% PS and 50 μM beta-mercaptoethanol. The cells were cultured in an incubator with 5% carbon dioxide ($CO_2$) at 37 °C and fresh medium was changed every two days.

For GSIS, the isolated islets, MIN6 or INS-1E cells were washed twice with Krebs buffer containing 2 mM glucose and 0.1 % fatty acid-free BSA. The cells were then incubated with the same buffer for 90 minutes, followed by stimulation with Krebs buffer containing 2 mM or 20 mM glucose for 30 minutes. The insulin secreted into the conditional medium was measured using a wide-range insulin ELISA according to the manufacturer's manual and normalized with protein concentration or islet size.

### 2.2.6 siRNA and plasmid transfection

$5 \times 10^4$ INS-1E cells were seeded into each well of a 24-well-plate and cultured overnight. Fresh medium was changed at least 2 hours before transfection. For siRNA transfection, 20 pmol siRNA oligos and 1 μL of Lipofectamine 3000 reagent were

diluted in 50 μL of Opti-MEM separately before mix by pipetting gently. The mixture was incubated at room temperature for 15 minutes and then added to the cells. Fresh medium was changed 7 hours after transfection and analyses were performed 48 hours after transfection. For co-transfection with siRNA against *APPL2* or scramble and/or plasmid overexpressing *Rac1Q61L*, transfection with plasmid was performed 7 hours after siRNA transfection. 0.5 μg of plasmid DNA and 0.5 μL of Lipofectamine 3000 reagent were diluted in 25 μL of Opti-MEM separately and then mixed gently by pipetting. The mixture was added to cells after incubation at room temperature for 15 minutes. Analyses were performed 48 hours after siRNA transfection.

### 2.2.7 Immunoblotting

INS-1E cells were subjected to different treatments as indicated in each figure legend. The treated cells were lysed in cell lysis buffer and protein concentration was determined by BCA protein quantification assay kit. Cells were denatured with SDS loading buffer at 100 °C for 10 minutes. An equal amount of proteins was loaded into and separated by sodium dodecyl sulphate-polyacrylamide gel electrophoresis (SDS-PAGE), and then transferred to PVDF membrane. After blocking with 5 % non-fat milk in 1 X TBST for 1 hour at room temperature, the membrane was probed with different primary antibodies in 5 % BSA in 1 X TBST at 4 °C for overnight. The membrane was washed with 1 X TBST for three times (5 minutes each) and subsequently incubated with HRP-conjugated secondary antibody prepared in 5 % non-fat milk in 1 X TBST for 90 minutes at room temperature. Afterwards, the membrane was washed with 1 X TBST for four times (10 minutes each). The specific signal of protein was visualized by ECL western blot detection kit and developed in Fuji medical X-Ray film. The

intensity of protein bands was quantified by the Image J software.

### 2.2.8 Histological and immunohistochemical staining

#### 2.2.8.1 Tissue collection and processing

The freshly isolated pancreas was fixed in 10 % neutral formalin overnight and dehydrated using the following protocol: 70 % ethanol for 30 minutes, 95 % ethanol I for 60 minutes, 95 % ethanol II for 60 minutes, 100 % ethanol I for 60 minutes, 100 % ethanol II for 60 minutes, 100 % ethanol III for 60 minutes, 1:1 ethanol/ xylene for 30 minutes, xylene I for 60 minutes, xylene II for 60 minutes, wax I for 60 minutes and wax II for overnight. The processed pancreas was then embedded into paraffin wax.

#### 2.2.8.2 Hematoxylin and eosin (H&E) staining

The paraffin-embedded pancreatic blocks were cut into 5-μm-thick sections, which were deparaffinized and rehydrated by xylene (15 minutes, twice), 100 % ethanol (5 minutes, twice), 90 % ethanol (3 minutes, twice), 70 % ethanol (2 minutes, once) and then rinsed in tap water. For H&E staining, the sections were stained with hematoxylin for 10 minutes and eosin for 3 minutes, followed by rinse in tap water and dehydration. Finally, the stained sections were immersed in xylene for at least 30 minutes and then mounted with DPX mounting medium.

#### 2.2.8.3 Immunohistochemical and immunofluorescent staining (IHC and IMF)

The paraffine pancreatic sections were deparaffinized and rehydrated as described above. The slides were immersed into preheated solution of citrate retrieval buffer and heated for 20 minutes, and then cooled down to room temperature. For IHC, the slides were treated with 3% hydrogen peroxide ($H_2O_2$) for 15 minutes at room temperature in

the dark for quenching of internal peroxidases. The slides were then blocked with 10 % FBS in 3 % BSA in 1X PBST for 1 hour at room temperature. After rinse with 1X PBST for three times (5 minutes each), the slides were incubated with primary antibodies against BCKDH-A (1:200), phosphorylated-BCKDH-A (1:200), PPM1K (1:200) and insulin (1:500) at 4 °C overnight, followed by incubation with HRP-conjugated secondary antibodies (1:300) for 1 hour at room temperature, and finally protein signal was developed by DAB.

For IMF, the slides after antigen retrieval were blocked and incubated with primary antibodies against glucagon (1:200) and insulin (1:500) as specified above. Afterwards, the slides were incubated with secondary antibodies (Alexa Fluor 594 anti-Rabbit IgG and Alexa Fluor 488 anti-Mouse IgG, 1:500) at room temperature for 1 hour, and then mounted with a mounting medium with DAPI.

### 2.2.9 Measurement of mitochondrial membrane potential

MIN6 cells were seeded into black 96- well plate with clear bottom and culture with or without 30 μM BCKA for 48 hours. 100 μL of 200 nM TMRE (prepared by dilution of TMRE stock solution into the 1 X assay buffer provided in the TMRE assay kit) was added into each cell well and incubated for 30 minutes at 37 °C. The medium was removed and the cells were gently rinsed twice with 1 X assay buffer, followed by the addition of another 100 μL of 1 X assay buffer and measurement of fluorescence intensity at excitation/emission 530/580 nm.

### 2.2.10 Measurement of ATP production

MIN 6 cells and INS-1E cells were seeded into black 96- well plate with clear bottom and subjected to treatments as specified in each figure legend. The cells were starved in the Krebs buffer with 2 mM glucose for 90 minutes, followed by stimulation with 100 μL of Krebs buffer containing 2 mM or 20mM glucose for 10 minutes. ATP level was measured using the Luminescence ATP detection kit according to the manufacturer's instruction and normalized with protein concentration. Briefly, 50 μL of cell lysis buffer was added into each well and vortexed for 5 minutes, followed by adding 50 μL of detection reagent and vortexed for another 5 minutes. The luminescence intensity was measured using a luminescent microplate reader.

### 2.2.11 Measurement of ECAR and OCR

MIN 6 cells and INS-1E cells were seeded into XF24 V7 PS tissue culture microplate and cultured overnight to reach around 50-60 % confluency. The cells were subjected to treatment as specified in each figure legend. XFe24 sensor cartridge was rinsed in Seahorse XF calibrant solution and kept in a 37 °C non-$CO_2$ incubator one day before the assay. The cells were rinsed twice with XF Base medium (PH7.4) and cultured with 500 μL of XF Base medium in the 37 °C non-$CO_2$ incubator for 1 hour. Afterwards, the culture plate was loaded into the Agilent Seahorse XFe24 Extracellular Flux Analyser and treated with 20 mM glucose, 5 μM oligomycin and 50 μM 2-DG sequentially through injection ports for the measurement of ECAR and OCR.

### 2.2.12 Quantitative real-time PCR

Total RNA was extracted from INS-1E cells using Trizol reagent and 1 μg of total RNA was used for cDNA synthesis by reverse transcription. Specific primers targeting to *PPM1K* and *GAPDH* and SYBR Green QPCR kit were used for the reaction of quantitative real-time PCR. The PCR reaction was performed by the Applied Biosystems Real-Time PCR system. The mRNA expression of *PPM1K* was normalized by mRNA level of *GAPDH*.

### 2.2.13 Live cell imaging

Pancreatic islets isolated from RIP-APPL2 KO mice and their WT controls were seeded into 8-well Nunc™ Lab-Tek™ II Chambered Coverglass and cultured for at least 24 hours to allow the islets to attach to coverglass. Islets were incubated with 200 μL of Krebs buffer containing 2.8 mM glucose and F-actin fluorescent probe SPY555-actin (1000 X dilution according to manufacturer's instruction) at 37 °C for 90 minutes. After labelling, real-time images of F-actin signals were captured for 10 minutes using a Leica TCS SP8 MP multiphoton/confocal microscope with temperature and CO2 concentration control at basal condition, which was served as photobleaching control. The islets were then stimulated with 16.7 mM glucose by adding 200 μL of Krebs buffer containing 30.6 mM glucose and dynamic changes of F-actin signal was recorded every 70s for 10 minutes. F-actin fluorescence intensity in an individual islet was quantified by ImageJ and normalized with islet size.

### 2.2.14 F-actin (Phalloidin) staining

The isolated islets were stimulated with 2.8 mM or 16.7 mM glucose for 10 minutes in Krebs buffer, and washed with PBS by centrifugation at 1,000 rpm for 5 minutes. Used PBS was discarded and islets were fixed with 4% formaldehyde in PBS at room temperature for 15 minutes. The fixed islets were rinsed with PBS for three times before incubation with Alexa Fluor 488 Phalloidin at room temperature for 15 minutes. After rinsing with PBS, islets were mounted onto slides by mounting medium with DPAI. The fluorescent images were captured using Nikon Eclipse C1 Confocal Microscope and F-actin fluorescence intensity in an individual islet was quantified by ImageJ and normalized with surface area.

### 2.2.15 Co-immunoprecipitation

HEK 293 cells and INS-1E cells were transfected with plasmids encoding HA-tagged human RacGAP1 and FLAG-tagged human full length APPL2 or its truncated mutants using Lipofectamine 3000 for 48 hours as described above. The transfected INS-1E cells were stimulated with 16.7 mM glucose for 0, 2, 5, 10 and 30 minutes before solubilization in cold cell lysis buffer. Cell lysates of HEK 293 cells and INS-1E cells were centrifuged at 13,000 rpm at 4°C for 10 minutes and supernatants were collected for co-immunoprecipitation. To immunoprecipitate HA-tagged protein, total cell lysate was incubated with mouse anti-HA antibody (1:100) by gently mixing on a rotator for 3 hours at 4 °C, followed by incubation with 10 μL of protein A/G agarose for 30 minutes. To immunoprecipitate FLAG-tagged protein, the lysate was incubated with 10 μL of anti-FLAG M2 Affinity Gel for 3 hours at 4 °C. To immunoprecipitate

endogenous RacGAP1, total cell lysate was pre-cleaned with protein A/G agarose at 4 °C for 60 minutes before incubation with an anti-RacGAP1 antibody overnight at 4 °C. The lysate-antibody mixture was centrifuged and supernatant was transferred for incubation with protein A/G agarose at 4 °C for 60 minutes. Protein A/G agarose was washed with lysis buffer for three times before use. The immunocomplex was centrifuged at 4,000 rpm for 1 minute and supernatant was discarded. The bead mixture was washed with cold lysis buffer for three times to remove nonspecific binding, followed by elution using SDS sample loading dye by heating at 99 °C for 5 minutes. The eluted immunocomplex and total cell lysate were subjected to western blot analysis to check the interaction of proteins

### 2.2.16 Statistical analysis

Figures were generated by GraphPad Prism and statistical analysis were performed using either SPSS or GraphPad Prism. All results are presented as mean ± s.d. Significance was determined using two-sided Student's t-test or one-way ANOVA with Bonferroni correction. Correlation and regression analysis were performed using Spearman analysis. A p-value of less than 0.05 represented a statistical significance.

# Chapter 3 BCAA catabolism in pancreatic β-cells is impaired in T2D

## 3.1 Introduction

Insulin resistance and pancreatic β-cell dysfunction are two leading causes contributing to the onset and progress of type 2 diabetes (T2D). Defective BCAA catabolism in peripheral tissues, such as liver, muscle, and adipose tissue, are associated with the development of insulin resistance, obesity, and future risk of T2D (34, 63). However, the role of BCAA catabolism in pancreatic β-cells under the physiological and pathophysiological conditions, such as obesity and T2D, has not been clearly established yet.

In this chapter, *in vitro* and *ex vivo* approaches were employed to examine whether BCAA catabolism takes place in pancreatic β-cells and whether this pathway is altered in pancreatic islets under diabetic condition.

## 3.2 Result

### 3.2.1 BCAA and its downstream metabolites are detected by LC-MS/MS

BCAA catabolic flux has now been clearly identified as illustrated in Figure 3.1A. BCAA is gradually catabolized by the enzymes BCATm and BCKDH-A to generate various small molecules and Co-A derivates which finally enter the TCA cycle or fatty acid synthesis pathways. To examine the catabolites (including leucine, isoleucine, valine, KIC, KMV, KIV, C3-acylcarnitine, and C5-acylcarnitine) in the BCAA catabolic pathway, a targeted metabolomic protocol for metabolite characterization and detection was established using the liquid chromatography tandem-mass spectrometry (LC-MS/MS) system with high analytical performance. The aforementioned BCAA-

related metabolites in standard mixtures and serum samples were firstly separated by High Performance Liquid Chromatography (HPLC) connected to columns with different binding capacities to retain polar or nonpolar analytes. The separated analytes were detected by Electrospray Ionization Triple Quadrupole Mass Spectrometer based on their specific mass-to-charge ratio (m/z). Representative chromatograms and retention time of each analytes are shown (Figure 3.1. B) and key parameters for LC-MS/MS detection are indicated in Figure 3.1. C. Specific and high signal-chromatogram could be identified and low background noise was found. Besides, standard curves with blank correction for each metabolite were also well established, indicating this metabolomic protocol displayed a good performance in the measurement of BCAA and its downstream catabolites.

It has been reported that circulating levels of BCAA are increased in Chinese people with hyperglycemia, insulin resistance, obesity and diabetes (38, 113-116). However, the profile of BCAA downstream intermediates in the aforementioned metabolic disorders has never been studied in the Chinese population before. To answer this question, BCAA related catabolites in plasma samples collected from age-matched normoglycemic and hyperglycemic human were detected. These plasma samples were collected from the hospital and were kind gifts from Dr. Parco Siu (110). Characteristics of human samples and plasma levels of BCAA associated catabolites are summarized in Table 3.1. Compared with normoglycemic human samples, hyperglycemic samples displayed aberrantly higher fasting blood glucose and fasting blood insulin, indicating the development of insulin resistance in these people, evidenced by the increased value of HOMA-IR (index of insulin resistance). In line with previous animal studies (110), circulating levels of BCAA (leucine, isoleucine, valine) and BCKA(KIC, KMV, and KIV), were significantly raised in hyperglycemic human. Additionally, both total

circulating levels of both BCAA and BCKA were positively related to fasting blood glucose in normoglycemic and hyperglycemic human (Figure 3.2. A-B), highlighting that BCAA pathway might play a critical role in controlling glucose metabolism.

A

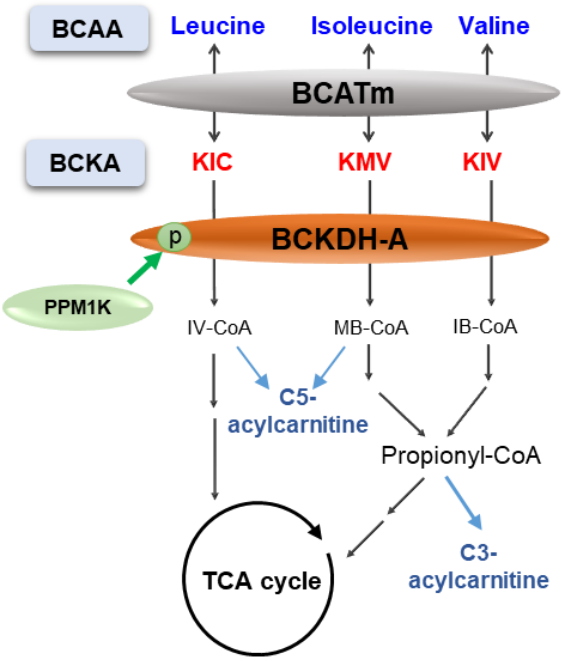


B

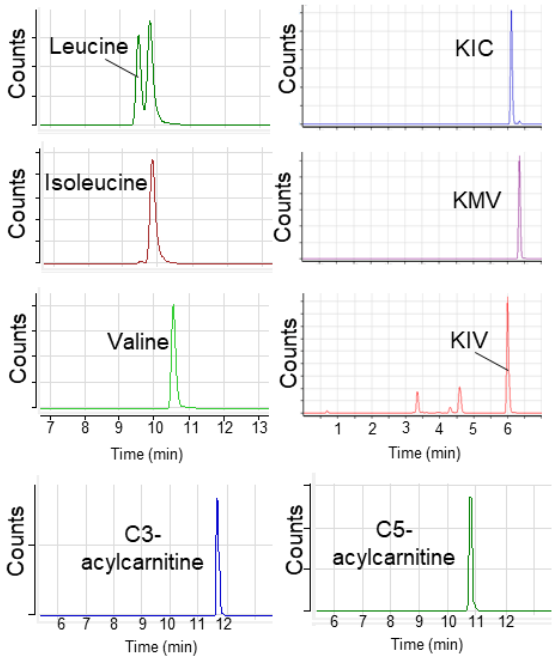


C

| Analyte | ESI model | Retention time (min) | Precursor →Product ions (m/z) |
|---|---|---|---|
| Leucine | + | 9.36 | 132.1 → 86.1 |
| Isoleucine | + | 9.84 | 132.1 → 69.2 |
| Valine | + | 10.53 | 118.1 → 72.2 |
| KIC | + | 6.11 | 203.2 → 161.2 |
| KMV | + | 6.35 | 203.0 → 174.2 |
| KIV | + | 6.02 | 189.1→ 119.3 |
| C2-acylcarnitine | + | 12.12 | 204.0 → 85.0 |
| C3-acylcarnitine | + | 11.64 | 218.0 → 85.0 |
| C5-acylcarnitine | + | 10.76 | 246.0 → 85.0 |
| D8-valine | + | 10.53 | 126.0 → 80.0 |
| D7-KIV | + | 6.02 | 196.0 → 126.0 |

**Figure 3.1. Detection of BCAA and its downstream metabolites by LC-MS/MS.** *(A)* Overview of BCAA catabolism. BCAA including leucine, isoleucine and valine are first transaminated into α-ketoisocaproate (KIC), α-ketomethylvaleric acid (KMV) and α-ketoisovaleric acid (KIV), respectively, by mitochondrial branched chain aminotransferase (BCATm). These three branched-chain α-keto acids (BCKA) are oxidatively decarboxylated via BCKDH-A to generate the Co-A derivatives, which are further metabolized by multiple mitochondrial-matrix enzymes, and eventually enter the TCA cycle. In response to elevated BCAA/ BCKA levels, protein phosphatase 1K (PPM1K) activates BCKDH-A by inducing dephosphorylation. *(B)* Different catabolites were detected by LC-MS/MS and representative chromatograms are shown. *(C)* Parameters of LC-MS/MS detection. Retention time for metabolites separation and m/z ratio of the metabolites are shown. Positive electrospray ionization (ESI) model was used in metabolite detection. m/z (mass-to-charge ratio). Noted that linear standard curve for each metabolite was established (r>0.99) .

**Table 3.1. Circulating levels of BCAA and its downstream metabolites in normoglycemic and hyperglycemic human.**

| | Normoglycemia | Hyperglycemia |
|---|---|---|
| Age | 68 - 85 | 68 - 85 |
| Sex | Male (19); Female (40) | Male (17); Female (38) |
| Waist (cm) | 78.07 ± 8.816 | 90.31 ± 8.002 ** |
| Blood glucose (mM) | 4.886±0.3082 | 6.538±1.456 ** |
| Blood insulin (ng/ml) | 4.283±2.393 | 8.725±4.584** |
| HOMA-IR | 0.95±0.56 | 2.58±1.90** |
| HOMA-beta (%) | 59.85±30.02 | 63.19±33.51 |
| Plasma leucine (μM） | 174.78±47.56 | 212.25±56.65** |
| Plasma isoleucine (μM） | 114.73±43.34 | 135.01±47.80* |
| Plasma valine (μM） | 129.55±27.07 | 157.87±30.57** |
| Plasma KIC (μM） | 24.75±6.73 | 33.51±7.36** |
| Plasma KMV (μM） | 13.82±3.27 | 18.30±4.66** |
| Plasma KIV (μM） | 11.65±2.41 | 14.56±2.38** |
| Plasma C2 acylcarnitine (μM） | 24.37±7.86 | 22.79±9.25 |
| Plasma C3 acylcarnitine (nM） | 29.01±13.12 | 35.54±17.34 |
| Plasma C5 acylcarnitine (nM） | 6.27±3.04 | 7.33±3.03 |

All results are presented as mean ± s.d. Significance was determined using Student's t-test. *$p < 0.05$ and **$p < 0.01$.

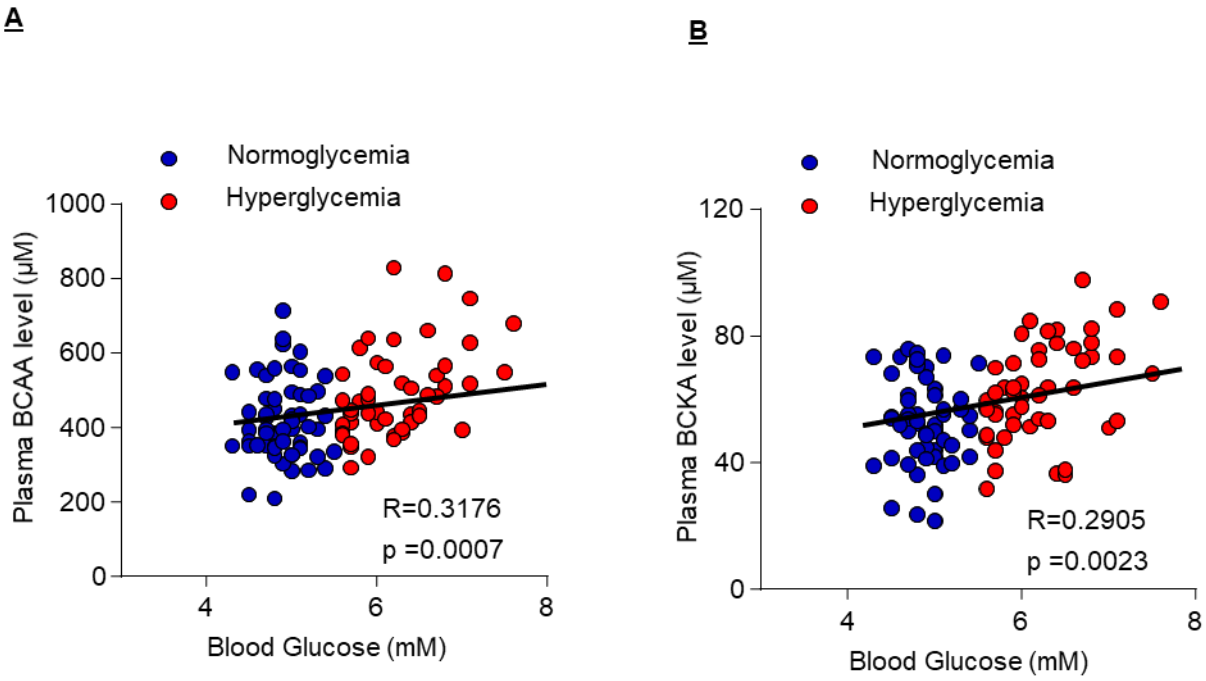


**Figure 3.2. Fasting blood glucose is positively associated with circulating BCAA and BCKA in human.** Positive association was found between fasting glucose and *(A)* circulating BCAA and *(B)* BCKA in normoglycemic and hyperglycemic human. Association was accessed by Spearman correlation test. n = 55-59.

### 3.2.2 Pancreatic β-cells are capable of BCAA catabolism

To investigate whether BCAA catabolism takes place in pancreatic β-cells, the expression of BCATm and BCKDH-A (the key enzymes responsible for the first two steps of BCAA degradation) were examined in insulinoma INS-1E β-cells. Immunoblotting analysis demonstrated that both BCATm and BCKDH-A were abundantly expressed in INS-1E β-cells (Figure 3.3. A-B). Stimulation with BCAA or BCKA in the culture medium induced activation of BCKDH-A via dephosphorylation at serine 293 (Figure 3.3. A-B). This finding suggests BCAA catabolic pathway is also activated in INS-1E β-cells upon stimulation with BCAA and BCKA.

To further confirm the capacity of pancreatic β-cells for BCAA catabolism, INS-1E β-cells were cultured with low or high concentration of BCAA in the medium for two hours, followed by targeted metabolomic analysis to reveal the alteration in intracellular levels of BCAA-related catabolites. As expected, intracellular levels of all BCAA (leucine, isoleucine and valine) were increased in INS-1E β-cells after incubation with high concentration of BCAA (Figure 3.4. A). Downstream catabolites BCKA including KIC, KMV, and KIV were also increased (Figure 3.4. B), which was consistent with the activation of BCKDH-A activity upon BCAA and BCKA stimulation. Noted that C5-acylcarnitine (one end-product of BCAA catabolism) was remarkably increased in INS-1E β-cells, but another end-product, C3-acylcarnitine, only slightly increased but no significant difference could be found (Figure 3.4. C).

The aforementioned study was repeated *ex vivo*. Pancreatic islets were isolated from 16-week-old male C57BL/J mice. Islets with similar size were handpicked under a microscope into two groups treated with low or high concentration of BCAA for two hours. Similar to the observations in INS-1E β-cells, BCAA dramatically accumulated

in islets upon treatment with high concentration of BCAA (Figure 3.4. D), accompanied by an elevation in downstream catabolites BCKA (Figure 3.4. E), end-products C3-acylcarnitine and C5-acylcarnitine (Figure 3.4. F). Taken together, these data suggest that pancreatic β-cells consist of intact BCAA catabolic pathway and thus they are able to take up and metabolize BCAA.

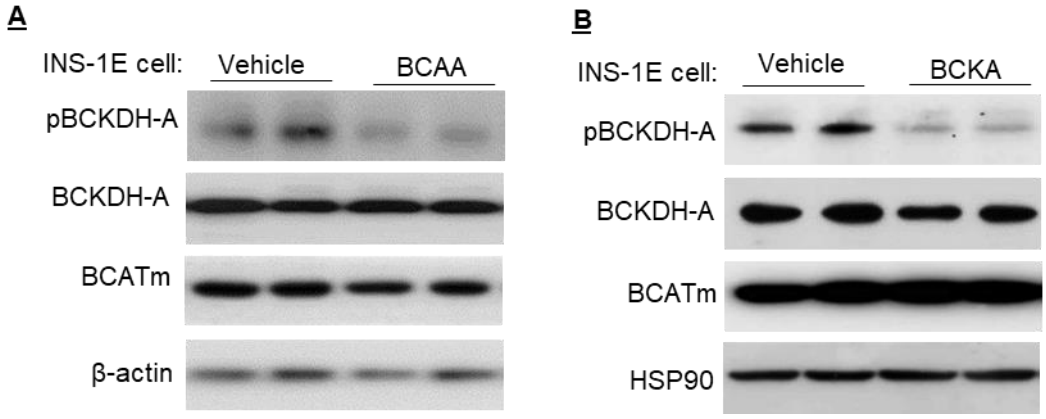


**Figure 3.3. Expression of BCAA catabolic gene in pancreatic β cells.** *((A-B)* INS-1E pancreatic β-cells were subjected to serum and amino acid starvation in Krebs buffer for 1 hour, followed by stimulation with *(A)* BCAA (leucine, isoleucine and valine [5 mM each]) and *(B)* BCKA (KIC, KMV and KIV [5 mM each]) or vehicle for 5 minutes. Total cell lysates were collected for immunoblotting analysis using antibodies against total BCKDH-A, phospho-BCKDH-A (pBCKDH-A, serine 293), BCATm, β-actin and HSP90.

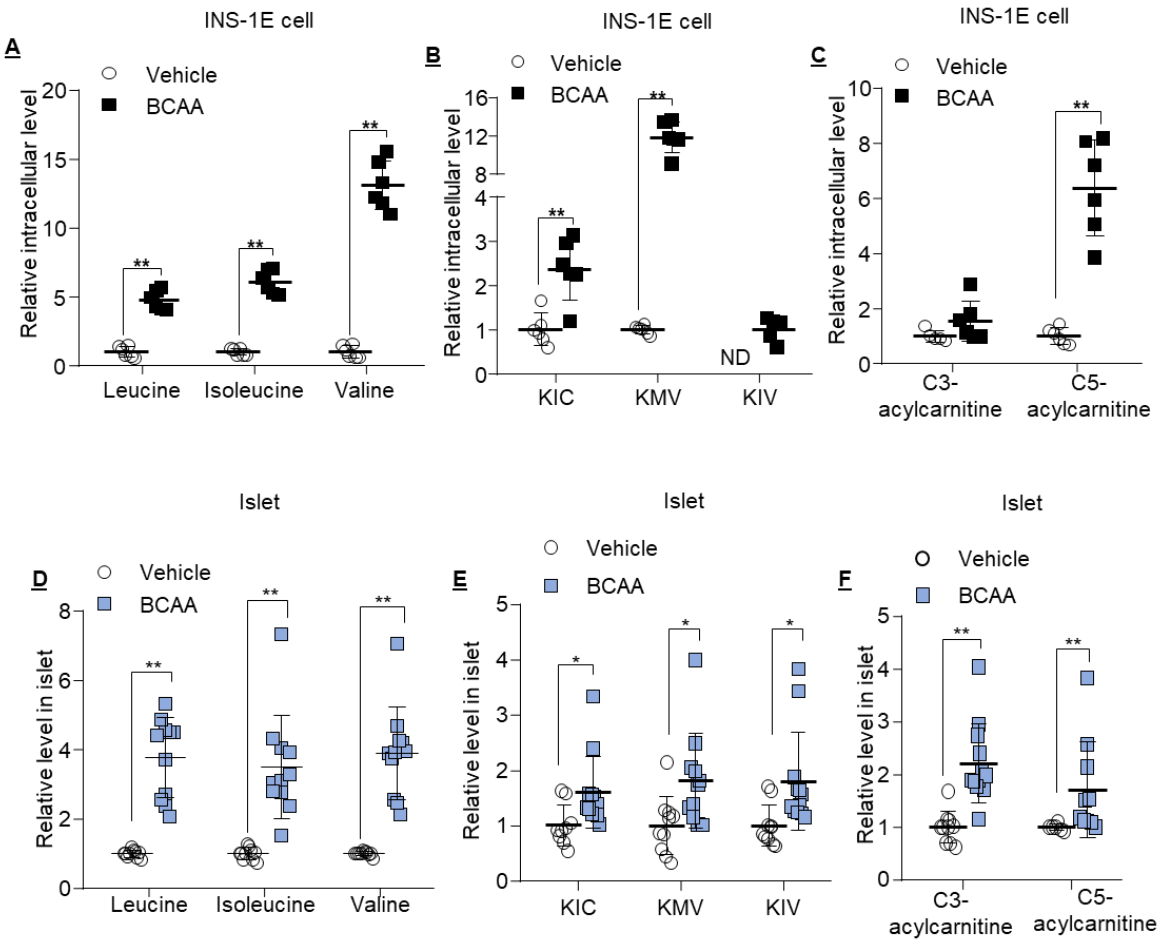


**Figure 3.4. Pancreatic β cells are able to catabolize BCAA.** *(A-C)* INS-1E cells were starved in the Krebs buffer for 1 hour, followed by administration with vehicle or 5 mM BCAA for 2 hours. Intracellular levels of *(A)* BCAA, *(B)* BCKA and *(C)* C3- and C5-acylcarnitine were measured by LC-MS/MS and normalized with protein concentration. n=5-6. *(D-F)* Pancreatic islets isolated from 16-week-old C57BL/J male mice were starved in the Krebs buffer for 1 hour, followed by administration with vehicle or 5 mM BCAA for 2 hours. Intracellular levels of *(D)* BCAA, *(E)* BCKA and *(F)* C3- and C5-acylcarnitine were measured by LC-MS/MS and normalized with islet number. n=6-11. ND (Not detectable). All results are presented as mean ± s.d. Significance was determined using Student's t-test. *$p < 0.05$ and **$p < 0.01$.

### 3.2.3 Leucine catabolic flux was monitored by isotopic carbon tracing analysis in INS-1E β-cells

BCAA metabolism connects with multiples pathways in cells, such as protein degradation, protein synthesis, glycolysis, TCA cycle, and fatty acid synthesis, and so on. To confirm that BCKA and C5-acylcarnitine derive from BCAA catabolism but not from other metabolic pathways, isotopic labeling analysis was performed to trace leucine metabolic flux in INS-1E β-cells.

Figure 3.5. A illustrates how isotopic carbon derived from $^{13}C_6$ leucine (6 carbons labeled with stable isotope $^{13}C$) incorporates into downstream metabolites KIC and C5-acylcarnitine. INS-1E β-cells were incubated with medium containing vehicle, low or high concentration of $^{13}C_6$ leucine for 9 or 24 hours. In INS-1E cells with isotopic leucine treatment, a dramatic accumulation in intracellular leucine M+6 and KIC M+6 (the direct isotope product of $^{13}C_6$ leucine) was observed at a time and dose-dependent manner while endogenous leucine (leucine M+0) also seemed slightly increased (Figure 3.5. B and C). To our surprise, isotopic C5-acylcarnitine in INS-1E β-cells incubated with a low concentration of $^{13}C_6$ leucine was not detectable, which might be due to low production or inadequate cell number.

Interestingly, the generation of isotopic C5-acylcarnitine (M+5) was increased at the 9th hour but later decreased at the 24th hour in β-cells treated with a high concentration of 13C-tracer. Meanwhile, compared with the vehicle group, endogenous C5-acylcarnitine (M+0) also significantly increased in cells treated with exogenous isotopic leucine, which might due to the generation of isotopic C5-acylcarnitine. As a result, less endogenous C5-acylcarnitine was required and utilized (Figure 3.5. D). Together with the alteration in the labeled KIC, chronic treatment with excessive leucine induced

accumulation of KIC but less C5-acylcarnitine in pancreatic β-cells compared with those with short term treatment, which leads to speculation that long-term overload of BCAA disrupts BCAA catabolic capacity in pancreatic β-cells. Overall, all the above data demonstrate an intact BCAA catabolic pathway in pancreatic β-cells.

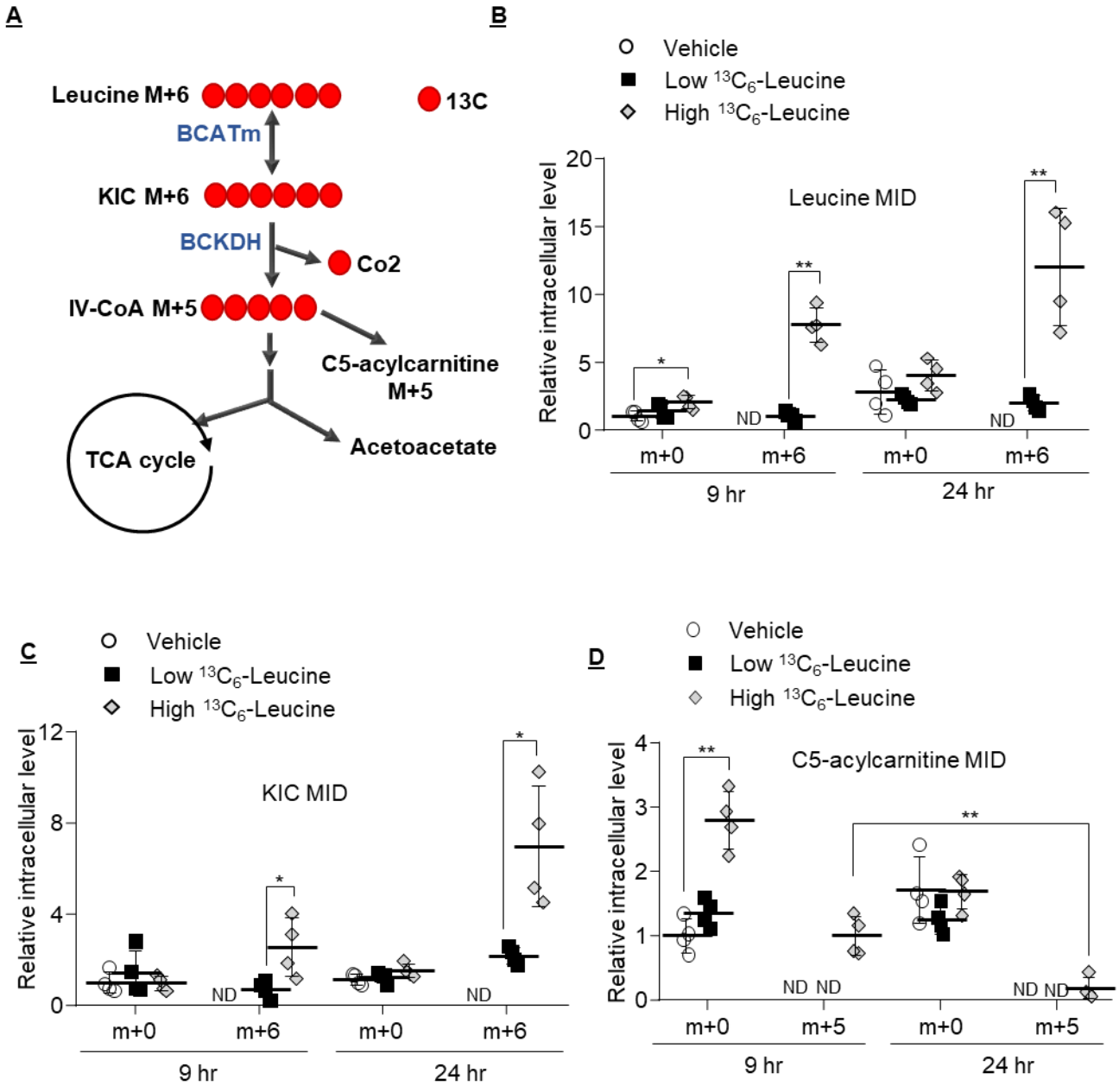


**Figure 3.5. Isotopic carbon tracing analysis of $^{13}C_6$ leucine in INS-1E cells.** *(A)* Diagram of isotopic leucine catabolic pathway. Red circles indicate 13C-labeled carbons. *(B-D)* INS-1E cells were cultured with leucine free RPMI 1640 medium supplemented with vehicle, low (300 μM) or high (2000 μM) concentration of 13C6-labelled leucine for 9 or 24 hours as indicated in each figure. Intracellular levels of *(B)* leucine, *(C)* KIC and *(D)* C5-acylcarnitine were measured by LC-MS/MS. MID indicates mass isotopologue distribution. n=4. ND (Not detectable). All results are presented as mean ± s.d. Significance was determined using Student's t-test or one-way ANOVA with Bonferroni correction. *$p < 0.05$ and **$p < 0.01$.

### 3.2.4 BCAA catabolism is defective in diabetic islets

The above data demonstrated the BCAA catabolic pathway in normal pancreatic β-cells and islets. Whether this pathway is aberrant in the diabetic condition is unknown. To address this question, *db/db* mice were used for the following studies. *db/db* mouse is a typical example of type 2 diabetes model with a spontaneous point mutation in leptin receptor, leading to the development of obesity and subsequent type 2 diabetes. Compared with control of lean littermates (*db/+*), *db/db* diabetic mice displayed a much higher fasting blood glucose level (Figure 3.6. A) and pancreatic β-cell dysfunction, as evidenced by blunted glucose-induced insulin secretion (Figure 3.6. B). In line with human data, circulating levels of BCAA and BCKA were elevated in *db/db* diabetic mice (Figure 3.6. C-D).

We next compared BCAA catabolism in islets isolated from *db/db* mice and lean controls by measuring BCAA related catabolites and expression of BCAA related enzymes. Except for C3-acylcarnitine, more BCAA and its catabolites BCKA (KIC, KMV, KIV) and C2/C5-acylcarnitine were accumulated in pancreatic islets isolated from *db/db* mice than those isolated from lean controls (Figure 3.7. A). These findings suggest that BCAA catabolic capacity was impaired under diabetic condition. Next, pancreatic sections were subjected to immunohistochemistry analyses of BCKDH-A (the key enzyme responsible for the rate-limiting step of BCAA catabolism) and its phosphorylation at serine 293. Although the phosphorylation level appeared to be comparable in pancreatic islets between the two groups, expression of total BCKDH-A tended to be reduced in diabetic islets. Indeed, increased ratio of phosphoBCKDH-A to total BCKDH-A was found in diabetic islets, suggesting that total activity of BCKHD-A was undermined and therefore capacity of BCKA clearance might be

impaired in diabetic islets (Figure 3.7. B and C). In addition, the increased ratio of phosphoBCKDH-A to total BCKDH-A was accompanied by a reduced expression of PPM1K, a phosphatase reducing phosphorylation of BCKHD-A at serine 293 (Figure 3.7. B and D). Taken together, these data suggest that BCAA catabolic pathway is altered in pancreatic islets under diabetic condition.

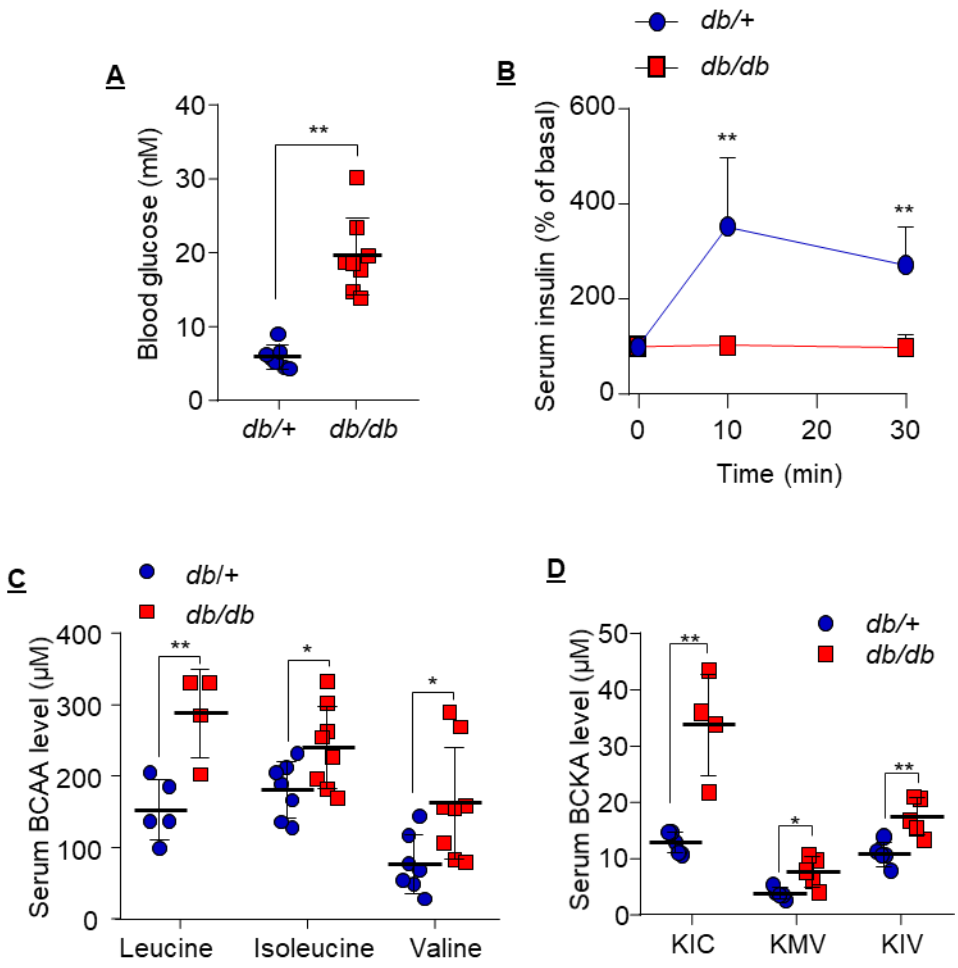


**Figure 3.6. Impaired insulin secretion is associated with increased circulating BCAA metabolites in *db/db* diabetic mice.** *(A)* Blood glucose and *(B)* glucose-induced insulin secretion (1g glucose/kg) in 20 to 24-week-old *db/d*b diabetic mice and *db/+* mice (lean littermates) fasted overnight. The blood was collected via tail vein and blood glucose was detected with a glucose meter. The serum insulin was measured using an insulin ELISA kit. n=7-8. *(C-D)* Serum levels of *(C)* BCAA and *(D)* BCKA in 20 to 24-week-old male mice fasted overnight. n=4-8. All results are presented as mean ± s.d. Significance was determined using Student's t-test. *$p < 0.05$ and **$p < 0.01$.

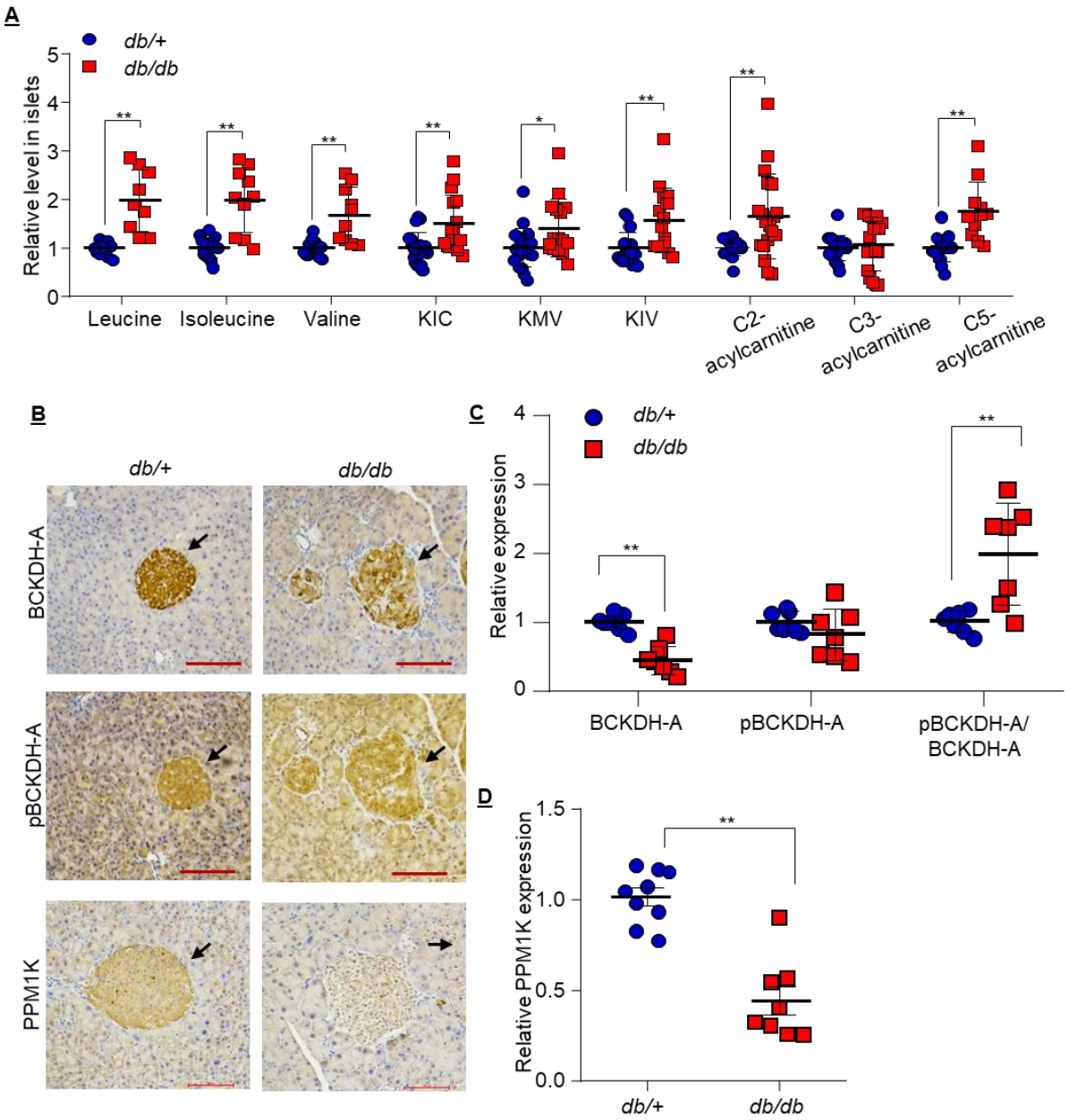


**Figure 3.7. Defective BCAA catabolism in diabetic islets.** *(A)* Islets isolated from 24-week-old *db/db* and lean littermates (*db/+*) were subjected to serum and amino acid starvation in Krebs buffer for 1 hour. Intracellular levels of BCAA, BCKA and acylcarnitines in islets were measured by LC-MS/MS. n=9-17. *(B)* IHC staining for total BCKDH-A, phosphoBCKDH-A (pBCKDH-A) and PPM1K in pancreatic sections of 24-week-old *db/db* mice and lean controls. *(C)* Quantification of expression of total BCKDH-A, pBCKDH-A and ratio of pBCKDH-A to BCKDH-A and *(D)* quantification of PPM1K expression in islets showed in *(B).* n=7-9. Scale bar: 100 µm.: All quantifications were performed using Image J software. All results are presented as mean ± s.d. Significance was determined using Student's t-test. *$p < 0.05$ and **$p < 0.01$.

## 3.3 Summary

BCAA catabolic pathway has not been fully characterized in pancreatic β-cells before. This chapter describes a successful establishment of method for detecting BCAA-related catabolites using LC-MS/MS targeted metabolomics. This technique and isotope tracing analysis demonstrated that pancreatic β-cells and islets are able to catabolize BCAA into downstream catabolites including BCKA and C3/C5 acylcarnitine. The existence of BCAA catabolic pathway in pancreatic β-cells was further supported by the expression of enzymes including BCATm and BCKDH-A.

In addition, I observed that pancreatic islets from *db/db* diabetic mice displayed defective BCAA catabolism compared to those from healthy controls. Given the importance of normal pancreatic β-cell function in the control of glucose homeostasis, it is worthwhile to further investigate whether defective BCAA catabolism plays a causal role in pancreatic β-cell failure during the development of T2D.

# Chapter 4 Defective BCAA catabolism impairs insulin secretion in pancreatic β-cells and induces glucose intolerance in mice

## 4.1 Introduction

In chapter 3, BCAA catabolism was shown altered in pancreatic islets under diabetic condition. However, it is unclear whether the defective BCAA catabolism and/or chronic exposure to a high concentration of BCAA catabolites have any effect on pancreatic β-cell function. This chapter explores the effect of an overload of BCAA related catabolites and disruption of BCAA metabolism on insulin secretion using *in vitro* approaches and animal models.

## 4.2 Result

### 4.2.1 BCKA, but not other BCAA catabolites impairs insulin secretion

To investigate whether chronic exposure of excessive BCAA and its related catabolites triggers pancreatic β-cell dysfunction, insulinoma MIN6 β-cells were selected for insulin secretion assay since MIN6 cells display better insulin secretory ability than INS-1E cells. MIN6 cells were incubated with medium containing basal or high concentration of different BCAA catabolites for 48 hours. The concentrations of BCAA and its catabolites used in the *in vitro* studies are similar to those we observed in the circulation of *db/db* mice, which mimic the diabetic conditions. After exposure to the catabolites, MIN6 β-cells were subjected to glucose-stimulated insulin secretion (GSIS) assay. In brief, the treated cells were stimulated with basal (2 mM) or 20 mM glucose for 30 minutes, and insulin secreted into the conditional medium was measured using an insulin ELISA. Basal insulin secretion under low concentration of glucose was comparable between β-cells cultured with or without a high concentration of catabolites. The mixture of BCKA (KIC, KMV and KIV) displayed a significant inhibitory effect

on insulin secretion (Figure 4.1. B), whereas BCAA (a mixture of leucine, isoleucine and valine) and C3 or C5 acylcarnitine alone had no obvious effect on insulin secretion (Figure 4.1. A and C). Further investigation revealed that individual BCKA was not sufficient to impair GSIS (Figure 4.1. D). Therefore, BCKA mixture (KIC, KMV and KIV) was used for the following functional studies unless otherwise specified. The adverse effect of BCKA overload on GSIS was also observed in the isolated pancreatic islets (Figure 4.1. E). To conclude, these data suggest that the toxic downstream catabolite - BCKA, but not BCAA per se, contributes to pancreatic β-cell dysfunction.

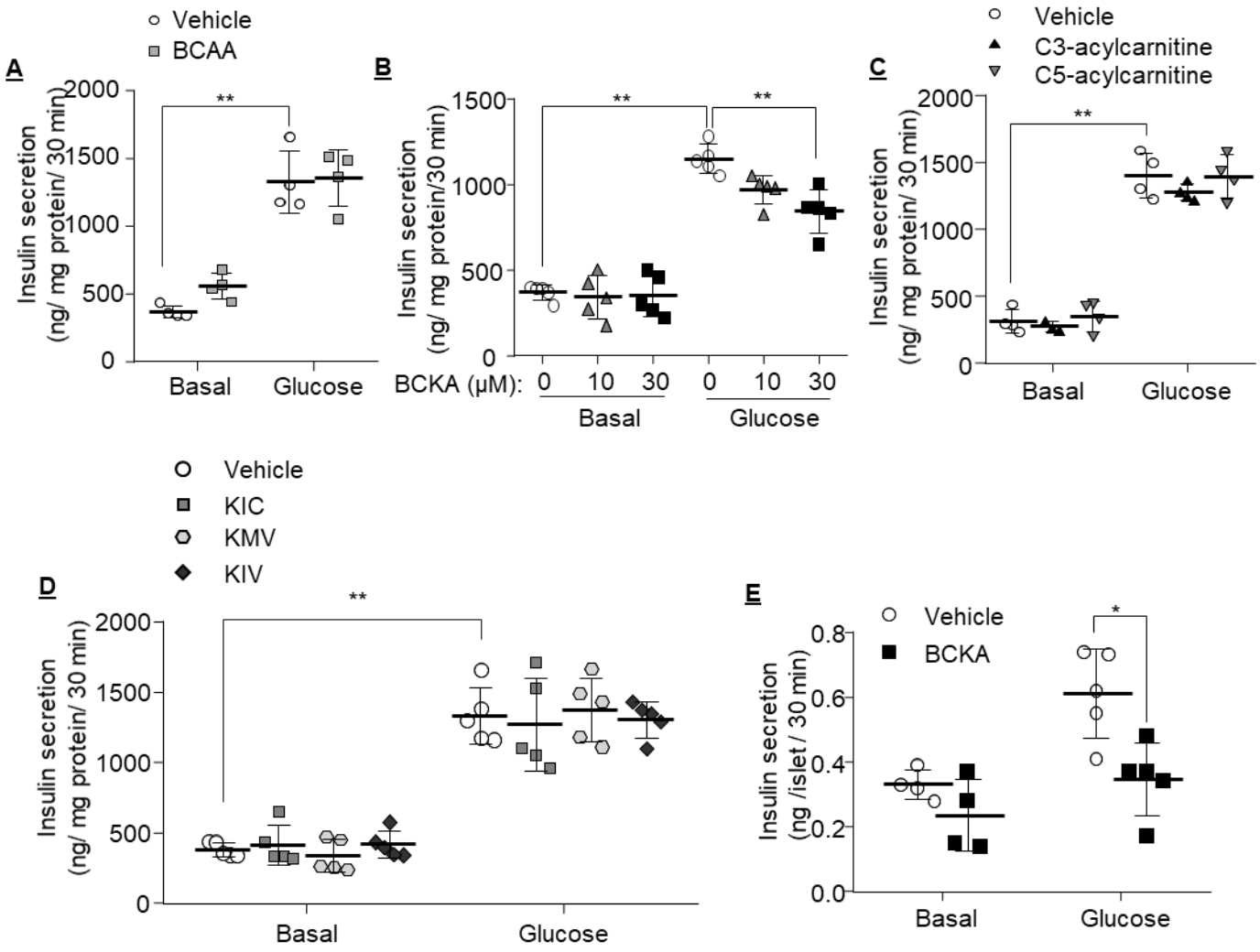


**Figure 4.1. Effect of chronic exposure of BCAA and its downstream metabolites on insulin secretion.** *(A-D)* The MIN6 β-cells were cultured in medium supplemented with *(A)* vehicle or 1.6 mM BCAA, *(B)* vehicle, 10 μM or 30 μM BCKA, *(C)* vehicle, 2μM C3-acylcarnitine or 0.3 μM C5-acylcarnitine, *(D)* vehicle or 30 μM individual KIC, KMV or KIV for 48 hours. The treated cells were incubated with Krebs buffer containing 0.1% fatty acid-free BSA and 2 mM glucose for 90 min, followed by stimulation with 2 mM (basal) or 20 mM glucose for 30 min. The secreted insulin into the conditional medium was measured using an insulin ELISA kit and normalized by protein concentration. n=*3-5*. *(E)* Islet isolated from 12-week–old C57BL/J mice were incubated with or without 30 μM BCKA for 48 hours, followed by static GSIS as described above and insulin secretion was normalized with islet size. n=4-5. All results are presented as mean ± s.d. Significance was determined using Student's t-test or one-way ANOVA with Bonferroni correction. *$p < 0.05$ and **$p < 0.01$.

### 4.2.2 Feeding with BCKA impairs insulin secretion and induces glucose intolerance in mice

To further confirm the detrimental effect of BCKA on pancreatic β-cells, 16-week-old C57BL/J mice were treated vehicle or BCKA via drinking water. Circulating levels of BCKA were gradually increased in mice treated with BCKA, and the levels were similar to that in *db/db* diabetic mice (Figure 4.2. A). Glucose tolerance test (GTT) revealed that treatment with BCKA for 2 weeks induced glucose intolerance (Figure 4.2. B). Besides, circulating insulin concentrations during GTT were significantly reduced in BCKA-fed mice (Figure 4.2. C). On the other hand, BCKA treatment did not alter insulin sensitivity in mice as demonstrated by insulin tolerance test (ITT) performed at week-3 (Figure 4.2. D). Arginine-stimulated insulin secretion was performed to determine whether BCKA caused a generalized or a specific defect in insulin secretion. No obvious difference in arginine-stimulated insulin secretion was found between the two groups (Figure 4.2. E). GTT and GSIS experiments were repeated in mice treated with BCKA for four weeks. Severe glucose intolerance and defective GSIS were observed with a longer treatment of BCKA (Figure 4.2. F and G). On the other hand, BCKA feeding did not change food intake, body weight, short-term fasting blood glucose, and blood insulin (Table 4.1). Although the mice with BCKA feeding displayed an elevation in circulating level of BCKA, their circulating BCAA levels were similar to the mice treated with vehicle (Table 4.1). These observations in cells and animal studies lead to a speculation that BCKA but not BCAA exerts a toxic effect on pancreatic β-cell function.

To explore the potential causes for the detrimental effect of BCKA on pancreatic β-cell function, the mice were sacrificed after 4-week feeding with vehicle or BCKA

supplementation. Pancreatic sections were prepared for immunohistochemistry analyses and histological analyses. H&E staining revealed that there was no difference in the morphology and size of islet between the two groups (Figure 4.3. A and B). To measure insulin content, immunochemical staining of insulin was performed in the pancreatic sections. This assay showed no difference in the islet insulin content between the mice treated with BCKA or vehicle (Figure 4.3. C and D). Additionally, percentages of α and β-cells, visualized by immunofluorescent staining of glucagon and insulin, respectively, were also similar between the two groups. (Figure 4.3. E and F). These data exclude the possibility that above factors involve in the regulation of GSIS by BCKA.

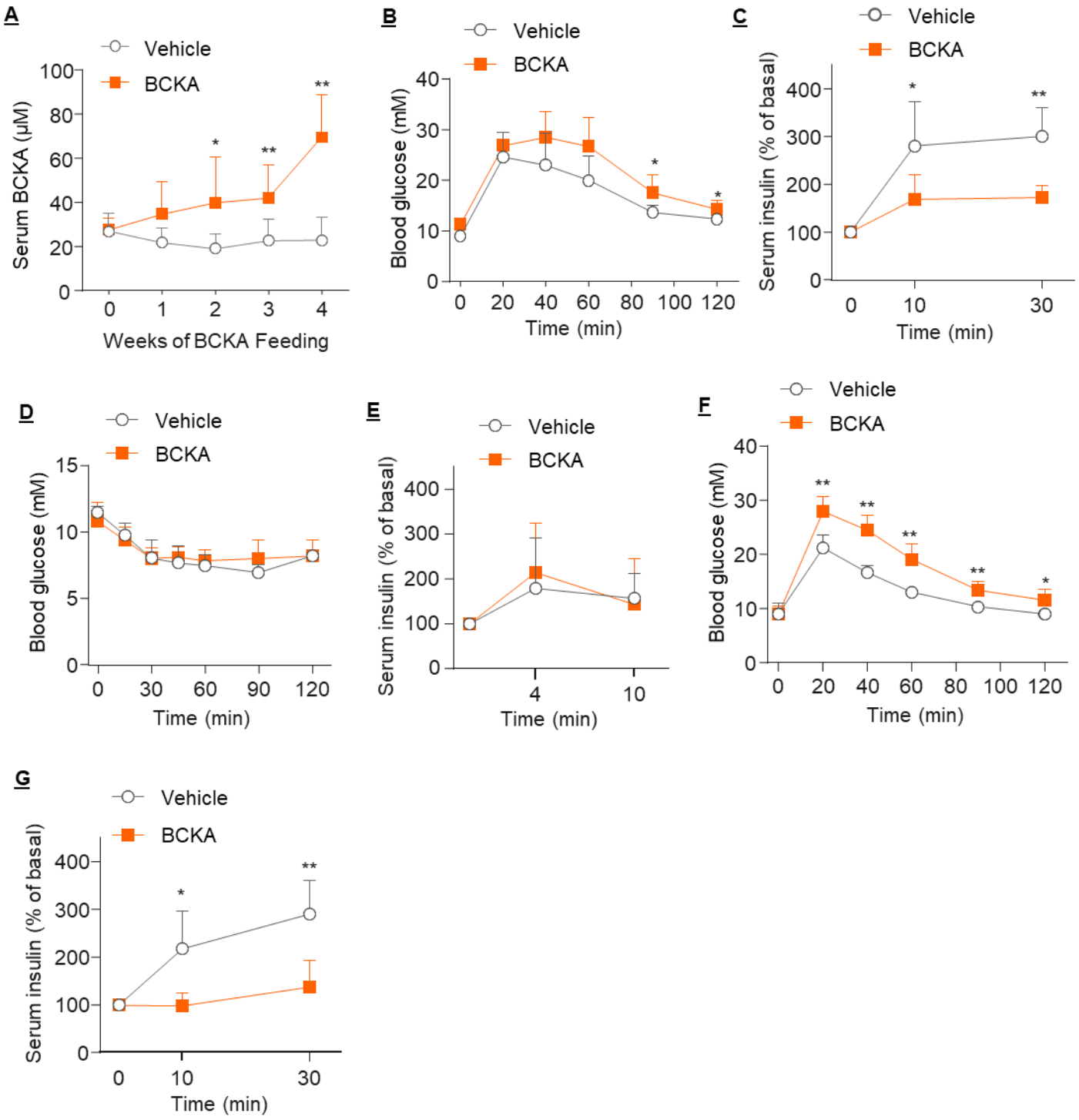


**Figure 4.2. Feeding with BCKA impairs insulin secretion and induces glucose intolerance in mice.** *(A-G)* 16-week-old male C57BL/J mice were randomly assigned into two groups having free access to drinking water supplemented with or without BCKA (5mg/ml of KIC, KMV and KIV each) for 4 weeks. *(A)* Circulating levels of BCKA during feeding. *(B)* GTT in 6-hour-fasted mice in the 2ed week of feeding (2 g glucose/kg). *(C)* GSIS in the 2ed week. Serum insulin were measured by an insulin ELISA kit. *(D)* ITT in 6-hour-fasted mice in the 3rd week (0.5 IU insulin/kg). *(E)* Arginine induced insulin secretion in overnight fasted-mice in the 4th week (1g arginine/kg). *(F)* GTT after BCKA feeding for 4 weeks. *(G)* GSIS after BCKA feeding for 4 weeks. n=6-7. All results are presented as mean ± s.d. Significance was determined using Student's t-test. *$p < 0.05$ and **$p < 0.01$.

**Table 4.1. Circulating levels of BCAA related catabolites after treatment with BCKA**

| | Vehicle | BCKA |
|---|---|---|
| Age (week) | 16 | 16 |
| Sex | Male (6) | Male (6) |
| Food intake (g/day) | 3.67±0.55 | 4.11±0.44 |
| Body weight (g) | 28.84±0.69 | 29.63±1.14 |
| Fasting glucose (mM) | 7.10±1.05 | 6.63±1.96 |
| Fasting insulin (ng/ml) | 0.259±0.307 | 0.247±0.341 |
| Serum leucine (μM) | 209.49±12.22 | 212.26±9.56 |
| Serum isoleucine (μM) | 122.43±18.62 | 130.28±17.56 |
| Serum valine (μM) | 201.76±22.20 | 192.39±11.98 |
| Serum KIV (μM) | 9.63±2.00 | 19.90±5.42* |
| Serum KIC (μM) | 6.69±1.17 | 16.59±2.17** |
| Serum KMV (μM) | 13.92±4.19 | 37.96±4.00** |

16-week-old male C57BL/J mice were fed with BCKA or vehicle in drinking water for 4 weeks. Fasting glucose was measured after 6-hour fasting. Results are presented as means ± s.d. *$p < 0.05$ and **$p < 0.01$.

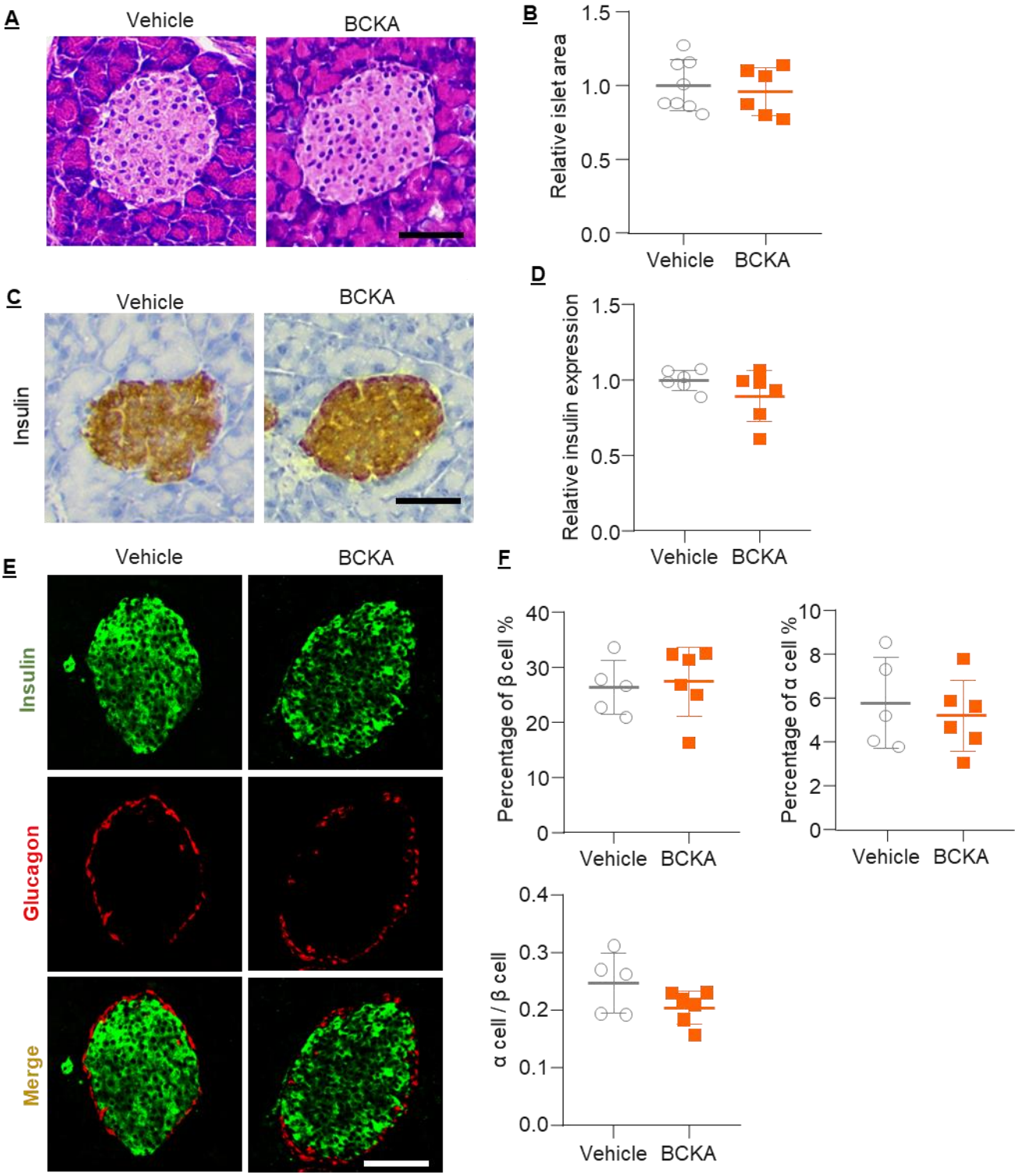


**Figure 4.3. Effect of BCKA on pancreatic islet size, insulin content and islet morphology.** 16-week-old male C57BL/J mice were fed with drinking water with or without BCKA supplementation (5 mg/ml) for 4 weeks. Pancreatic sections were prepared for following analyses. *(A)* H&E staining. *(B)* Area of islets as quantified from the result of H&E staining. n=6-8. *(C)* IHC staining of insulin and *(D)* relative expression of insulin was quantified. n=6. *(E)* Immunofluorescence staining of insulin (green) and glucagon (red). *(F)* Proportions of pancreatic β-cell (insulin positive), α-cell (glucagon positive) and ratio of α-cell to β-cell in pancreatic islets in panel *(E)* were quantified. n=5-6. Scale bar: 50 μm. All quantifications were performed using Image J software. All results are presented as mean ± s.d. Significance was determined using Student's t-test.

### 4.2.3 Downregulation of PPM1K induces excessive accumulation of BCKA and defective insulin secretion in pancreatic β cells

PPM1K is the key protein to upregulate BCAA catabolic flux by inducing dephosphorylation of the enzyme BCKDH-A (Figure 4.4. A). Chapter 3 showed that the expression of PPM1K was largely reduced in diabetic islets compared with healthy controls (Figure 3.7. B). In addition, an excessive amount of BCKA impaired GSIS. Therefore, I speculated that reduction of PPM1K caused excessive accumulation of BCKA, which in turn caused defective GSIS. To test this, siRNA was employed to silence *PPM1K*. After that, BCAA catabolism and GSIS were assessed in INS-1E cells. INS-1E cells were selected due to higher transfection efficiency than MIN6 cells. The knockdown efficiency by siRNA transfection was validated by immunoblotting analysis. INS-1E cells transfected with siRNA against *PPM1K* showed a remarkable reduction of PPM1K protein when compared to those transfected with *scrambled* control (Figure 4.4. B). In line with the phosphatase function of PPM1K on BCKDH-A activity, knockdown of PPM1K expression induced around a two-fold increase in the phosphorylation of BCKDH-A, while expression of total BCKDH-A remained unchanged, suggesting that BCKDH-A was inactivated in PPM1K deficient pancreatic β-cells (Figure 4.4. B and C).

To further demonstrate that knockdown of PPM1K expression led to attenuated BCAA metabolism in pancreatic β-cells, intracellular BCKA (KIC, KMV and KIV) was measured in INS-1E cells cultured with normal medium. KIC and KMV but not KIV were significantly accumulated in INS-1E cells with downregulation of PPM1K (Figure 4.4. D). A higher elevation of intracellular BCKA was observed when PPM1K deficient β-cells were cultured with media containing a high concentration of BCAA (Figure 4.4.

E). These data suggest the reduction of PPM1K expression significantly abrogates BCKA catabolism, leading to an increased accumulation of BCKA in β-cells.

Similar to treatment with excessive BCKA, knockdown of PPM1K expression also caused defective GSIS in INS-1E cells (Figure 4.4. F). To further confirm the role of PPM1K in GSIS, islets were isolated from WT and *PPM1K* knockout mice. *PPM1K* knockout mice were obtained from Dr. Yinbing Wang from the University of California at Los Angeles (49, 82) (the pioneer in BCAA research, who discovered PP1MK as a phosphatase of BCKDH-A). As expected, PPM1K deficient islets exhibited diminished GSIS compared with WT islets (Figure 4.4. G). Taken together, these data suggest that deficiency of PPM1K induces accumulation of BCKA and defective insulin secretion in pancreatic β-cells.

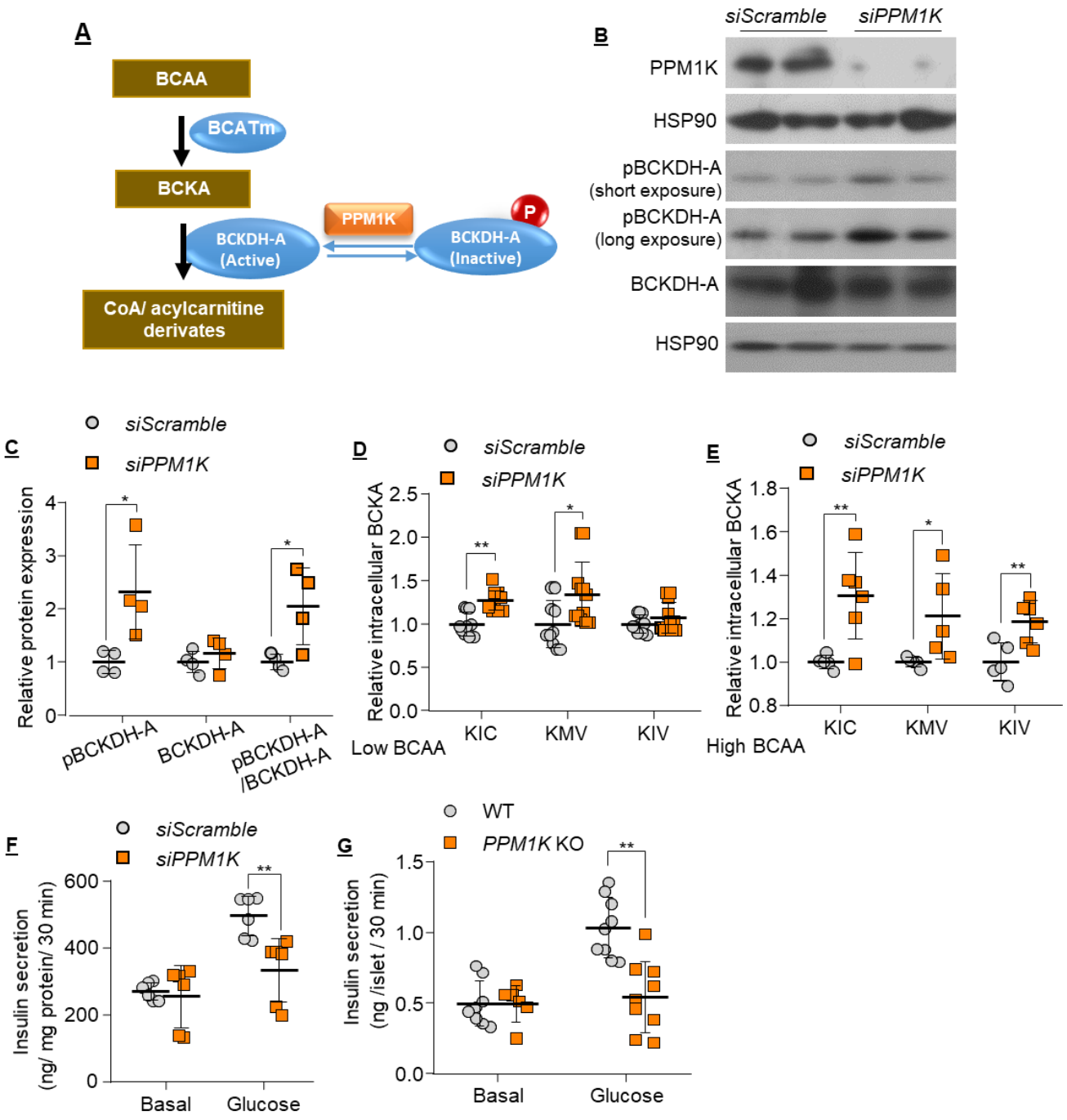


**Figure 4.4. Downregulation of PPM1K induces excessive accumulation of BCKA and defective insulin secretion in pancreatic β-cells.** *(A)* Diagram showing PPM1K enhances BCKDH-A activity by inducing dephosphorylation. *(B-F)* INS-1E cells were transfected with siRNA against *PPM1K* or *scramble* for 48 hours. *(B)* Knockdown of *PPM1K* expression was confirmed by immunoblotting analysis, which also showed an induction of BCKDH-A phosphorylation. *(C)* Quantification of relative abundance of pBCKDH-A, total BCKDH-A and ratio of pBCKDH-A to BCKDH-A normalized with HSP90. n=4. *(D-E)* The transfected cells were treated with *(D)* low BCAA (0.3 mM) or *(E)* high BCAA (5 mM) for 8 hours, followed by measurement of intracellular levels of BCKA by LC-MS/MS. *(D)* n=10-12. *(E)* n=5-6. *(F)* Static GSIS normalized to total protein. n=4-6. *(G)* Islets isolated from 12-week-old male WT and *PPM1K* KO mice were subjected to static GSIS and insulin secretion was normalized with islet size. n=6-9. All results are presented as mean ± s.d. Significance was determined using Student's t-test. *$p < 0.05$ and **$p < 0.01$.

### 4.2.4 BT2 treatment prevents BCKA accumulation and alleviates BCKA-induced defective insulin secretion in pancreatic β-cells

The above experiments demonstrated that overload of BCKA impaired insulin secretion in pancreatic β-cells. Next, I questioned whether such a detrimental effect could be alleviated by enhancing BCAA catabolism using the pharmacological activator 3,6-dichlorobenzo[b]thiophene-2-carboxylic acid (BT2). A previous study identified that BT2 activates the activity of BCKDH-A by binding to BDK, leading to dissociation of BDK from the BCKDH complex (79). First, whether or not BT2 could promote BCAA catabolism in INS-1E β-cells was tested. As expected, treatment with BT2 induced dephosphorylation of BCKDH-A at serine 293 (Figure 4.5. A), indicating the enzyme activity of BCKDH-A was activated. Intracellular levels of BCKA were dramatically increased in pancreatic β-cells upon incubation with a medium containing high concentration of BCAA or BCKA, but the elevation could be prevented by treatment with BT2 (Figure 4.5. B and C). More importantly, treatment with BT2 reversed the defective GSIS in pancreatic β-cells induced by chronic exposure to high BCKA. These findings further confirm the cytotoxic impact of BCKA on pancreatic β-cell function.

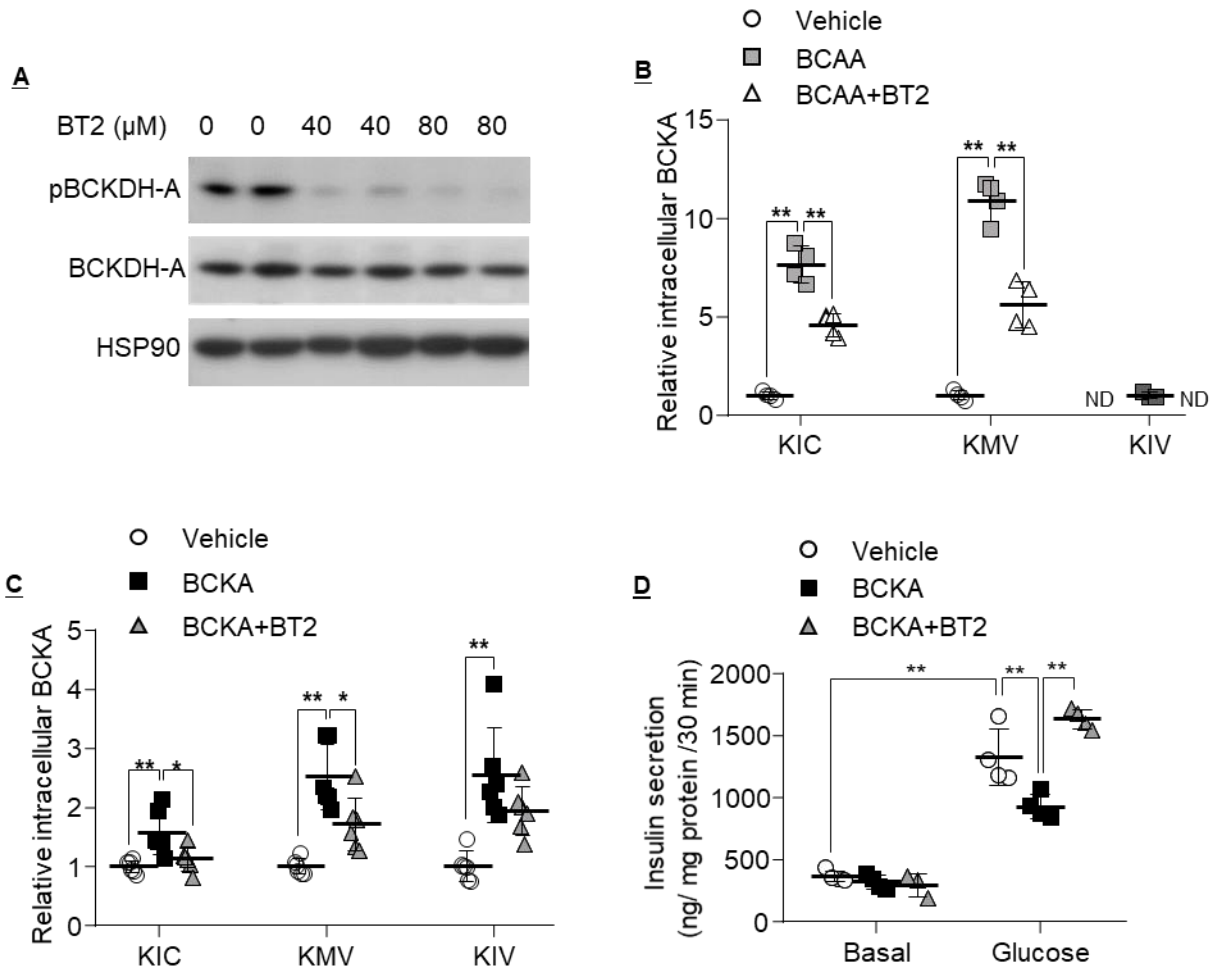


**Figure 4.5. BT2 prevents BCKA accumulation and alleviates BCKA-induced defective insulin secretion in pancreatic β cells.** *(A)* INS-1E cells were treated with different concentrations of BT2 for 1 hour. Total cell lysates were subjected to immunoblotting analysis for pBCKDH-A (serine 293), total BCKDH-A and total HSP90. *(B)* INS-1E cells were treated with vehicle or 5 mM BCAA and/or 40 μM BT2 for 2 hours. n=3-4. *(C)* MIN6 cells were treated with vehicle or 30 μM BCKA and/or 40 μM BT2 for 2 hours. n=6. *(B-C)* Intracellular levels of BCKA were detected by LC-MS/MS. ND (Not detectable). *(D)* The MIN6 β cells were cultured in medium supplemented with vehicle or 30 μM BCKA and/or 10 μM BT2 for 48 hours, followed by static GSIS. n=3-4. All results are presented as mean ± s.d. Significance was determined using Student's t-test or one-way ANOVA with Bonferroni correction. *$p < 0.05$ and **$p < 0.01$.

### 4.2.5 Treatment with BT2 improves glucose intolerance and glucose-stimulated insulin secretion in *db/db* diabetic mice

The above studies demonstrated that BT2 exerts a protective effect against BCKA-induced pancreatic β-cell dysfunction *in vitro*. Next, *db/db* diabetic mice were used to examine whether treatment with BT2 could alleviate β-cell dysfunction and improve glucose homeostasis in T2D. 20-24-week old *db/db* mice were assigned into two groups according to their short-term fasting blood glucose levels. No difference was found in fasting glucose level between the two groups before BT2 treatment. The mice were intraperitoneally injected with BT2 at a dose of 20 mg/kg or vehicle (diluted into 5 % DMSO in 0.1 M sodium bicarbonate, pH 9.0) for 4 weeks. After treatment with BT2 for one week, serum samples were collected for the measurement of BCAA and BCKA. Targeted metabolomics analysis showed a dramatic reduction in both circulating BCAA and BCKA in *db/db* diabetic mice treated with BT2 compared with those treated with vehicle control (Figure 4.6. A and B).

GTT was performed after treatment with BT2 for 1 week. As indicated in Figure 4.6. C, after glucose injection, *db/db* mice with BT2 treatment displayed improved glucose tolerance. These mice had a relatively lower blood glucose than the mice treated with vehicle. More importantly, the improved glucose tolerance in BT2 treated *db/db* mice was accompanied by an enhanced GSIS. Serum insulin concentration was significantly increased at the 10-minute and 30-minute after glucose injection in the BT2-treated diabetic mice, whereas serum insulin level remained unchanged in the controls treated with vehicle (Figure 4.6. D-E). Given that blood glucose is collectively controlled by the amount of insulin released from pancreatic β-cells and insulin signaling pathway in the peripheral tissues, ITT was performed to evaluate insulin sensitivity. No difference

in insulin sensitivity was found between mice treated with vehicle or BT2 (Figure 4.6. F). These data suggest that BT2 improves glucose intolerance in *db/db* diabetic mice by promoting insulin secretion.

Apart from glucose, arginine is also known to act as an insulinotropic signal to directly trigger insulin secretion by inducing β-cell membrane depolarization. The mechanism underlying insulin secretion induced by glucose is distinct from that induced by arginine. It was interesting to find that BT2 treatment did not alter arginine-induced insulin release (Figure 4.6. G), suggesting that BT2 and BCAA catabolism might specifically regulate glucose-mediated insulin secretion.

Metabolic parameters of *db/db* diabetic mice with BT2 and vehicle treatment were listed in Table 4.2. No significant difference was found in food intake, body weight, fasting blood glucose, and fasting insulin between the two groups. Noted that there was also no difference in HOMA-IR, the index for assessing insulin resistance.

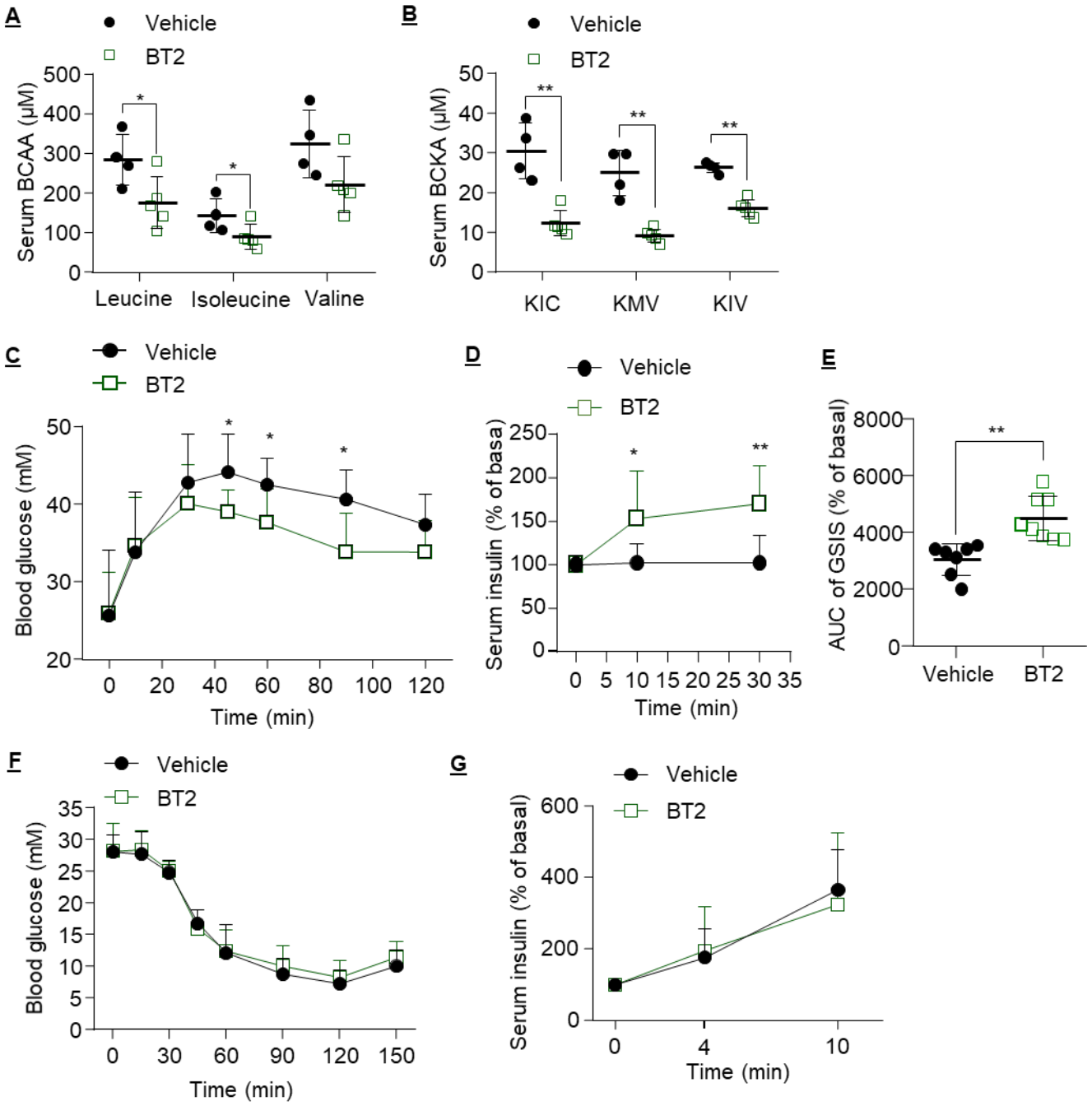


**Figure 4.6. Treatment with BT2 improves glucose intolerance and glucose-stimulated insulin secretion in *db/db* diabetic mice.** 20 to 24-week-old male and female *db/db* mice were intraperitoneally injected with BT2 at a dose of 20 mg/kg or vehicle for 4 weeks. (*A-B)* Circulating levels of *(A)* BCAA and *(B)* BCKA in the 7th day of treatment. n=4-5. *(C)* GTT in overnight fasted-mice with treatment for 1 weeks (1 g glucose/kg). *(D)* GSIS and *(E)* AUC of GSIS in *(C).* Serum insulin were measured by an insulin ELISA kit. *(F)* ITT in 6-hour-fasted mice after 2 weeks of treatment (1.25 IU insulin/kg). *(G)* Arginine induced insulin secretion in overnight fasted-mice after 3 weeks of treatment (1g arginine/kg). n=6. All results are presented as mean ± s.d. Significance was determined using Student's t-test. *$p < 0.05$ and **$p < 0.01$.

**Table 4.2. Effect of BT2 treatment on food intake, body weight, blood glucose and insulin in *db/db* diabetic mice.**

| | *db/db* -Vehicle | *db/db* -BT2 |
|---|---|---|
| Age (week) | 20-24 | 20-24 |
| Sex | Male (4); Female (2) | Male (4); Female (2) |
| Food intake (g/ day) | 6.641±3.551 | 7.246±3.241 |
| Body weight (g) | 50.51±10.15 | 50.17±3.38 |
| Fasting glucose (mM) | 18.08±2.93 | 14.52±3.67 |
| Fasting insulin (ng/ml) | 4.55±2.98 | 3.385±1.499 |
| HOMA-IR | 65.67±37.32 | 60.18±17.06 |
| HOMA-beta | 90.58±70.16 | 99.43±44.61 |

*db/db* mice were intraperitoneally injected with BT2 at a dose of 20 mg/kg or vehicle control for 4 weeks. All results are presented as mean ± s.d. Significance was determined using Student's t-test. *$p < 0.05$ and **$p < 0.01$.

## 4.3 Summary

This chapter aims to explore the association between defective BCAA catabolism and pancreatic β-cell function. BCKA, but neither BCAA nor acylcarnitine, negatively regulated pancreatic β-cell function. Chronic overload of BCKA impaired insulin secretion in pancreatic β-cell lines and mice. Such a detrimental effect could be alleviated by the BCKDH activator BT2, which enhanced BCAA catabolic flux and reduced BCKA in cells and diabetic mice model. Furthermore, disruption of BCAA catabolism by downregulation of *PPM1K* caused BCKA accumulation in pancreatic β-cells and defect in insulin secretion. Taken together, these data highlight the possibility of improving pancreatic β-cell function by manipulation with BCAA catabolic pathway. Additionally, our animal study showed that BCKA feeding had no obvious impact on pancreatic islet size, insulin content, and islet morphology.

# Chapter 5 Defective BCAA catabolism diminishes insulin secretion by interrupting glucose metabolism in pancreatic β-cells

## 5.1 Introduction

Glucose is a major nutrient signal to trigger insulin release from pancreatic β-cells. This complex process involves multiple steps. In brief, glucose is transported into pancreatic β-cells and then metabolized by glycolysis and TCA cycle to produce ATP. The increase of ATP/ADP ratio induces a closure of the ATP-sensitive K+ (KATP) channel, leading to membrane depolarization and Ca2+ influx, which in turn triggers first-phase insulin secretion (93). The subsequent second-phase insulin secretion requires multiple coupling factors and F-actin remodeling for exocytosis of insulin granules (95). Diminished first- and second-phase GSIS are both observed in T2D (93), yet the underlying pathogenic mechanism remains elusive.

The inhibitory effect of BCKA on GSIS raised the possibility that defective BCAA catabolism disrupts glucose metabolism in pancreatic β-cells. In this chapter, I aim to investigate how defective BCAA catabolism impairs glucose metabolism that couples insulin secretion in pancreatic β-cells.

## 5.2 Result

### 5.2.1 BCKA impairs ATP production in pancreatic β-cells

To pinpoint the precise step by which BCKA affects GSIS, first, glucose uptake was measured in MIN6 cells by using an assay kit. 2-Deoxy-d-glucose (2-DG) is a stable glucose analogue thant cannot be metabolited by glycolysis. Therefore, intracellular 2-DG is able to directly reflect glucose uptake rate. Glucose uptake rate was comparable in MIN6 β-cells treated with vehicle or BCKA. (Figure 5.1. A). Next, mitochondrial membrane potential was assessed using a probe TMRE by detection of fluorescence intensity, which did not show any alteration by BCKA treatment in β-cells (Figure 5.1. B). Interestingly, ATP production upon glucose stimulation was significantly reduced in BCKA-treated β-cells, despite the fact that no change was observed under basal condition (Figure 5.1. C). On the other hand, non-glucose stimulator KCl could directly trigger insulin secretion without affecting glucose metabolism. BCKA treatment had no effect on KCl-induced insulin secretion (Figure 5.1. D), reinforcing the idea that BCKA selectively affects glucose-induced insulin secretion. Therefore, it was likely that glucose metabolism was disrupted by overexposure to BCKA.

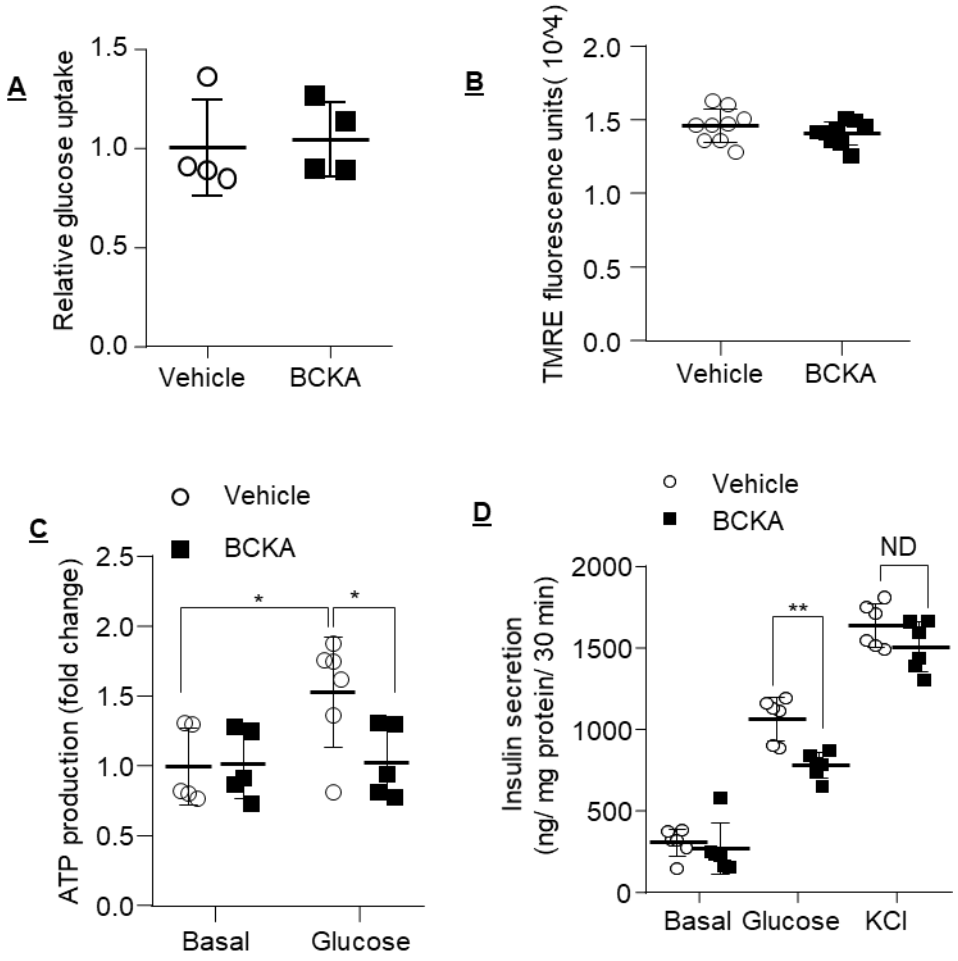


**Figure 5.1. BCKA impairs ATP production in pancreatic β-cells.** The MIN6 β-cells were cultured in medium supplemented with vehicle or 30 μM BCKA for 48 hours. *(A)* Glucose uptake in the treated cells. *(B)* The treated cells were incubated with 100 nM TMRE for 30 min, followed by measurement of fluorescence at 530/580nm. Loss of mitochondrial membrane potential was reflected by an increase in fluorescence intensity. n=9. *(C)* ATP production upon stimulation with 2 mM (basal) or 20 mM glucose for 10 min. n=5-6. *(D*) Static insulin secretion stimulated by 2 mM glucose, 20 mM glucose or 50 mM KCl for 30 min. n=6.*(C-D)* Results were normalized with protein concentration. All results are presented as mean ± s.d. Significance was determined using Student's t-test. *$p < 0.05$ and **$p < 0.01$

### 5.2.2 Overload of BCKA diminishes glucose metabolism in pancreatic β-cells

Glucose induces ATP production mainly via glycolysis in the cytosol and oxidative phosphorylation in the mitochondria. Therefore, effect of BCKA on glycolysis and mitochondrial oxidation was assessed using a Seahorse XF analyzer. This analysis allowed to monitor the dynamic change of glucose metabolism in live cells at a real-time manner. Extracellular acidification rate (ECAR) reflects glycolytic flux, while oxygen consumption rate (OCR) is an indicator of aerobic metabolism of glucose via TCA cycle and mitochondrial oxidative phosphorylation. Chronic treatment with BCKA reduced both ECAR and OCR in MIN6 β-cells under a high glucose condition, but had no effect under a basal glucose condition (Figure 5.2. A and B). The reduction in ECAR and OCR could be reversed by treatment with the BCAA catabolic activator BT2 (Figure 5.2. C and D). These data suggest that excessive amount of BCKA diminished glucose metabolism in the step of glycolysis and/or TCA cycle.

To further delineate how BCKA affects glucose metabolism, intracellular metabolites generated from glycolysis and TCA cycle were measured using Capillary Electrophoresis–Mass Spectrometry (CE-MS) with the help from Dr. Hailong Piao from Dalian Institute of Chemical Physics, Chinese Academy of Sciences. Multiple metabolites generated from glycolysis and TCA cycle were identified by the CE-MS analysis. There was no change in the intracellular concentrations of fructose-6-phosphate, fructose-1,6-diphosphate, glycerol-3-phosphate, 3-phosphoglyceric acid, lactate, acetyl CoA, citrate, succinate, fumarate, and malate. However, dihydroxyacetone phosphate (DHAP) and pyruvate from glycolysis and α-Ketoglutarate (α-KG) from TCA cycle (Figure 5.3. A) were reduced in BCKA-treated MIN6 β-cells upon glucose stimulation. No signal of these metabolites could be

detected under basal condition, perhaps the sensitivity of the detection was not high enough and/or the metabolite concentrations were extremely low (Figure 5.3. B-D). The drop in glycolytic metabolites proved that chronic treatment with BCKA inhibited glycolysis in pancreatic β-cells. On the other hand, it still remained elusive whether BCKA had an effect on TCA cycle since the reduction in α-KG could result from either defective glycolysis or defective TCA cycle. Another question was that no significant alteration could be identified in other metabolites as mentioned above, which might result from a compensation from other metabolic pathways which cross-link with glycolysis and TCA cycle.

Taken together, I speculated that BCKA mainly affects glycolysis in pancreatic β-cells. Indeed, methyl pyruvate (end-product of glycolysis)-stimulated insulin secretion was not inhibited by BCKA treatment (Figure 5.3. E). These data argue that BCKA selectively affects the generation of pyruvate from glucose, which is required for the production of ATP and other coupling factors in TCA cycle for insulin secretion.

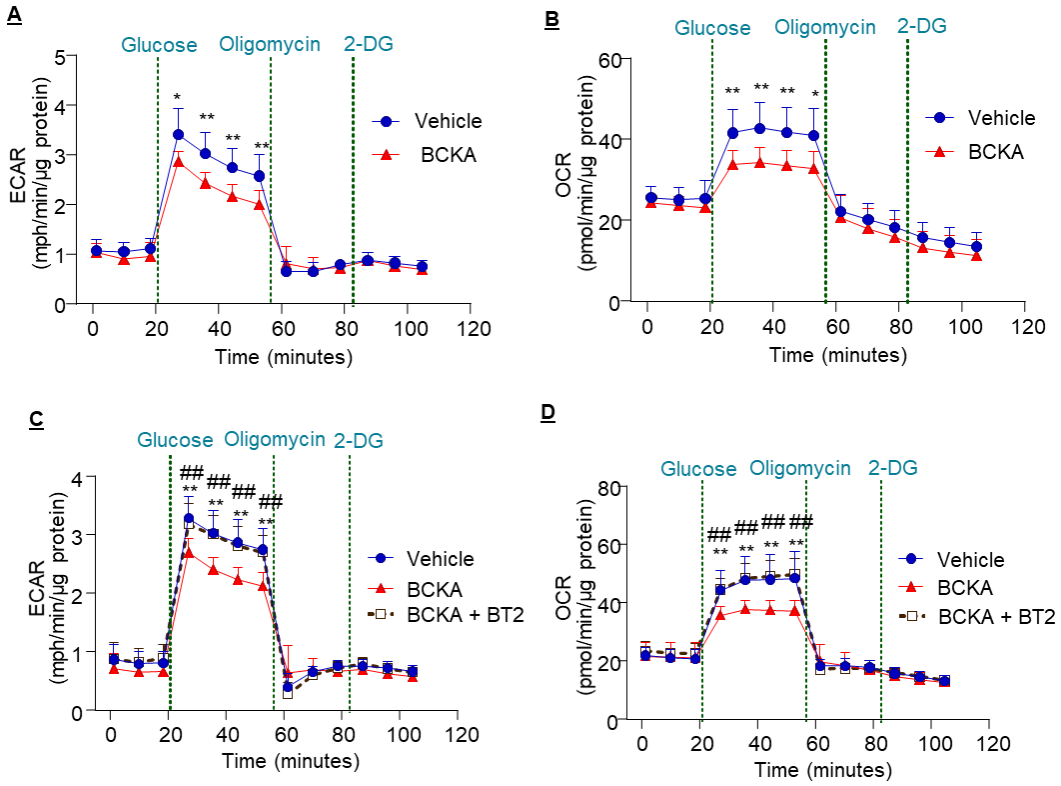


**Figure 5.2. Overload of BCKA diminishes glucose metabolism in pancreatic β-cells.** *(A-B)* The MIN6 β-cells were cultured in medium supplemented with vehicle or 30 µM BCKA for 48 hours. *(A)* ECAR and *(B)* OCR in the treated MIN6 cells in response to various stimuli as indicated. n=7. *(C-D)* The MIN6 β-cells were cultured in medium supplemented with vehicle or 30 µM BCKA and/or 10 µM BT2 for 48 hours**.** *(C)* ECAR and *(D)* OCR in the treated MIN6 cells in response to various stimuli as indicated. n=7. Results were normalized with protein concentration. All results are presented as mean ± s.d. Significance was determined using Student's t-test. *$p < 0.05$ and **$p < 0.01$

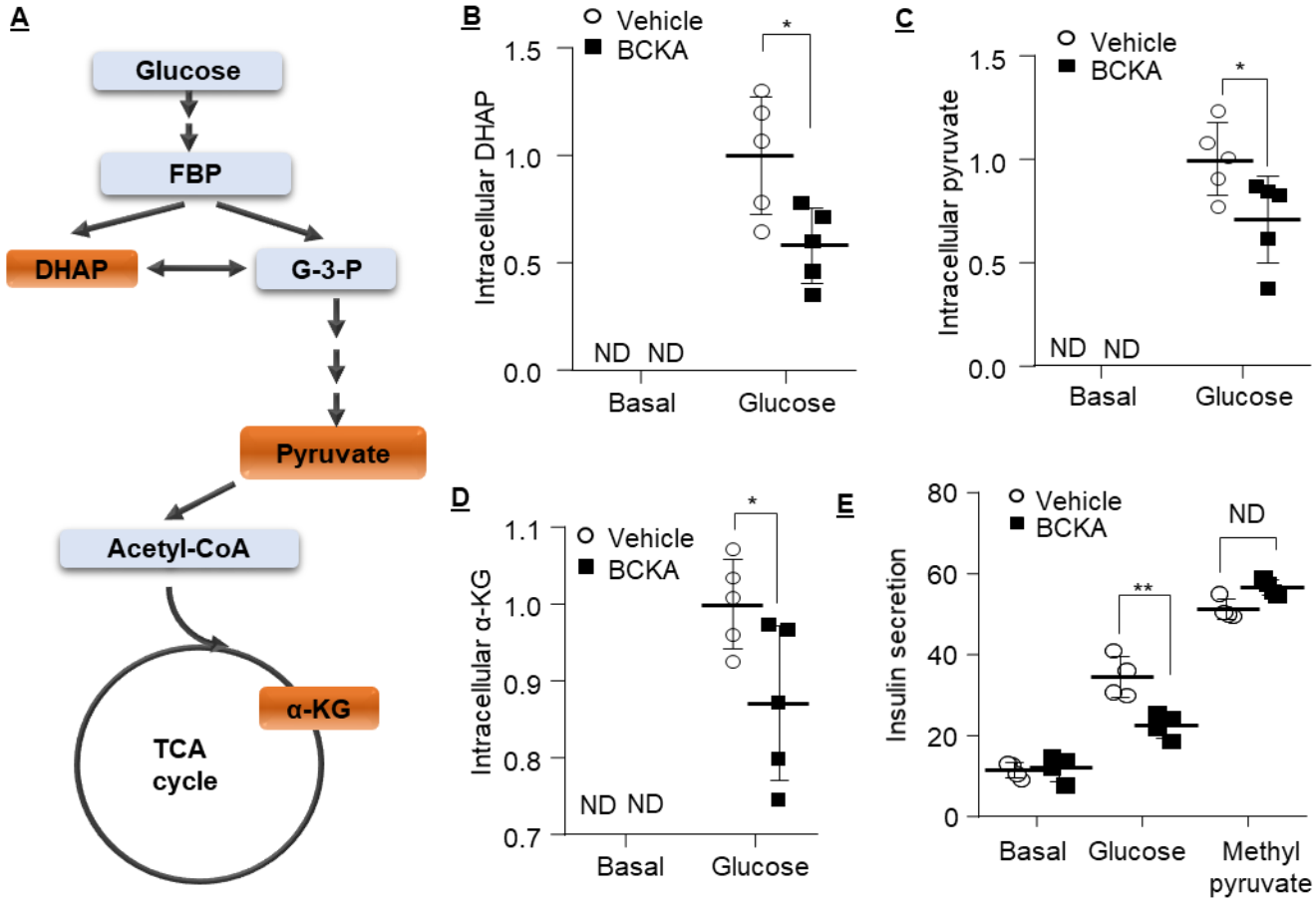


**Figure 5.3. Chronic treatment with BCKA inhibits production of glycolytic metabolites in pancreatic β cells.** *(A)* Diagram of glucose metabolism. *(B-E)* MIN6 cells were cultured with vehicle or 30 μM BCKA for 48 hours and then incubated with Krebs buffer containing 2 mM glucose for 90 min, followed by stimulation with 2 mM (basal) or 20 mM glucose for 30 min. Intracellular levels of glycolytic and TCA metabolites were detected by CE-MS. Metabolites in brown rectangles indicated in *(A)* displayed a reduction in BCKA-treated cells upon 20 mM glucose treatment, as showed in *(B)* DHAP, *(C)* pyruvate and *(D)* α-KG. n=5. *(E)* Static insulin secretion in the treated MIN6 cells stimulated by 2 mM glucose, 20 mM glucose or 40 mM methyl pyruvate for 30 min. n=3-4. All results are presented as mean ± s.d. Significance was determined using Student's t-test or one-way ANOVA with Bonferroni correction. *Vehicle vs BCKA, *$p < 0.05$ and **$p < 0.01$; #BCKA vs BCKA+BT2, #$p < 0.05$ and ## $p < 0.01$;

### 5.2.3 Downregulation of PPM1K disrupts glucose-induced ATP production.

Chapter 4 showed that disruption of BCAA catabolism by PPM1K downregulation caused an accumulation of BCKA and defective GSIS in β-cells. Therefore, I speculated that PPM1K downregulation might also impair glucose metabolism, in particular glycolysis. To test this, INS-1E β-cells were transfected with siRNA against Scramble or PPM1K, followed by the assays assessing glucose metabolism. siRNA-mediated downregulation of PPM1K did not affect glucose uptake rate but significantly reduced glucose-stimulated ATP production in INS-1E cells (Figure 5.4. A-B). Consistently, β-cells with PPM1K deficiency displayed a dramatic reduction of glycolysis and mitochondrial oxidation under a high glucose condition, as revealed by the Seahorse XF analyzer. (Figure 5.4. C-D). These data suggest that disrupted BCAA catabolism by PPM1K downregulation impairs glycolysis and glucose-induced ATP production, leading to defective insulin secretion in pancreatic β-cells.

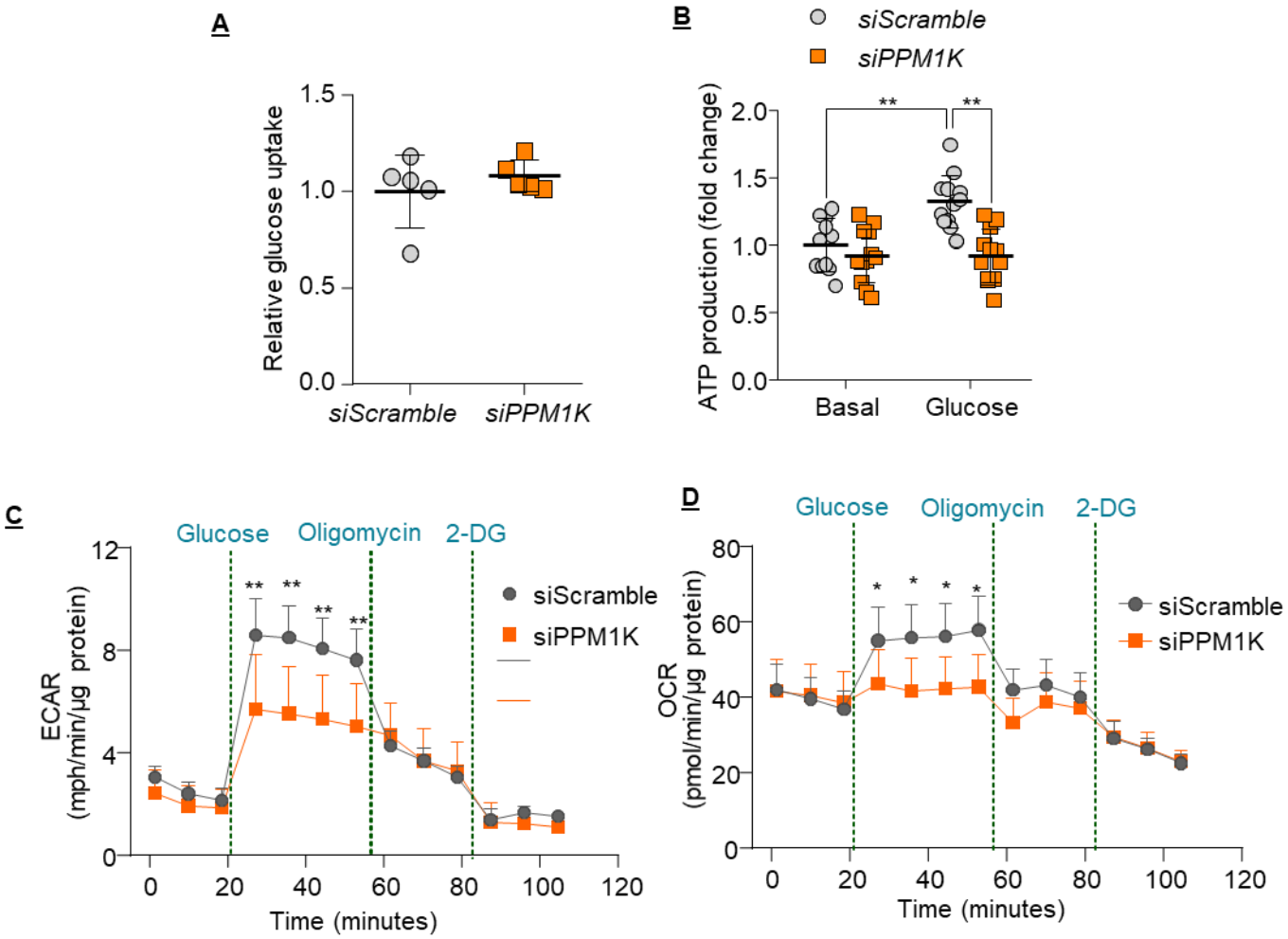


**Figure 5.4. Downregulation of PPM1K impaired glucose induced ATP production.** *(A-D)* INS-1E cells were transfected with siRNA against *PPM1K* or *scramble* for 48 hours, followed by analysis of *(A)* glucose uptake and *(B)* ATP production as described above. *(A)* n=4-5. *(B)* n=11-12. *(C)* ECAR and *(D)* OCR in the transfected INS-1E cells in response to various stimuli as indicated. n=6-8. All results are presented as mean ± s.d. Significance was determined using Student's t-test or one-way ANOVA with Bonferroni correction. *$p < 0.05$ and **$p < 0.01$

## 5.3 Summary

Glycolysis is the first step of intracellular glucose utilization, and it is essential for coupling glucose with pancreatic β-cell insulin secretion. Pyruvate, the end-product of glycolysis, fuels the mitochondrial TCA cycle and oxidative phosphorylation to drive the production of ATP, leading to insulin secretion. In this chapter, disrupted glucose metabolism was identified as a leading cause for the defective GSIS in pancreatic β-cells with BCKA overload or PPM1K downregulation. BCKA-induced disruption in glucose metabolism could be reversed by BT2 treatment. Taken together, these data suggest that defective BCAA catabolism diminishes insulin secretion by interrupting glucose metabolism in pancreatic β-cells.

# Chapter 6 The adaptor protein APPL2 controls F-actin remodeling and GSIS via RacGAP1-Rac1 signaling axis in pancreatic β-cells

## 6.1 Introduction

### 6.1.1 Adaptor proteins APPL1 and APPL2

Adaptor proteins containing an N-terminal Bin/Amphiphysin/Rvs (BAR) domain, a central pleckstrin homology (PH) domain, and a C-terminal phosphotyrosine binding (PTB) domain 1 and 2, refer as APPL1 and APPL2, respectively. Human APPL1 and APPL2 are highly homologous and both present in early endosomes, cytoplasm and nucleus. Originally, APPL1 and APPL2 emerged as the interacting partners of the small GTPase Rab5 and are known to regulate membrane trafficking and cell signaling transduction (117). Subsequent studies showed they have similar or opposite functions in glucose homeostasis in different cell types and contexts (118-120). In particular, APPL1 sensitizes adiponectin and insulin actions, whereas APPL2 exerts opposite actions. On the other hand, both APPL1 and APPL2 positively regulate insulin secretion in pancreatic β-cells. In human, APPL1 expression is positively correlated GSIS in the pancreatic islets, and its loss-of-function mutations were identified in the family with diabetic history (121). APPL1 was shown to enhance the effect of adiponectin on GSIS via the AMPK signaling pathway (122). APPL1 potentiates the first phase GSIS by increasing the expression of soluble N-ethylmaleimide-sensitive factor attachment protein receptor (SNARE) proteins, which serve as exocytotic machinery (123). Besides, in type 1 diabetic mouse model, APPL1 prevents inflammation and apoptosis in pancreatic β-cells by inhibition of nuclear factor NF-kappaB (124). These studies clearly indicate the protective effects of APPL1 on β-cells. However, it is unclear whether APPL2, the close homolog of APPL1, also plays a role in the regulation of β-cell function.

### 6.1.2 APPL2 deficiency impairs GSIS and glucose-stimulated F-actin remodeling (results by Baile Wang)

A previous study by Baile Wang (we are collaborators of this new study and co-first authors of the publication) showed that APPL2 expresses in both pancreatic islets and exocrine cells (125), but the effect of APPL2 on β-cell function is unknown. To answer this question, APPL2 was specifically deleted in β-cells by crossing *APPL2*$^{floxed/floxed}$ mice with β-cell-specific Cre transgenic mouse (Cre recombinase under the control of rat insulin promoter) (125). Baile Wang demonstrated that RIP-APPL2 KO mice displayed impaired glucose tolerance and GSIS at the age of 16 weeks, whereas insulin sensitivity was not altered. *Ex vivo*, consistent with the animal study, GSIS was reduced in pancreatic islets isolated from RIP-APPL2 KO mice when compared with those isolated from WT littermates. Potassium chloride-stimulated insulin secretion did not differ between APPL2 WT and KO islets, indicating the defective insulin secretion by APPL2 deficiency might be specifically related to glucose stimulation and/or the downstream of calcium influx. Further investigation showed that both first- and second-phase GSIS (first 9 minutes and 10-42 minutes of high glucose stimulation, respectively) were significantly diminished in APPL2 KO islets. These data suggest APPL2 is crucial for GSIS in pancreatic β-cells.

Multiple potential factors might contribute to defective GSIS, including reduced β-cell mass and insulin content, change in β-and α-cell area, disrupted glucose metabolism and/or its downstream signal transduction in β-cells. Among them, disrupted glucose-stimulated F-actin remodeling was identified as a potential cause for the defective GSIS in APPL2 KO islets. Previous studies showed that the BAR domain containing proteins play a role in the regulation of F-actin remodeling (126). It has been demonstrated

APPL2 is a key regulator for small GTPase activity through direct interaction with small GTPase such as Rab5 and Rab31 or GAP protein such as TBC1 Domain Family Member 1 (TBC1D1) (127, 128). In our study, siRNA was employed to knockdown APPL2 in INS-1E cells. Consistently, impaired GSIS was observed in β-cells with APPL2 downregulation. Next, intracellular F-actin actin was visualized by an F-actin fluorescent probe SPY-555. Real-time live-cell imaging revealed that glucose-stimulated F-actin depolymerization was abolished in INS-1E cells transfected with siAPPL2. The defective GSIS in APPL2 KO islets was partially rescued by promoting F-actin depolarization using latrunculin A which could disrupt F-actin structure. Furthermore, APPL2 deficiency diminished glucose-induced activation of Ras-related C3 botulinum toxin substrate 1 (Rac1), a guanosine triphosphatase (GTPase) of Rho family that is known to control insulin granule trafficking via F-actin remodeling and required for GSIS (129, 130).

Taken together, the findings from islets and INS-1E cells suggest that APPL2 deficiency impairs GSIS by abrogating F-actin remodeling.

## 6.2 Result

### 6.2.1 The defective GSIS in APPL2 deficient islets is due to impaired glucose-induced F-actin remodeling and Rac1 activation.

The works from Baile Wang demonstrated that APPL2 deficiency disturbs glucose-stimulated F-actin and subsequent GSIS in INS1-E cells. To further confirm this finding, F-actin distribution was examined in islets from RIP-APPL2 KO and WT mice using a real-time live-cell imaging approach. F-actin was visualized by fluorescent probe SPY555-actin, which is membrane permeable and specifically binds to endogenous F-actin filaments. The F-actin probe was validated by monitoring the change of F-actin in WT islets incubated with latrunculin A (a compound that depolymerizes actin filaments) for an hour. In line with previous studies (131, 132), the morphology of islets was obviously changed, and small clusters of F-actin were observed by stimulation with latrunculin A (Figure 6.2.1. A), proving the reliability of this method.

Next, the dynamic change of F-actin was monitored in islets isolated from RIP-APPL2 KO and WT mice with stimulation of low or high concentration of glucose for 10 minutes. No noticeable change of F-actin signal was found in islets maintained at low glucose condition, which served as a negative control to exclude the effect of photobleaching on F-actin fluorescent signal (Figure 6.2.1. B). Similar to the results in IN1S-E cells, glucose reduced F-actin signal in WT islets at a time-dependent manner, but this effect was dampened in APPL2 deficient islets (Figure 6.2.2. A-C). To further support the above finding, a second approach, phalloidin staining was employed to examine F-actin remodeling. Consistent with previous studies (96, 133), phalloidin staining revealed that glucose-stimulated significant F-actin depolymerization in WT islet, but this effect was abolished by APPL2 deficiency (Figure 6.2.2. D-E). To test

whether defective GSIS by APPL2 deficiency could be rescued by induction of F-actin deploymerization, islets from RIP-APPL2 KO mice and WT littermates were treated with cytochalasin B, a F-actin depolymerization agent. Latrunculin A and cytochalasin B are actin-depolymerizing agents that block F-actin assembly by sequestering binding of monomeric G-actin to the end of actin filaments, respectively (134, 135). Cytochalasin B partially rescued the defective GSIS in APPL2 deficient islets (Figure 6.2.2. F). Taken together, these data suggest that the defective GSIS in APPL2 deficient islets might be a result of aberrant F-actin depolymerization.

F-actin disassembly-mediated insulin granule trafficking is dependent on the activation of small GTPase including Rac1 and cell division cycle 42 (Cdc42) (96, 129, 130). Work by Baile Wang showed that APPL2 downregulation dramatically abrogated glucose-induced Rac1 activation, and here I demonstrated that APPL2 downregulation did not alter glucose-stimulated activation of Cdc42 (Figure 6.2.3. A). To confirm APPL2 regulates GSIS and F-actin remodeling via Rac1 activation, APPL2-knockdown INS-1E cells were transfected with a vector overexpressing constitutively active mutant of human Rac1 (Q61L) or an empty vector control (Figure 6.2.3. B). Rac1-Q61L possesses constitutively GTP-bound and unresponsive to its upstream GAP (136). As expected, constitutively active Q61L mutant strikingly reversed the defective GSIS in β-cells with APPL2 knockdown (Figure 6.2.3. C). These data suggest that APPL2 might regulate GSIS via Rac1-dependent F-actin remodeling.

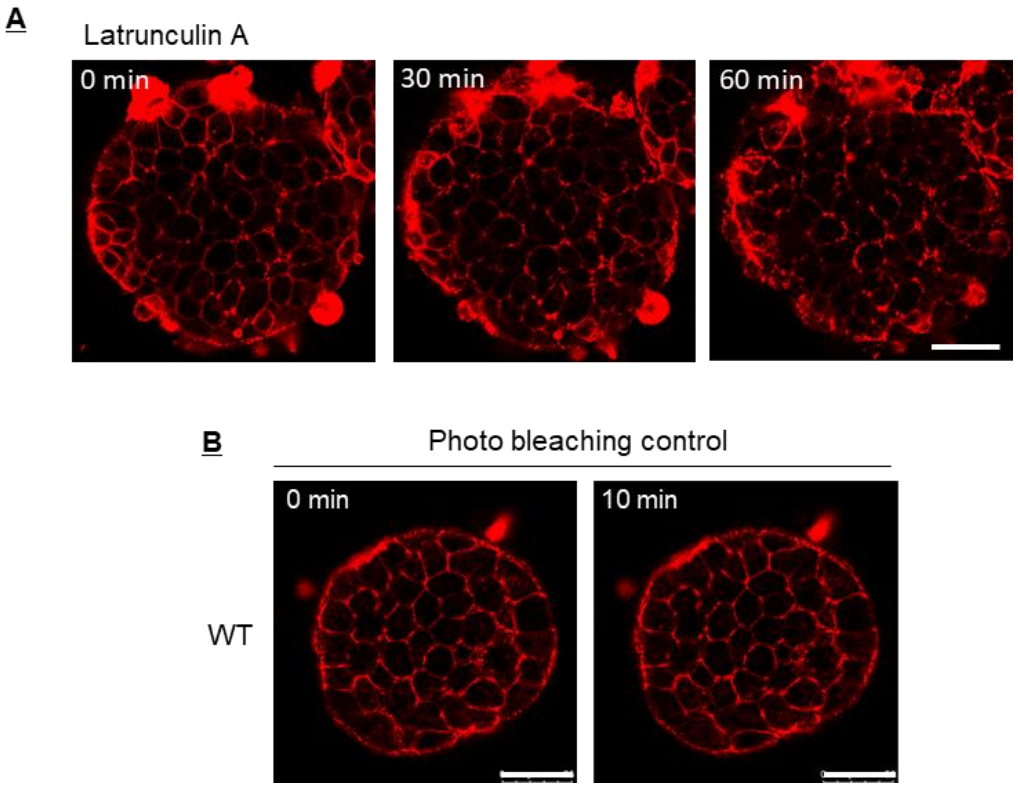


**Figure 6.2.1. Effect of Latrunculin A on F-actin structure in pancreatic islets.** Pancreatic islets isolated from WT mice labelled with SPY555-actin probe (red) were treated with Latrunculin A (0.5 μM) for 60 min. Representative two-photon confocal images captured at indicated time point upon Latrunculin A treatment were shown. Scale bar: 25 μm. (B) WT islets labeled with SPY555-actin probe (red) were incubated with a Krebs buffer with 2.8 mM glcuose, followed by two-photon confocal imaging for 10 min. This experiment acts as photobleaching control. Scale bar: 25 μm. Representative images were shown.

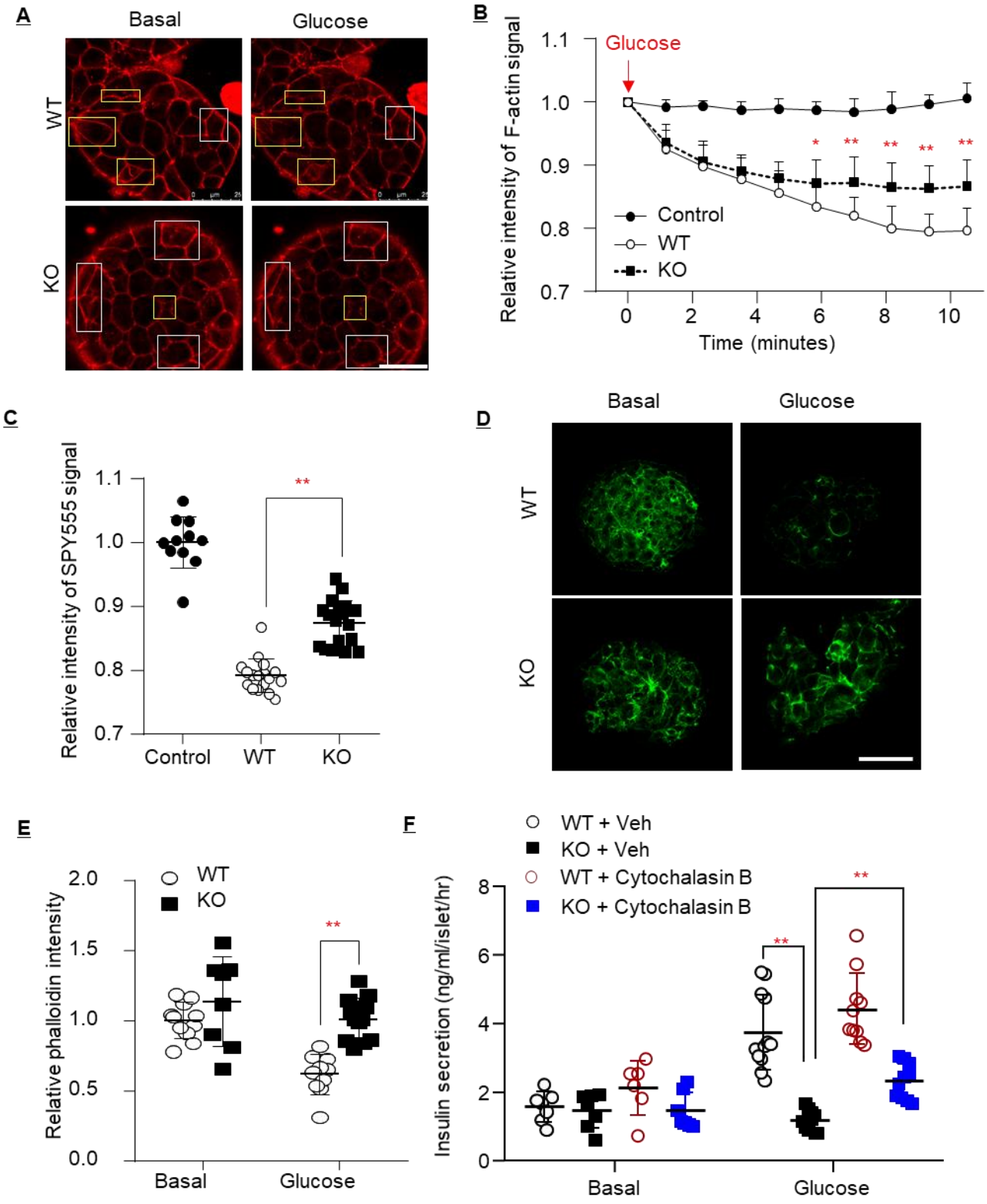
A
Basal
Glucose
WT
KO
B
Glucose
Relative intensity of F-actin signal
1.1
1.0
0.9
0.8
0.7
Control
WT
KO
0
2
4
6
8
10
Time (minutes)
C
Relative intensity of SPY555 signal
Control
WT
KO
D
Basal
Glucose
WT
KO
E
Relative phalloidin intensity
WT
KO
Basal
Glucose
F
WT + Veh
KO + Veh
WT + Cytochalasin B
KO + Cytochalasin B
Insulin secretion (ng/ml/islet/hr)
Basal
Glucose

**Figure 6.2.2. The defective glucose-stimulated insulin secretion in APPL2 deficient islets is attributed to impaired glucose-induced F-actin remodeling.** Pancreatic islets isolated from 16-week-old male RIP-APPL2 KO mice and their WT littermates under STC diet were used. (A-C) The islets were incubated in Krebs buffer containing 2.8 mM glucose (basal) and SPY555-actin probe for 90 min, followed by 16.7 mM glucose (glucose) stimulation for 10 min. Live cell imaging of F-actin (red) was visualized by SPY555-actin probe in the islets at basal level and subsequent 16.7 mM glucose stimulation for 10 mins. Yellow rectangles indicate the region with the most obvious difference while white rectangles indicate the region with no obvious difference before and after high glucose stimulation. Scale bar: 25 μM. (B) Quantification of dynamic change of SPY555-actin signal intensity. (C) Relative intensity of SPY555-actin signal upon high glucose stimulation at 0-min and 10-min. n=11-18. (D-E) The islets were stimulated with glucose (16.7 mM) for 10 min, followed by staining with Alexa Fluor 488® phalloidin (green). (E) Quantification of fluorescence intensity of phalloidin signal relative to WT-basal. n=8-12. Scale bar: 50 μM. (F) Pancreatic islets isolated from 16-week-old male RIP-APPL2 KO mice and WT controls were pretreated with cytochalasin B (5 μM) or vehicle for 90 min, followed by static GSIS as Figure 2A. Insulin secretion in the conditioned medium was measured and normalized with islet number. n=6-12. All data are presented as the mean±s.d. Significance was determined using Student's t-test or one-way ANOVA with Bonferroni correction. *$p<0.05$, **$p<0.01$. Representative images were shown.

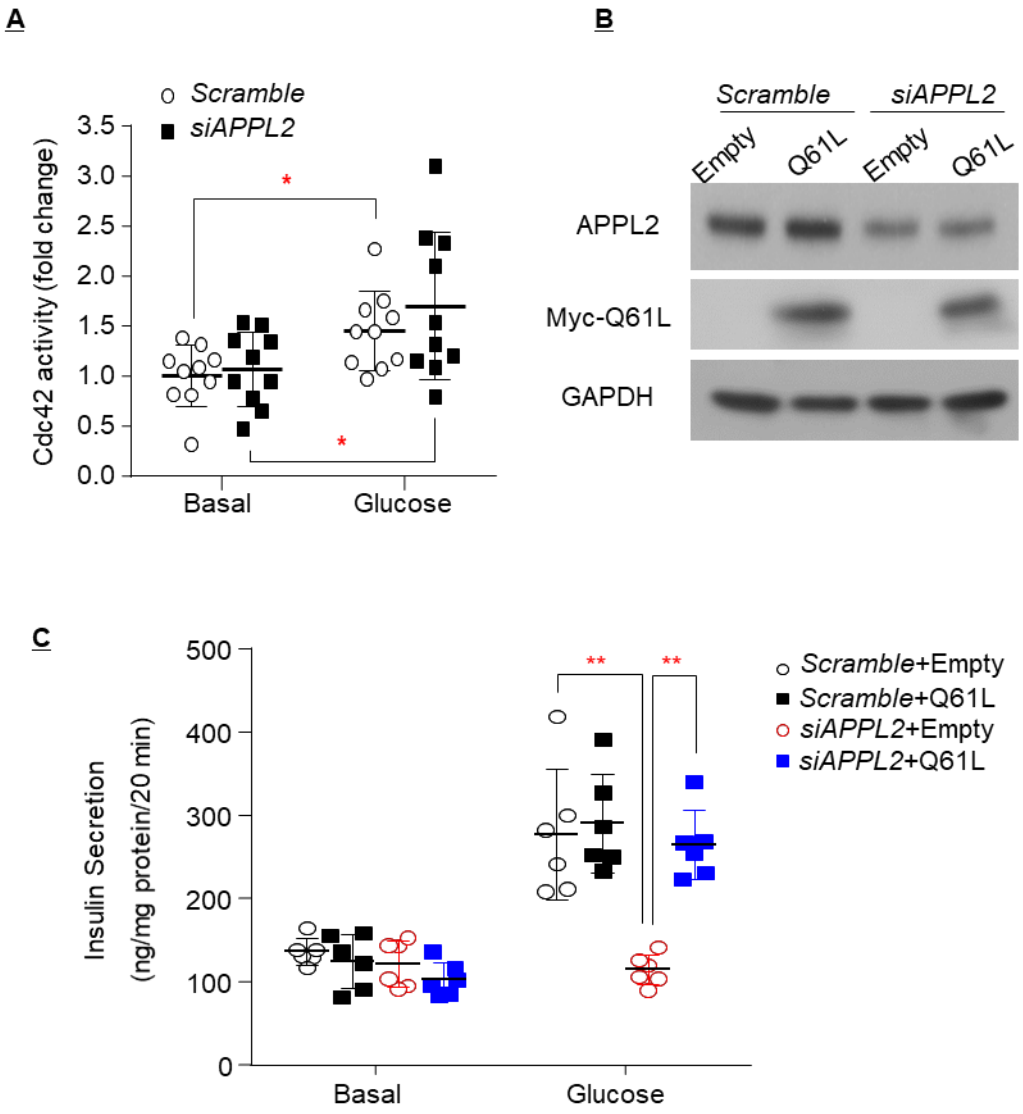


**Figure 6.2.3. APPL2 regulates glucose-stimulated insulin secretion via Rac1 activation.** (A-C) INS-1E cells were co-transfected with siRNA against *scrambled* control or *APPL2* and/or empty vector or plasmid encoding Rac1-Q61L mutant (active form of Rac1) for 48 hours. (A) Cdc42 activity in the transfected cells under basal level or after high glucose stimulation for 3 min. n=10. The transfected cells were subjected to immunoblotting analysis (B) and static GSIS (C). n=6All data are presented as the mean±s.d. Significance was determined using one-way ANOVA with Bonferroni correction. *p<0.05, **p<0.01. Representative images were shown.

### 6.2.2 APPL2 interacts with RacGAP1 to regulate F-actin remodeling and GSIS

Our research group previously identified that APPL2 is an interacting partner of Rac GTPase activating protein 1 (RacGAP1) (127), which is known to inactivate Rac1 during cytokinesis (137, 138). The RacGAP1 and Rac1 interaction occurs in INS-1E cells, but its biological function is unknown (139). We hypothesized that the regulation of APPL2 in Rac1 activation is dependent on the interaction between APPL2 and RacGAP1. To test this, HEK293 cells were transfected with plasmid expressing FLAG-tagged APPL2 and/or HA-tagged RacGAP1(Figure 6.2.4. A-B). Co-immunoprecipitation assay detected the interaction between APPL2 and RacGAP. Further analysis indicated that the BAR-PH domain of APPL2 appears to be the functional unit responsible for RacGAP1 interaction, while weak or no interaction could be observed between RacGAP1 and BAR, PH or the PTB domain alone (Figure 6.2.4. C-D). Apart from HEK293 cells, endogenously expressed APPL2 and RacGAP1 also interacted with each other in INS-1E cells, and this interaction could be potentiated by glucose stimulation at a time-dependent manner (Figure 6.2.4 E-F).

To examine whether APPL2 regulates GSIS and Rac1 activation depending on the interaction with RacGAP1, we employed siRNAs for concomitant knockdown of APPL2 and RacGAP1 in INS-1E cells. Downregulation of protein expression of APPL2 and RacGAP1 was confirmed in INS-1E cells transfected with siRNA against *APPL2* and/or *RacGAP1* (Figure 6.2.5 A). As expected, the downregulation of APPL2 expression impaired GSIS, but concomitant knockdown of RacGAP1 largely reversed this impairment (Figure 6.2.5 B). In addition, works from Baile Wang and my teammate Wenqi LV demonstrated that APPL2 deficiency-induced defective Rac1 activation and F-actin depolymerization were also reversed when RacGAP1 was concomitantly

downregulated. Taken together, these data suggest that APPL2 controls GSIS by antagonizing the inhibitory effect of RacGAP1 on Rac1 activation and F-actin remodeling in pancreatic β cells.

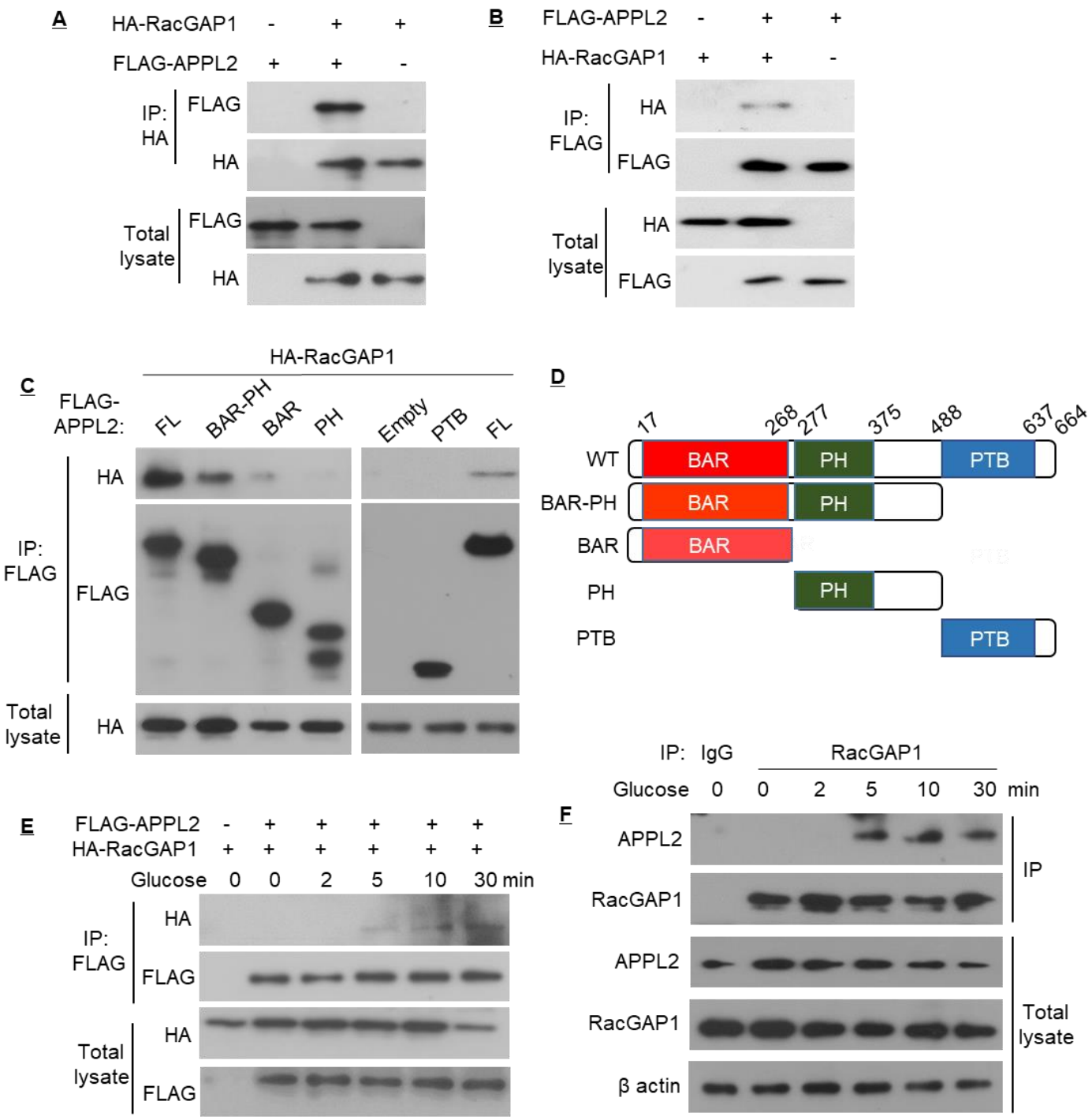


**Figure 6.2.4. APPL2 interacts with RacGAP1 in a glucose-dependent manner in INS-1E cells.** HEK293 cells (A-B) or INS-1E cells (E) were co-transfected with plasmids encoding FLAG-tagged APPL2 and HA-tagged RacGAP1 for 48 hours. INS-1E cells were stimulated with glucose (16.7 mM) for indicated time points. The transfected cells were subjected to immunoprecipitation (IP) using an antibody against HA tag (A) or FLAG tag (B and E). (C) HEK293 cells were transfected with indicated APPL2 plasmids and HA-RacGAP1, followed by IP and immunoblotting analysis. (D) Schematic diagram of FLAG-tagged full-length (FL) APPL2 and its truncated mutants. (F) INS-1E cells stimulated with glucose (16.7 mM) were subjected to IP using anti-RacGAP1 antibody or non-specific IgG as a negative control, followed by immunoblotting analysis as indicated. Representative images were shown from three independent experiments.

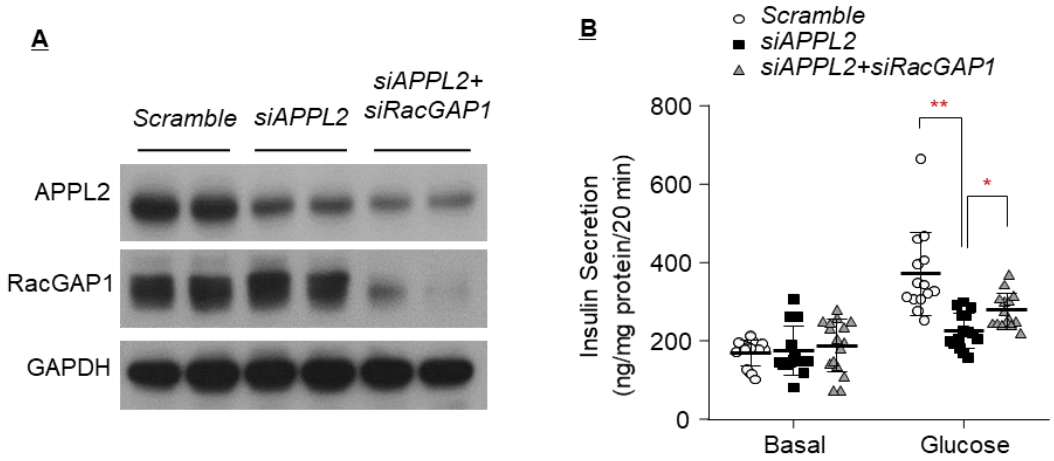


**Figure 6.2.5. APPL2 regulates GSIS via RacGAP1.** (A-B) INS-1E cells were co-transfected with siRNA against *APPL2*, *RacGAP1* and/or *scrambled* control for 48 hours, followed by (A) immunoblotting analysis of APPL2, RacGAP1 and GAPDH. (B) Static GSIS. n=11-16. All data are presented as mean±s.d. Significance was determined using one-way ANOVA with Bonferroni correction. *p<0.05, **p<0.01. Representative images were shown.

## 6.3 Summary and discussion

Previously we found that the adaptor protein APPL2 positively regulates GSIS and glucose homeostasis in mice. Such effects were associated with glucose-stimulated F-actin remodeling in pancreatic islets. My study demonstrated the mechanism underlying the regulation of APPL2 in glucose-stimulated F-actin remodeling. Live cell imaging and phalloidin staining revealed that F-actin remodeling is disrupted in APPL2 deficient islets. Promoting F-actin depolymerization by cytochalasin B could rescue the defective GSIS. Overexpression of constitutively active Rac1, the positive regulator of F-actin remodeling, largely reversed the defective GSIS in INS1-E cells with APPL2 knockdown. In addition, APPL2 interacts with RacGAP1 in INS-1E cells under high glucose condition and this interaction mainly depends on the BAR-PH domain of APPL2. My teammates and I collectively demonstrated that concomitant knockdown of RacGAP1 expression reverted APPL2 deficiency-induced defective GSIS, F-actin remodeling and Rac1 activation in INS-1E cells. Taken together, APPL2 promotes Rac1 activation by interacting with RacGAP1, leading to enhanced glucose-stimulated F-actin remodeling and GSIS (Figure 6.2.6)

Physiologically, F-actin serves as a barrier that restricts the translocation of secretory insulin granules to the plasma membrane. Glucose-stimulated F-actin remodeling is essential for exocytosis. Dysregulated cytoskeletal remodeling has been implicated in the progress of type 2 diabetes since it is associated with defective GSIS (129, 130), but the upstream regulatory mechanism is poorly characterized. In this study, I showed that APPL2 controls the disassembly of actin cytoskeleton via the RacGAP1-Rac1 signaling axis. APPL2 deficiency in pancreatic β-cells leads to defective F-actin remodeling and GSIS. The role of APPL2 in the regulation of pancreatic β-cell function has not hitherto

been examined. Our study proposes a novel function and the underlying mechanism for APPL2 to emerge as a positive regulator of β-cell function.

Activation of Rac1 is a crucial factor for cytoskeletal remodeling, which allows insulin granules fusion and trafficking for exocytosis (95, 130, 140, 141). We found that knockdown of APPL2 expression impairs glucose-induced Rac1 activation. Loss of Rac1 was shown to impair F-actin remodeling and GSIS (130). Similarly, we also observed a defective F-actin remodeling and GSIS in APPL2 deficient β-cells. The defective GSIS can be reversed by treatment with cytochalasin B.

The activity of Rac1 is positively controlled by its upstream regulator guanine exchange factors (GEF), and negatively controlled by Rho GDP-dissociation inhibitors (Rho-GDIs) and GAPs. Up to date, several GEFs and Rho-GDI have been identified to involve in the regulation of Rac1-mediated GSIS (142-147). However, to my knowledge, no GAP has been discovered to regulate Rac1 activation in β-cells. Protein interaction analysis by a recent proteomics study identified RacGAP1 as a potential regulator of Rac1(139), but the functional link remains to be examined. RacGAP1 enable to inactivate Rac1 by promoting GTP hydrolysis. Of note, RacGAP1 was found to abundantly express in human and rodent islets (138, 139). This study showed that simultaneous downregulation of RacGAP1 or ectopic expression of constitutively active Rac1 mutant could reverse the defective GSIS in INS1-E cells with APPL2 downregulation. However, the rescue effect of concomitant knockdown of RacGAP1 on GSIS is partial, indicating that an additional pathway which is independent of RacGAP1 might mediate the APPL2 actions in pancreatic β-cells. Another question is that Rac1 deficient islets display impaired second- but not first-phase GSIS (130). In our study, however, both first- and second-phases GSIS were diminished in APPL2

deficient islets. Further investigation on whether activation of Rac1 or inactivation of RacGAP1 is able to rescue the defective first- and second-phase GSIS in APPL2 deficient islets is required.

Our group previously reported that BAR domain containing proteins could interact with and affect the activity of GAP (127, 148). Of note, APPL2 belongs to the classical crescent-shape BAR domain subfamily. Besides, APPL2 was found to prevent insulin-elicited phosphorylation of the GAP domain of TBC1D1, which in turn inhibits glucose uptake in the skeletal muscles (127). This study demonstrated both exogenous and endogenous interaction between APPL2 and RacGAP1, and this interaction is BAR-PH domain-dependent and enhanced by glucose stimulation. Taken together, we speculate that the BAR-PH domain of APPL2 is able to antagonize the inhibitory effect of RacGAP1 on Rac1 activation via protein-protein interaction (Figure 6.3.1).

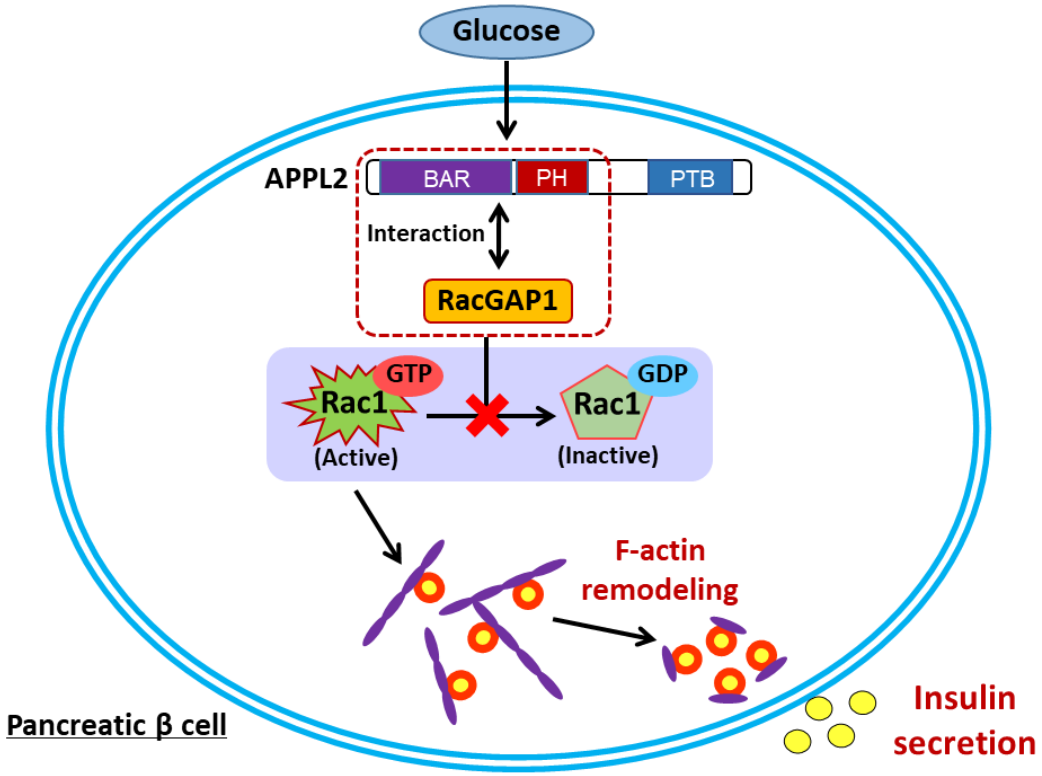


**Figure 6.3.1. Working model**

# Chapter 7 General Discussion

## 7.1 BCAA catabolism in pancreatic β-cell under healthy and metabolic disorder

BCAA catabolic pathway has been demonstrated in multiple tissues, especially in the liver, skeletal muscle and adipose tissue (51). Systematic isotope BCAA tracing revealed that pancreas also exhibits pronounced BCAA uptake and oxidation (51). However, BCAA catabolism most likely takes place in the exocrine pancreas, which makes up the majority of the pancreas mass (9). Current investigations on BCAA metabolism in the pancreas mainly focus on the pancreatic ductal adenocarinoma (PDAC), a type of exocrine pancreatic cancer with decreased BCAA uptake and mRNA expression of proteins responsible for BCAA catabolism (98, 149). Although insulin-producing β-cells are the endocrine unit of pancreas, BCAA catabolism in the endocrine and exocrine pancreas could largely differ. Immunohistochemical staining showed that BCATm was abundantly expressed in the exocrine pancreas but almost absent in rat islet, while expression of BCKDH-A was comparably expressed in both islet and exocrine cells (92). This finding suggests that islets are capable of BCAA utilization and possibly possess a BCAA pathway different from that in the exocrine pancreas. However, BCAA catabolic pathway and its function in islet is poorly unknown.

To delineate the BCAA catabolic pathway in the pancreatic β-cells, expression of BCATm and BCKDH-A, two enzymes involved in the first two steps of BCAA catabolism, was confirmedi in INS-1E β-cells. Besides, stimulation with BCAA or BCKA increased activity of BCKDH-A by inducing dephosphorylation. Out of my expectation, abundant expression of BCATm was observed in INS-1E β-cells, whereas the previous report suggested that rat islet is lack of BCATm expression (92). Expression of BCKDH-A was also examined in islets from healthy mice using

immunohistochemical staining. However, expression of BCKDH-A was strikingly higher in islets than exocrine cells, but not comparable between the two cell types as previously described (92). Of note, a proteomics analysis in mouse islets identified 19 proteins of BCAA catabolic pathway, including upstream BCATm, BCKDH-A and other downstream enzymes (150). Further investigation using different approaches to examine the expression of BCATm and downstream enzymes in islets is required. Importantly, LC-MS/MS targeted metabolomics and isotope-labeled leucine tracing analysis showed that BCAA uptake and its catabolism occur in both pancreatic islets and β-cells. These data demonstrate that pancreatic β-cells also have the BCAA catabolic machinery.

Normally, in healthy human, circulating concentration of total BCAA ranges from 400 to 600 μM, and this value will be increased by at least 1.5-fold in obese human (30-32). Circulating level of BCAA is found decreased by 30 % with aging (151). In addition, all BCAA catabolites show higher concentrations in males compared with that in women (152). These differences are believed to be mainly associated with body protein composition and metabolic rate. Change of circulating BCAA in T1D is similar as T2D. BCAA levels increase with the progress of T1D at different ages, but the biological link remained unclear (153).

Defective BCAA catabolism has been demonstrated in the skeletal muscle, liver and adipose tissue under metabolic disorders such as insulin resistance, obesity and type 2 diabetes (41, 59-62). Type 1 diabetes (T1D) happens when insufficient or no insulin is produced by pancreatic β-cells. In T1D, insulin-producing β-cells are destroyed by immune cells such as inflammatory T cells and macrophages (1, 5).In islets from type 1 diabetic mice, proteomics analysis showed modest declines in the expression of BCAA catabolic enzymes when compared with those isolated from healthy controls. These enzymes included BCKDH-A, methylcrotonoyl-CoA carboxylase β chain

(MCC2), methylglutaconyl-CoA hydratase (AUH), isobutyryl-CoA dehydrogenase (ACAD8) and short-branched chain specific acyl-CoA dehydrogenase (ACADSB) (150). The current studies investigating the function of BCAA in T1D are limited. To my knowledge, BCAA metabolism in pancreatic β-cells under T2D has not been explored. In this study, I compared BCAA catabolism in islets from healthy and *db/db* type 2 diabetic mice. BCAA, BCKA and C3/C5-acylcarnitine were elevated in diabetic islets. This was associated with reduced expression of BCKDH-A and an increased ratio of phosphorylated BCKDH-A to total BCKDH-A. The alteration in BCKDH-A phosphorylation might due to decreased expression of PPM1K. These data suggest BCAA catabolism in islets is impaired in the diabetic condition.

The cause for the diminished expression of BCKDH-A in diabetic islets is unknown. Inflammation and ER stress might play a role as they are important factors for pancreatic β-cell dysfunction in diabetes (14, 15, 19, 20). In adipocytes, inflammation and ER stress have been shown to downregulate the expression of BCAA catabolism-related proteins including BCKDH-A (62). Further investigation is required to explore the pathogenesis of defective BCAA metabolism in diabetic islets.

## 7.2 Chronic exposure to BCKA triggers pancreatic β-cell dysfunction

In healthy condition, leucine and its direct catabolite KIC can evoke acute insulin secretion in pancreatic islets (87-89). However, prospective cohort studies revealed that chronic elevation of circulating BCAA was positively associated with future pancreatic β-cell dysfunction (86, 154). Moreover, in mice with progressive T2D, the elevation in circulating BCAA-related metabolites was shown to precede pancreatic β-cell failure and severe hyperglycemia (39). These findings suggest a potential causative link between BCAA catabolism and pancreatic β-cells dysfunction in T2D, yet the pathophysiological pathway has not been clearly elucidated.

This study demonstrates that chronic treatment with BCKA (a mixture of KIC, KMV and KIV), but not BCAA nor C3/C5-acylcarnitine (upstream and downstream metabolites of BCKA, respectively), diminished GSIS in MIN6 β-cells and pancreatic islets. It was reported that exposure to leucine for 72 hours impaired GSIS in both mouse islets and insulinoma INS-1E cells (94). However, leucine at a concentration of 10 mM was used. This concentration was too high as circulating BCAA ranges from around 80-200 μM under physiological condition and increases to around 200-600 μM in diabetes, which was observed in my study and analyses by others (30-32). To better mimic the pathological condition, leucine at a concentration of 1.6 mM was used as a treatment and basal DMEM cell culture medium containing 0.8 mM leucine was used as a control in my study. The detrimental effect of BCKA on pancreatic β-cell function was also demonstrated *in vivo*. Compared with mice fed with vehicle control, mice fed with BCKA displayed significant glucose intolerance and impaired GSIS. LC-MS/MS targeted metabolomics revealed that after BCKA feeding, circulating levels of BCKA were strikingly increased, whereas levels of BCAA remained unchanged. These data

reinforce that accumulation of BCKA but not BCAA catabolites is detrimental to pancreatic β-cells.

Previous studies showed that BT2 strikingly reduced the circulating levels of BCAA and BCKA in mice (63, 78, 155), suggesting BCKA oxidation was enhanced in peripheral tissues. Consistently, in our study, both circulating BCAA and BCKA reduced in *db/db* mice with BT2 treatment compared with mice treated with vehicle. What's more, BT2 treatment significantly improved GSIS and glucose tolerance in diabetic mice. This is the first direct evidence to show that promoting BCAA catabolism is able to enhance insulin secretion. However, it is unclear whether such an effect was due to decreased circulating BCKA and/or improved BCAA catabolism in pancreatic β-cells. In pancreatic sections, BT2 treatment increased the expression of BCKDH-A but had no effect on its phosphorylation. As a result, the actual activity of BCKDH-A was estimated to be enhanced and thus BCKA oxidation was potentiated in islets from mice with BT2 treatment. Further animal study on whether direct and specific regulation of BCAA catabolism in islet improves insulin secretion is required.

## 7.3 PPM1K improves BCAA catabolism and GSIS

The irreversible oxidation of BCKA is the rate-limiting step of BCAA catabolism, which is positively regulated by PPM1K and negatively regulated by BDK via regulating phosphorylation of BCKDH-A at serine 293, respectively (49, 50). Compared with healthy subjects, mice with obesity or T2D displayed downregulated PPM1K in the liver and adipose tissue but no change was found in the skeletal muscle. On the contrary, expression of BDK was dramatically enhanced in the liver, adipose tissue and skeletal muscle in mice with obesity or T2D (64). Similar to the above observations, this study identified a significant reduction in PPM1K expression in diabetic islets compared with healthy controls, accompanied by a decreased ratio of phospho-BCKDH-A to total BCKDH-A. Our further study indicate that downregulation of PPM1K leads to an excessive amount of BCKA, which in turn causes defective GSIS in the progress of T2D.

Of note, PPM1K and BDK were shown to regulate lipid metabolism via a BCAA-independent pathway. Hepatic overexpression of BDK increased the phosphorylation of ATP-citrate lyase (ACL), leading to activation of *de novo* lipogenesis (78). In my study, downregulation of PPM1K alone was sufficient to disrupt GSIS. PPM1K deficiency remarkably increased the accumulation of intracellular BCKA in pancreatic β-cells upon BCAA stimulation. However, this effect was not less pronounced without BCAA stimulation, especially in the level of KIV. These data suggest PPM1K might regulate insulin secretion partially via BCAA pathway. Further investigation to determine whether PPM1K regulates pancreatic β-cells function is independent of BCAA pathway is warranted.

The whole BCAA catabolic pathway, including BDK, is poorly understood in β-cells.

The increased expression of BDK is believed to associate with abrogated BCAA catabolism in peripheral tissues (64). BDK can be inhibited by BT2, leading to activation of BCKDH-A (79). Therefore, our data in animals and cells with BT2 treatment also suggest that BDK is likely to involve in the regulation of β-cell function. It is speculated that expression of BDK is upregulated in diabetic islet. Surprisingly, a slight but significant reduction in BDK expression was identified in type 1 diabetic islet by proteomics (150). Whether BDK also plays a role in β-cells function remained to be further investigated.

## 7.4 Defective BCAA catabolism diminishes GSIS by modulating glucose metabolism

Glucose serves as a major nutrient signal to evoke insulin secretion. Several studies showed that glucose metabolism can be modulated by BCAA pathway. Treatment with BCAA and KIC suppressed the activity of pyruvate dehydrogenase (PDH) and α-ketoglutarate dehydrogenase (KGDH) in heart, respectively (101, 105). In the isolated liver mitochondria, BCKA repressed respiratory Complex II of oxidative phosphorylation (81). Additionally, gene deletion of PPM1K leads to impaired glucose metabolism in the heart, liver and hematopoietic stem cells (HSCs) (81, 101, 107). Similarly, a reduced glycolytic flux and subsequent ATP production were observed in β-cells with downregulated PPM1K. Moreover, BCKA treatment was also shown to impair glucose metabolism. Methyl pyruvate (end-product of glycolysis)-stimulated insulin secretion was not affected by BCKA. These data suggest that pyruvate production from glycolysis can be inhibited by defective BCAA catabolism.

Hepatic PPM1K deficiency resulted in excessive BCKA and altered glycolytic flux (81). Downstream intermediates of glycolysis including fructose-1,6-biphosphate, 3-phosphoglycerate were lower whereas upstream metabolites including glucose 6-phosphate and fructose 6-phosphate, were higher in the PPM1K deficient liver compared with WT controls (81). This study shows that BCKA treatment impaired glucose-stimulated production of DHAP, pyruvate and α-KG. Since DHPA is generated by the fourth step of glycolysis, these data indicate that BCKA might induce defect in the upstream of glucose metabolism. There was no change in intracellular concentrations of fructose-6-phosphate, fructose-1,6-diphosphate, glycerol-3-phosphate, 3-phosphoglyceric acid, lactate, acetyl CoA, citrate, succinate, fumarate and

malate. The potential possibility could be that glycolysis interacts with other metabolic pathways such as pentose phosphate pathway, gluconeogenesis, glycogenesis, glycogenolysis and TCA cycle and so on (156). Alteration in one metabolic pathway will be somehow compensated by the conjoint metabolic pathways. Despite the above findings, further investigation is required to identify which step of glucose metabolism in β-cells is disrupted by defective BCAA catabolism.

It is still unknown how BCAA pathway interacts with glucose metabolism in β-cells. There are several speculations. First, BCKA might affect transcription of glycolytic and TCA cycle proteins. In the liver, BCAA treatment increased expression of *Foxo1, PCK1* and *G6PC* (proteins for gluconeogenesis) (106). In HSCs, PPM1K deletion resulted in a downregulated expression of glycolysis-associated proteins (*Meis1, HIF1 α, Glut1* and *LDHA*) (107). Further investigation is essential to examine whether BCAA pathway manipulates mRNA transcription of glucose metabolism-associated proteins.

Second, BCAA pathway is likely to regulate glucose metabolism in the level of post-translational modification. Tao Li *et al.* identified a decreased O-linked-N-acetylglucosamine (O-GlcNAc) modification of PDH in rat cardiomyocytes by exposure to excessive BCAA and in mice heart by gene ablation of PPM1K. Reduced protein O-GlcNAc modification was shown to impair PDH activity and glycolysis (101). O-GlcNAc modification is emerging as a key factor to control enzyme activities of glycolysis (102-104). Claude Michalski *et al*. employed proteomics screening in muscle cells. Strikingly, all glycolytic enzymes were O-GlcNAcylated (157), although the effect of modification on each enzyme remains elusive and might varies (104). Based on above findings, O-GlcNAc modification could be a potential mechanism by which BCAA pathway regulates glucose metabolism in pancreatic β-cells.

The last speculation relates to the phosphatase function of PPM1K. With analysis of phosphoproteomics in the liver, Phillip J. White *et al.* identified that PPM1K substrates have common sequence motif SxS" or "RxxS" (78). Glycolytic enzymes might be potential targets of PPM1K. To test this, sequences of all glycolytic enzymes from human, mouse and rat were analyzed. Out of expectation, almost all of these enzymes possess at least one PPM1K-targeted motif. Next, PhosphoSitePlus is a database which provides information of phosphorylation site collected from clinical researches and phosphoproteomics analyses (158). In this database, around 55 reported phosphorylation sites were found in glycolytic enzymes from human, mouse and rat. To find out the potential PPM1K targets in pancreatic β-cells and islets, the aforementioned phosphorylation sites were compared with those reported in MIN6 cells, INS-1E cells and islets (150, 159, 160). The results were put together to find out which enzyme fulfills all screening conditions. Three glycolytic zymes were finally identified as potential targets of PPM1K in β-cells. These enzymes are phosphofructokinase (PFKM), aldolase A and pyruvate dehydrogenase E1 alpha subunit (PDHA2). Further investigations into whether PPM1K plays a regulatory role in these glycolytic enzymes are warranted.

## 7.5 Conclusion

This study demonstrates that BCAA catabolism is crucial in the regulation of pancreatic β-cells function. In type 2 diabetes, elevated BCAA downstream catabolites in islets are associated with defective BCAA catabolic pathway. Overload of BCKA, but not BCAA or acylcarnitine, impairs GSIS in pancreatic β-cells and mice. On the contrary, promoting BCKA oxidation improves glucose tolerance and GSIS in type 2 diabetic mice. Further investigation identified an adverse effect of defective BCAA catabolism on glucose metabolism in β-cells. Taken together, this study proposes that excessive BCKA and defective BCAA catabolic pathway in pancreatic β-cells impair GSIS by disruption of glucose metabolism, leading to the progress of pancreatic β-cell dysfunction and subsequent type 2 diabetes (Figure 7.1). To my knowledge, the association between defective BCAA catabolism and pancreatic β-cell function has not been reported. This study sheds new light on the critical role of BCAA catabolism in the regulation of pancreatic β-cell function, thereby providing prospective therapeutic targets for the prevention and treatment of T2D.

Apart from BCAA study, I also showed that the adaptor protein APPL2 interacts with RacGAP1 and thus antagonizes the inhibitory effect of RacGAP1 on Rac1 activation, leading to enhanced glucose-induced F-actin remodeling and GSIS in pancreatic β-cells.

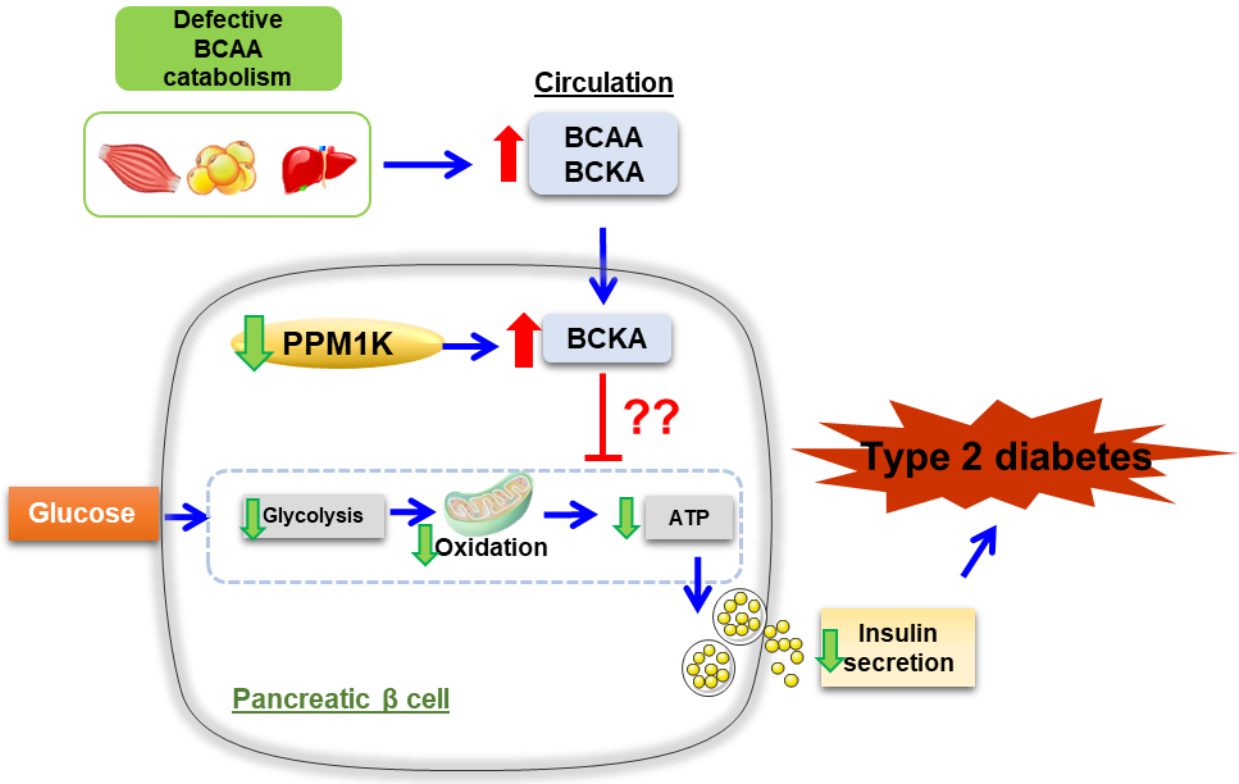


**Figure 7.1. Hypothetic model of this study:**

BCAA catabolic pathway is disrupted (such as unrestrained phosphorylation of BCKDH-A due to reduced expression of PPM1K) in pancreatic β cells. Together with chronic elevation of circulating BCKA, excessive cytotoxic BCKA is accumulated in pancreatic β cells, which in turn impairs glucose metabolism and subsequent glucose–induced insulin secretion in pancreatic β-cells, contributing to overt type 2 diabetes.

## 7.6 Future work

Despite the exciting findings in this study, there are still several questions remained unanswered. For one, I have demonstrated that chronic treatment with BCKA and downregulation of PPM1K disturb the production of glycolytic metabolites and ATP, but the underlying mechanism remains unknown. Based on our current findings and literature review, we have three speculations for the potential mechanisms by which defective BCAA catabolism disrupts glucose metabolism in pancreatic β-cells. The first speculation involves regulation in the transcriptional level of glycolytic enzymes. To test this, we are employing real-time quantitative PCR analysis to examine and compare the expression of glycolytic enzymes in pancreatic β-cells with or without BCKA treatment. If alteration in mRNA expression was found, we will continue to test their protein expression. The second speculation proposes that BCKA and/or PPM1K might regulate activities of glycolytic enzymes via O-linked-N-acetylglucosamine (O-GlcNAc) modification, which has been generally shown to control enzyme activities of glycolysis (102-104). To test this, O-GlcNAc modification upon glucose stimulation will be examined in pancreatic β-cells with defective BCAA catabolism.

The last speculation relies on the fact that PPM1K is a phosphatase, which enable to regulate protein activity by inducing dephosphorylation. The common motif (SxS or RxxS) of PPM1K substrates has been identified (78). Together with the information of phosphorylated peptide provided by the phosphorylation site database (158), I found PFKM, aldolase A and PDHA2 possess the common PPM1K substrates motif. Moreover, phosphorylation sites in these three enzymes are also indicated by phosphoproteomics analyses of pancreatic β cells and islets (150, 159, 160), yet the physiological meaning remains to be examined. To test if PPM1K interacts with the

glycolytic enzymes, exogenous co-immunoprecipitation will be performed in HEK 293 cells. The plasmids overexpressing PPM1K and glycolytic enzymes have been ready for cell transfection. Besides, the co-immunoprecipitated protein complex will be subjected to immunoblotting analysis using anti-phosphorylated serine antibody. The result will suggest whether PPM1K controls glycolytic enzymes via modulation of phosphorylation.

Another major problem of this study is that in animal studies, it is uncertain whether BCAA metabolism in pancreatic islets was altered by treatment with BCKA and BT2. To further confirm that BCAA metabolism in pancreatic β-cells is crucial to β-cell function, adeno-associated virus (AAV) will be employed to selectively overexpress PPM1K in pancreatic β-cells under control of a modified mouse insulin promoter as we previously reported (124, 161). Besides, Cre/loxP system will be used to generate pancreatic β-cell-specific or inducible knockout mice. We have generated $PPM1K^{flox/flox}$ mice, which will be crossed with mice carrying the transgene encoding Cre recombinase enzyme under the control of a rat insulin promoter. Alternatively, AAV will be used to selectively express Cre in pancreatic β-cells and thus PPM1K will be specifically knocked out in pancreatic β-cells. The mice will be subjected to metabolic characterizations, including GTT, GSIS and ITT. In summary, more investigations are essential to examine whether specific manipulation of BCAA catabolism in pancreatic β-cells improves β-cell function and prevents diabetes in mice.

# References

**Uncategorized References**


1. WHO (2016) Global report on diabetes. *World Health Organization*.

2. Papatheodorou K, Banach M, Bekiari E, Rizzo M, & Edmonds M (2018) Complications of Diabetes 2017. *Journal of diabetes research* 2018:3086167.

3. Harding JL, Pavkov ME, Magliano DJ, Shaw JE, & Gregg EW (2019) Global trends in diabetes complications: a review of current evidence. *Diabetologia* 62(1):3-16.

4. Ogurtsova K, *et al.* (2017) IDF Diabetes Atlas: Global estimates for the prevalence of diabetes for 2015 and 2040. *Diabetes research and clinical practice* 128:40-50.

5. Katsarou A, *et al.* (2017) Type 1 diabetes mellitus. *Nature Reviews Disease Primers* 3(1):17016.

6. Hu C & Jia W (2018) Diabetes in China: Epidemiology and Genetic Risk Factors and Their Clinical Utility in Personalized Medication. *Diabetes* 67(1):3-11.

7. Weng J, *et al.* (2016) Standards of care for type 2 diabetes in China. *Diabetes/metabolism research and reviews* 32(5):442-458.

8. DeFronzo RA, *et al.* (2015) Type 2 diabetes mellitus. *Nature Reviews Disease Primers* 1(1):15019.

9. Da Silva Xavier G (2018) The Cells of the Islets of Langerhans. *Journal of clinical medicine* 7(3).

10. Steiner DJ, Kim A, Miller K, & Hara M (2010) Pancreatic islet plasticity: interspecies comparison of islet architecture and composition. *Islets* 2(3):135-145.

11. Cerf ME (2013) Beta cell dysfunction and insulin resistance. *Frontiers in endocrinology* 4:37.

12. El Ouaamari A, *et al.* (2016) SerpinB1 Promotes Pancreatic β Cell Proliferation. *Cell metabolism* 23(1):194-205.

13. Shirakawa J, *et al.* (2017) Insulin Signaling Regulates the FoxM1/PLK1/CENP-A Pathway to Promote Adaptive Pancreatic β Cell Proliferation. *Cell metabolism* 25(4):868-882.e865.

14. Eizirik DL, Cardozo AK, & Cnop M (2008) The role for endoplasmic reticulum

stress in diabetes mellitus. *Endocrine reviews* 29(1):42-61.

15. Rabhi N, Salas E, Froguel P, & Annicotte JS (2014) Role of the unfolded protein response in β cell compensation and failure during diabetes. *Journal of diabetes research* 2014:795171.

16. Butler AE, *et al.* (2003) Beta-cell deficit and increased beta-cell apoptosis in humans with type 2 diabetes. *Diabetes* 52(1):102-110.

17. Masini M, *et al.* (2009) Autophagy in human type 2 diabetes pancreatic beta cells. *Diabetologia* 52(6):1083-1086.

18. Talchai C, Xuan S, Lin HV, Sussel L, & Accili D (2012) Pancreatic β cell dedifferentiation as a mechanism of diabetic β cell failure. *Cell* 150(6):1223-1234.

19. Robertson R, Zhou H, Zhang T, & Harmon JS (2007) Chronic oxidative stress as a mechanism for glucose toxicity of the beta cell in type 2 diabetes. *Cell biochemistry and biophysics* 48(2-3):139-146.

20. Gerber PA & Rutter GA (2017) The Role of Oxidative Stress and Hypoxia in Pancreatic Beta-Cell Dysfunction in Diabetes Mellitus. *Antioxidants & redox signaling* 26(10):501-518.

21. Nie C, He T, Zhang W, Zhang G, & Ma X (2018) Branched Chain Amino Acids: Beyond Nutrition Metabolism. *Int J Mol Sci* 19(4).

22. Harper AE, Miller RH, & Block KP (1984) Branched-chain amino acid metabolism. *Annual review of nutrition* 4:409-454.

23. Ren M, Zhang SH, Zeng XF, Liu H, & Qiao SY (2015) Branched-chain Amino Acids are Beneficial to Maintain Growth Performance and Intestinal Immune-related Function in Weaned Piglets Fed Protein Restricted Diet. *Asian-Australasian journal of animal sciences* 28(12):1742-1750.

24. Ren M, *et al.* (2016) Different Lipopolysaccharide Branched-Chain Amino Acids Modulate Porcine Intestinal Endogenous β-Defensin Expression through the Sirt1/ERK/90RSK Pathway. *J Agric Food Chem* 64(17):3371-3379.

25. Ma N, *et al.* (2018) Nutrients Mediate Intestinal Bacteria-Mucosal Immune Crosstalk. *Frontiers in immunology* 9:5.

26. Qin LQ, *et al.* (2011) Higher branched-chain amino acid intake is associated with a lower prevalence of being overweight or obese in middle-aged East Asian and Western adults. *The Journal of nutrition* 141(2):249-254.

27. Chen H, Simar D, Ting JH, Erkelens JR, & Morris MJ (2012) Leucine improves glucose and lipid status in offspring from obese dams, dependent on diet type, but not caloric intake. *Journal of neuroendocrinology* 24(10):1356-1364.

28. Doi M, *et al.* (2005) Isoleucine, a blood glucose-lowering amino acid, increases glucose uptake in rat skeletal muscle in the absence of increases in AMP-

activated protein kinase activity. *The Journal of nutrition* 135(9):2103-2108.

29. Du Y, Meng Q, Zhang Q, & Guo F (2012) Isoleucine or valine deprivation stimulates fat loss via increasing energy expenditure and regulating lipid metabolism in WAT. *Amino acids* 43(2):725-734.

30. Zhou Y, *et al.* (2013) Obesity and diabetes related plasma amino acid alterations. *Clinical biochemistry* 46(15):1447-1452.

31. Rietman A, *et al.* (2016) Associations between plasma branched-chain amino acids, beta-aminoisobutyric acid and body composition. *Journal of nutritional science* 5:e6.

32. Newgard CB, *et al.* (2009) A branched-chain amino acid-related metabolic signature that differentiates obese and lean humans and contributes to insulin resistance. *Cell metabolism* 9(4):311-326.

33. Felig P, Marliss E, & Cahill GF, Jr. (1969) Plasma amino acid levels and insulin secretion in obesity. *The New England journal of medicine* 281(15):811-816.

34. Wang TJ, *et al.* (2011) Metabolite profiles and the risk of developing diabetes. *Nature medicine* 17(4):448-453.

35. Floegel A, *et al.* (2013) Identification of serum metabolites associated with risk of type 2 diabetes using a targeted metabolomic approach. *Diabetes* 62(2):639-648.

36. Lee CC, *et al.* (2016) Branched-Chain Amino Acids and Insulin Metabolism: The Insulin Resistance Atherosclerosis Study (IRAS). *Diabetes care* 39(4):582-588.

37. Tillin T, *et al.* (2015) Diabetes risk and amino acid profiles: cross-sectional and prospective analyses of ethnicity, amino acids and diabetes in a South Asian and European cohort from the SABRE (Southall And Brent REvisited) Study. *Diabetologia* 58(5):968-979.

38. Chen T, *et al.* (2016) Branched-chain and aromatic amino acid profiles and diabetes risk in Chinese populations. *Scientific reports* 6:20594.

39. Li L, *et al.* (2019) Metabolomics Identifies a Biomarker Revealing In Vivo Loss of Functional β-Cell Mass Before Diabetes Onset. *Diabetes* 68(12):2272-2286.

40. Giesbertz P & Daniel H (2016) Branched-chain amino acids as biomarkers in diabetes. *Current opinion in clinical nutrition and metabolic care* 19(1):48-54.

41. Newgard CB (2012) Interplay between lipids and branched-chain amino acids in development of insulin resistance. *Cell metabolism* 15(5):606-614.

42. Fontana L, *et al.* (2016) Decreased Consumption of Branched-Chain Amino Acids Improves Metabolic Health. *Cell reports* 16(2):520-530.

43. Cummings NE, *et al.* (2018) Restoration of metabolic health by decreased

consumption of branched-chain amino acids. *The Journal of physiology* 596(4):623-645.

44. White PJ, *et al.* (2016) Branched-chain amino acid restriction in Zucker-fatty rats improves muscle insulin sensitivity by enhancing efficiency of fatty acid oxidation and acyl-glycine export. *Molecular metabolism* 5(7):538-551.

45. Xiao F, *et al.* (2014) Effects of individual branched-chain amino acids deprivation on insulin sensitivity and glucose metabolism in mice. *Metabolism: clinical and experimental* 63(6):841-850.

46. Xiao F, *et al.* (2011) Leucine deprivation increases hepatic insulin sensitivity via GCN2/mTOR/S6K1 and AMPK pathways. *Diabetes* 60(3):746-756.

47. Lynch CJ & Adams SH (2014) Branched-chain amino acids in metabolic signalling and insulin resistance. *Nature reviews. Endocrinology* 10(12):723-736.

48. Hull J, *et al.* (2012) Distribution of the branched chain aminotransferase proteins in the human brain and their role in glutamate regulation. *J Neurochem* 123(6):997-1009.

49. Lu G, *et al.* (2009) Protein phosphatase 2Cm is a critical regulator of branched-chain amino acid catabolism in mice and cultured cells. *The Journal of clinical investigation* 119(6):1678-1687.

50. Zhou M, Lu G, Gao C, Wang Y, & Sun H (2012) Tissue-specific and Nutrient Regulation of the Branched-chain α-Keto Acid Dehydrogenase Phosphatase, Protein Phosphatase 2Cm (PP2Cm). *The Journal of biological chemistry* 287(28):23397-23406.

51. Neinast MD, *et al.* (2019) Quantitative Analysis of the Whole-Body Metabolic Fate of Branched-Chain Amino Acids. *Cell metabolism* 29(2):417-429.e414.

52. Shimomura Y, *et al.* (2006) Nutraceutical effects of branched-chain amino acids on skeletal muscle. *J Nutr* 136(2):529S-532S.

53. Shin AC, *et al.* (2014) Brain insulin lowers circulating BCAA levels by inducing hepatic BCAA catabolism. *Cell metabolism* 20(5):898-909.

54. Hutson SM & Harper AE (1981) Blood and tissue branched-chain amino and alpha-keto acid concentrations: effect of diet, starvation, and disease. *Am J Clin Nutr* 34(2):173-183.

55. Suryawan A, *et al.* (1998) A molecular model of human branched-chain amino acid metabolism. *Am J Clin Nutr* 68(1):72-81.

56. Zimmerman HA, Olson KC, Chen G, & Lynch CJ (2013) Adipose transplant for inborn errors of branched chain amino acid metabolism in mice. *Mol Genet Metab* 109(4):345-353.

57. Mazariegos GV, *et al.* (2012) Liver transplantation for classical maple syrup

urine disease: long-term follow-up in 37 patients and comparative United Network for Organ Sharing experience. *J Pediatr* 160(1):116-121 e111.

58. Oh KJ, *et al.* (2016) Metabolic Adaptation in Obesity and Type II Diabetes: Myokines, Adipokines and Hepatokines. *International journal of molecular sciences* 18(1).

59. Lackey DE, *et al.* (2013) Regulation of adipose branched-chain amino acid catabolism enzyme expression and cross-adipose amino acid flux in human obesity. *American journal of physiology. Endocrinology and metabolism* 304(11):E1175-1187.

60. Herman MA, She P, Peroni OD, Lynch CJ, & Kahn BB (2010) Adipose tissue branched chain amino acid (BCAA) metabolism modulates circulating BCAA levels. *The Journal of biological chemistry* 285(15):11348-11356.

61. She P, *et al.* (2007) Obesity-related elevations in plasma leucine are associated with alterations in enzymes involved in branched-chain amino acid metabolism. *American journal of physiology. Endocrinology and metabolism* 293(6):E1552-1563.

62. Burrill JS, *et al.* (2015) Inflammation and ER stress regulate branched-chain amino acid uptake and metabolism in adipocytes. *Molecular Endocrinology* 29(3):411-420.

63. Zhou M, *et al.* (2019) Targeting BCAA Catabolism to Treat Obesity-Associated Insulin Resistance. *Diabetes* 68(9):1730-1746.

64. Lian K, *et al.* (2015) Impaired adiponectin signaling contributes to disturbed catabolism of branched-chain amino acids in diabetic mice. *Diabetes* 64(1):49-59.

65. Tiffin N, *et al.* (2006) Computational disease gene identification: a concert of methods prioritizes type 2 diabetes and obesity candidate genes. *Nucleic Acids Res* 34(10):3067-3081.

66. Taneera J, *et al.* (2012) A systems genetics approach identifies genes and pathways for type 2 diabetes in human islets. *Cell metabolism* 16(1):122-134.

67. Kettunen J, *et al.* (2012) Genome-wide association study identifies multiple loci influencing human serum metabolite levels. *Nat Genet* 44(3):269-276.

68. Biswas D, *et al.* (2020) Branched-chain ketoacid overload inhibits insulin action in the muscle. *The Journal of biological chemistry*.

69. Jang C, *et al.* (2016) A branched-chain amino acid metabolite drives vascular fatty acid transport and causes insulin resistance. *Nature medicine* 22(4):421-426.

70. Haufe S, *et al.* (2017) Branched-chain amino acid catabolism rather than amino acids plasma concentrations is associated with diet-induced changes in insulin

resistance in overweight to obese individuals. *Nutrition, metabolism, and cardiovascular diseases : NMCD* 27(10):858-864.

71. Pedersen A (2018) Higher concentrations of BCAAs and 3-HIB are associated with insulin resistance in the transition from gestational diabetes to type 2 diabetes.

72. Mardinoglu A, *et al.* (2018) Elevated Plasma Levels of 3-Hydroxyisobutyric Acid Are Associated With Incident Type 2 Diabetes. *EBioMedicine* 27:151-155.

73. Nilsen MS, *et al.* (2020) 3-Hydroxyisobutyrate, A Strong Marker of Insulin Resistance in Type 2 Diabetes and Obesity That Modulates White and Brown Adipocyte Metabolism. *Diabetes* 69(9):1903-1916.

74. Mai M, *et al.* (2013) Serum levels of acylcarnitines are altered in prediabetic conditions. *PloS one* 8(12):e82459.

75. Mihalik SJ, *et al.* (2010) Increased levels of plasma acylcarnitines in obesity and type 2 diabetes and identification of a marker of glucolipotoxicity. *Obesity (Silver Spring, Md.)* 18(9):1695-1700.

76. Koves TR, *et al.* (2008) Mitochondrial overload and incomplete fatty acid oxidation contribute to skeletal muscle insulin resistance. *Cell metabolism* 7(1):45-56.

77. Koves TR, *et al.* (2005) Peroxisome proliferator-activated receptor-gamma co-activator 1alpha-mediated metabolic remodeling of skeletal myocytes mimics exercise training and reverses lipid-induced mitochondrial inefficiency. *The Journal of biological chemistry* 280(39):33588-33598.

78. White PJ, *et al.* (2018) The BCKDH Kinase and Phosphatase Integrate BCAA and Lipid Metabolism via Regulation of ATP-Citrate Lyase. *Cell metabolism* 27(6):1281-1293.e1287.

79. Tso SC, *et al.* (2014) Benzothiophene carboxylate derivatives as novel allosteric inhibitors of branched-chain alpha-ketoacid dehydrogenase kinase. *The Journal of biological chemistry* 289(30):20583-20593.

80. She P, *et al.* (2007) Disruption of BCATm in mice leads to increased energy expenditure associated with the activation of a futile protein turnover cycle. *Cell metabolism* 6(3):181-194.

81. Wang J, *et al.* (2019) BCAA Catabolic Defect Alters Glucose Metabolism in Lean Mice. *Frontiers in physiology* 10:1140.

82. Lu G, *et al.* (2007) A novel mitochondrial matrix serine/threonine protein phosphatase regulates the mitochondria permeability transition pore and is essential for cellular survival and development. *Genes & development* 21(7):784-796.

83. Lu G, *et al.* (2009) Functional characterization of a mitochondrial Ser/Thr

protein phosphatase in cell death regulation. *Methods Enzymol* 457:255-273.

84. Oyarzabal A, *et al.* (2013) A Novel Regulatory Defect in the Branched-Chain - Keto Acid Dehydrogenase Complex Due to a Mutation in the PPM1K Gene Causes a Mild Variant Phenotype of Maple Syrup Urine Disease. *Hum Mutat* 34(2):355-362.

85. Lotta LA, *et al.* (2016) Genetic Predisposition to an Impaired Metabolism of the Branched-Chain Amino Acids and Risk of Type 2 Diabetes: A Mendelian Randomisation Analysis. *PLoS medicine* 13(11):e1002179.

86. Vangipurapu J, Stancakova A, Smith U, Kuusisto J, & Laakso M (2019) Nine Amino Acids Are Associated With Decreased Insulin Secretion and Elevated Glucose Levels in a 7.4-Year Follow-up Study of 5,181 Finnish Men. *Diabetes* 68(6):1353-1358.

87. Panten U, Christians J, von Kriegstein E, Poser W, & Hasselblatt A (1974) Studies on the mechanism of L-leucine-and alpha-ketoisocaproic acid-induced insulin release from perifused isolated pancreatic islets. *Diabetologia* 10(2):149-154.

88. Branstrom R, Efendic S, Berggren PO, & Larsson O (1998) Direct inhibition of the pancreatic beta-cell ATP-regulated potassium channel by alpha-ketoisocaproate. *The Journal of biological chemistry* 273(23):14113-14118.

89. Yang J, *et al.* (2006) Leucine Regulation of Glucokinase and ATP Synthase Sensitizes Glucose-Induced Insulin Secretion in Pancreatic β-Cells. *Diabetes* 55(1):193-201.

90. Liu Z, Jeppesen PB, Gregersen S, Larsen LB, & Hermansen K (2012) Chronic exposure to leucine in vitro induces beta-cell dysfunction in INS-1E cells and mouse islets. *The Journal of endocrinology* 215(1):79-88.

91. Anderson KA, *et al.* (2017) SIRT4 Is a Lysine Deacylase that Controls Leucine Metabolism and Insulin Secretion. *Cell metabolism* 25(4):838-855 e815.

92. Sweatt AJ, *et al.* (2004) Branched-chain amino acid catabolism: unique segregation of pathway enzymes in organ systems and peripheral nerves. *American journal of physiology. Endocrinology and metabolism* 286(1):E64-76.

93. Seino S, Shibasaki T, & Minami K (2011) Dynamics of insulin secretion and the clinical implications for obesity and diabetes. *The Journal of clinical investigation* 121(6):2118-2125.

94. Jitrapakdee S, Wutthisathapornchai A, Wallace JC, & MacDonald MJ (2010) Regulation of insulin secretion: role of mitochondrial signalling. *Diabetologia* 53(6):1019-1032.

95. Wang Z & Thurmond DC (2009) Mechanisms of biphasic insulin-granule exocytosis - roles of the cytoskeleton, small GTPases and SNARE proteins. *Journal of cell science* 122(Pt 7):893-903.

96. Kalwat MA & Thurmond DC (2013) Signaling mechanisms of glucose-induced F-actin remodeling in pancreatic islet beta cells. *Experimental & molecular medicine* 45:e37.

97. Green CR, *et al.* (2016) Branched-chain amino acid catabolism fuels adipocyte differentiation and lipogenesis. *Nature chemical biology* 12(1):15-21.

98. Mayers JR, *et al.* (2016) Tissue of origin dictates branched-chain amino acid metabolism in mutant Kras-driven cancers. *Science (New York, N.Y.)* 353(6304):1161-1165.

99. Shao D, *et al.* (2018) Glucose promotes cell growth by suppressing branched-chain amino acid degradation. *Nature communications* 9(1):2935.

100. Yoon I, *et al.* (2020) Glucose-dependent control of leucine metabolism by leucyl-tRNA synthetase 1. *Science (New York, N.Y.)* 367(6474):205-210.

101. Li T, *et al.* (2017) Defective Branched-Chain Amino Acid Catabolism Disrupts Glucose Metabolism and Sensitizes the Heart to Ischemia-Reperfusion Injury. *Cell metabolism* 25(2):374-385.

102. Nie H, *et al.* (2020) O-GlcNAcylation of PGK1 coordinates glycolysis and TCA cycle to promote tumor growth. *Nature communications* 11(1):36.

103. Koppe L, *et al.* (2016) Urea impairs β cell glycolysis and insulin secretion in chronic kidney disease. *The Journal of clinical investigation* 126(9):3598-3612.

104. Bacigalupa ZA, Bhadiadra CH, & Reginato MJ (2018) O-GlcNAcylation: key regulator of glycolytic pathways. *Journal of Bioenergetics and Biomembranes* 50(3):189-198.

105. Jackson RH & Singer TP (1983) Inactivation of the 2-ketoglutarate and pyruvate dehydrogenase complexes of beef heart by branched chain keto acids. *The Journal of biological chemistry* 258(3):1857-1865.

106. Zhao H, *et al.* (2020) Branched-Chain Amino Acids Exacerbate Obesity-Related Hepatic Glucose and Lipid Metabolic Disorders via Attenuating Akt2 Signaling. *Diabetes* 69(6):1164-1177.

107. Liu X, *et al.* (2018) PPM1K Regulates Hematopoiesis and Leukemogenesis through CDC20-Mediated Ubiquitination of MEIS1 and p21. *Cell reports* 23(5):1461-1475.

108. Bridi R, *et al.* (2005) alpha-keto acids accumulating in maple syrup urine disease stimulate lipid peroxidation and reduce antioxidant defences in cerebral cortex from young rats. *Metabolic brain disease* 20(2):155-167.

109. Funchal C, *et al.* (2006) Morphological alterations and induction of oxidative stress in glial cells caused by the branched-chain alpha-keto acids accumulating in maple syrup urine disease. *Neurochem Int* 49(7):640-650.

110. Giesbertz P, *et al.* (2015) Metabolite profiling in plasma and tissues of ob/ob

and db/db mice identifies novel markers of obesity and type 2 diabetes. *Diabetologia* 58(9):2133-2143.

111. Olson KC, Chen G, & Lynch CJ (2013) Quantification of branched-chain keto acids in tissue by ultra fast liquid chromatography-mass spectrometry. *Anal Biochem* 439(2):116-122.

112. Yan M, *et al.* (2019) Metabolomics profiling of metformin-mediated metabolic reprogramming bypassing AMPKα. *Metabolism: clinical and experimental* 91:18-29.

113. Sun L, *et al.* (2017) Association of circulating branched-chain amino acids with cardiometabolic traits differs between adults and the oldest-old. *Oncotarget* 8(51):88882-88893.

114. Xie G, *et al.* (2014) The metabolite profiles of the obese population are gender-dependent. *Journal of proteome research* 13(9):4062-4073.

115. Tai ES, *et al.* (2010) Insulin resistance is associated with a metabolic profile of altered protein metabolism in Chinese and Asian-Indian men. *Diabetologia* 53(4):757-767.

116. Wang SM, *et al.* (2018) Identification of serum metabolites associated with obesity and traditional risk factors for metabolic disease in Chinese adults. *Nutrition, metabolism, and cardiovascular diseases : NMCD* 28(2):112-118.

117. Miaczynska M, *et al.* (2004) APPL proteins link Rab5 to nuclear signal transduction via an endosomal compartment. *Cell* 116(3):445-456.

118. Cheng KK, Lam KS, Wang B, & Xu A (2014) Signaling mechanisms underlying the insulin-sensitizing effects of adiponectin. *Best practice & research. Clinical endocrinology & metabolism* 28(1):3-13.

119. Wang C, *et al.* (2009) Yin-Yang regulation of adiponectin signaling by APPL isoforms in muscle cells. *J Biol Chem* 284(46):31608-31615.

120. Wang B & Cheng KK (2018) Hypothalamic AMPK as a Mediator of Hormonal Regulation of Energy Balance. *Int J Mol Sci* 19(11).

121. Prudente S, *et al.* (2015) Loss-of-Function Mutations in APPL1 in Familial Diabetes Mellitus. *Am J Hum Genet* 97(1):177-185.

122. Wang C, *et al.* (2013) Deficiency of APPL1 in mice impairs glucose-stimulated insulin secretion through inhibition of pancreatic beta cell mitochondrial function. *Diabetologia* 56(9):1999-2009.

123. Cheng KK, *et al.* (2012) APPL1 potentiates insulin secretion in pancreatic beta cells by enhancing protein kinase Akt-dependent expression of SNARE proteins in mice. *Proceedings of the National Academy of Sciences of the United States of America* 109(23):8919-8924.

124. Jiang X, *et al.* (2017) APPL1 prevents pancreatic beta cell death and

inflammation by dampening NFkappaB activation in a mouse model of type 1 diabetes. *Diabetologia* 60(3):464-474.

125. Wang B, *et al.* (2018) Activation of hypothalamic RIP-Cre neurons promotes beiging of WAT via sympathetic nervous system. *EMBO reports*:e44977.

126. Qualmann B, Koch D, & Kessels MM (2011) Let's go bananas: revisiting the endocytic BAR code. *EMBO J* 30(17):3501-3515.

127. Cheng KK, *et al.* (2014) The adaptor protein APPL2 inhibits insulin-stimulated glucose uptake by interacting with TBC1D1 in skeletal muscle. *Diabetes* 63(11):3748-3758.

128. King GJ, *et al.* (2012) Membrane curvature protein exhibits interdomain flexibility and binds a small GTPase. *J Biol Chem* 287(49):40996-41006.

129. Wang Z, Oh E, & Thurmond DC (2007) Glucose-stimulated Cdc42 signaling is essential for the second phase of insulin secretion. *J Biol Chem* 282(13):9536-9546.

130. Asahara S, *et al.* (2013) Ras-related C3 botulinum toxin substrate 1 (RAC1) regulates glucose-stimulated insulin secretion via modulation of F-actin. *Diabetologia* 56(5):1088-1097.

131. Hoboth P, *et al.* (2015) Aged insulin granules display reduced microtubule-dependent mobility and are disposed within actin-positive multigranular bodies. *Proceedings of the National Academy of Sciences of the United States of America* 112(7):E667-676.

132. Mziaut H, *et al.* (2016) The F-actin modifier villin regulates insulin granule dynamics and exocytosis downstream of islet cell autoantigen 512. *Molecular metabolism* 5(8):656-668.

133. Thurmond DC, Gonelle-Gispert C, Furukawa M, Halban PA, & Pessin JE (2003) Glucose-stimulated insulin secretion is coupled to the interaction of actin with the t-SNARE (target membrane soluble N-ethylmaleimide-sensitive factor attachment protein receptor protein) complex. *Molecular endocrinology* 17(4):732-742.

134. Fujiwara I, Zweifel ME, Courtemanche N, & Pollard TD (2018) Latrunculin A Accelerates Actin Filament Depolymerization in Addition to Sequestering Actin Monomers. *Curr Biol* 28(19):3183-3192 e3182.

135. Theodoropoulos PA, *et al.* (1994) Cytochalasin B may shorten actin filaments by a mechanism independent of barbed end capping. *Biochemical pharmacology* 47(10):1875-1881.

136. Grand RJ & Owen D (1991) The biochemistry of ras p21. *Biochem J* 279 ( Pt 3):609-631.

137. Bastos RN, Penate X, Bates M, Hammond D, & Barr FA (2012) CYK4 inhibits

Rac1-dependent PAK1 and ARHGEF7 effector pathways during cytokinesis. *J Cell Biol* 198(5):865-880.

138. Jacquemet G, *et al.* (2013) Rac1 is deactivated at integrin activation sites through an IQGAP1-filamin-A-RacGAP1 pathway. *Journal of cell science* 126(Pt 18):4121-4135.

139. Damacharla D, *et al.* (2019) Quantitative proteomics reveals novel interaction partners of Rac1 in pancreatic beta-cells: Evidence for increased interaction with Rac1 under hyperglycemic conditions. *Mol Cell Endocrinol* 494:110489.

140. Li J, Luo R, Kowluru A, & Li G (2004) Novel regulation by Rac1 of glucose- and forskolin-induced insulin secretion in INS-1 beta-cells. *Am J Physiol Endocrinol Metab* 286(5):E818-827.

141. Veluthakal R, Kaur H, Goalstone M, & Kowluru A (2007) Dominant-negative alpha-subunit of farnesyl- and geranyltransferase inhibits glucose-stimulated, but not KCl-stimulated, insulin secretion in INS 832/13 cells. *Diabetes* 56(1):204-210.

142. Abe K, *et al.* (2000) Vav2 is an activator of Cdc42, Rac1, and RhoA. *J Biol Chem* 275(14):10141-10149.

143. Veluthakal R, Madathilparambil SV, McDonald P, Olson LK, & Kowluru A (2009) Regulatory roles for Tiam1, a guanine nucleotide exchange factor for Rac1, in glucose-stimulated insulin secretion in pancreatic beta-cells. *Biochem Pharmacol* 77(1):101-113.

144. Veluthakal R, *et al.* (2015) VAV2, a guanine nucleotide exchange factor for Rac1, regulates glucose-stimulated insulin secretion in pancreatic beta cells. *Diabetologia* 58(11):2573-2581.

145. Thamilselvan V & Kowluru A (2019) Paradoxical regulation of glucose-induced Rac1 activation and insulin secretion by RhoGDIbeta in pancreatic beta-cells. *Small GTPases*:1-8.

146. Wang Z & Thurmond DC (2010) Differential phosphorylation of RhoGDI mediates the distinct cycling of Cdc42 and Rac1 to regulate second-phase insulin secretion. *J Biol Chem* 285(9):6186-6197.

147. Kowluru A & Veluthakal R (2005) Rho guanosine diphosphate-dissociation inhibitor plays a negative modulatory role in glucose-stimulated insulin secretion. *Diabetes* 54(12):3523-3529.

148. Jian X, *et al.* (2009) Autoinhibition of Arf GTPase-activating protein activity by the BAR domain in ASAP1. *J Biol Chem* 284(3):1652-1663.

149. Lee JH, *et al.* (2019) Branched-chain amino acids sustain pancreatic cancer growth by regulating lipid metabolism. *Experimental & molecular medicine* 51(11):1-11.

150. Sacco F, *et al.* (2016) Glucose-regulated and drug-perturbed phosphoproteome reveals molecular mechanisms controlling insulin secretion. *Nature communications* 7:13250.

151. Foroumandi E, Alizadeh M, & Kheirouri S (2018) Age-dependent Changes in Plasma Amino Acids Contribute to Alterations in Glycoxidation Products. *Journal of medical biochemistry* 37(4):426-433.

152. Krumsiek J, *et al.* (2015) Gender-specific pathway differences in the human serum metabolome. *Metabolomics : Official journal of the Metabolomic Society* 11(6):1815-1833.

153. Lamichhane S, *et al.* (2019) Circulating metabolites in progression to islet autoimmunity and type 1 diabetes. *Diabetologia* 62(12):2287-2297.

154. Wang TJ, *et al.* (2011) Metabolite profiles and the risk of developing diabetes. *Nature medicine* 17(4):448-U483.

155. Uddin GM, *et al.* (2019) Impaired branched chain amino acid oxidation contributes to cardiac insulin resistance in heart failure. *Cardiovascular diabetology* 18(1):86.

156. Portais JC & Delort AM (2002) Carbohydrate cycling in micro-organisms: what can (13)C-NMR tell us? *FEMS microbiology reviews* 26(4):375-402.

157. Cieniewski-Bernard C, *et al.* (2004) Identification of O-linked N-acetylglucosamine proteins in rat skeletal muscle using two-dimensional gel electrophoresis and mass spectrometry. *Molecular & cellular proteomics : MCP* 3(6):577-585.

158. Hornbeck PV, *et al.* (2012) PhosphoSitePlus: a comprehensive resource for investigating the structure and function of experimentally determined post-translational modifications in man and mouse. *Nucleic acids research* 40(Database issue):D261-270.

159. Li J, *et al.* (2015) Quantitative Phosphoproteomics Revealed Glucose-Stimulated Responses of Islet Associated with Insulin Secretion. *Journal of proteome research* 14(11):4635-4646.

160. Han D, *et al.* (2012) Comprehensive phosphoproteome analysis of INS-1 pancreatic β-cells using various digestion strategies coupled with liquid chromatography-tandem mass spectrometry. *Journal of proteome research* 11(4):2206-2223.

161. Jiang X, *et al.* (2017) APPL1 prevents pancreatic beta cell death and inflammation by dampening NFκB activation in a mouse model of type 1 diabetes. *Diabetologia* 60(3):464-474.